

© Copyright by Yang Zheng 2015

All Rights Reserved

Applied and Fundamental Studies of LNT-SCR Dual-layer Monolithic Catalysts for Lean NO_x Emission Control

A Dissertation

Presented to

the Faculty of the Department of Chemical and Biomolecular Engineering

University of Houston

In Partial Fulfillment

of the Requirements for the Degree

Doctor of Philosophy

in Chemical Engineering

By

Yang Zheng

December 2015

Applied and Fundamental Studies of LNT-SCR Dual-layer Monolithic Catalysts for Lean NO_x Emission Control

Yang Zheng

Approved:

Chair of the Committee
Dr. Michael P. Harold
Professor and Chair
Chemical and Biomolecular Engineering

Committee Members:

Dr. Dan Luss
Professor
Chemical and Biomolecular Engineering

Dr. William S. Epling
Associate Professor
Chemical and Biomolecular Engineering

Dr. Stanko R. Brankovic
Associate Professor
Electrical and Computer Engineering

Dr. Allan Jacobson
Professor
Department of Chemistry

Dr. Suresh K. Khator, Associate Dean,
Cullen College of Engineering

Dr. Michael P. Harold, Professor and Chair,
Chemical and Biomolecular Engineering

Acknowledgments

I would like to gratefully thank my PhD advisors, Dr. Michael Harold and Dr. Dan Luss, for their continuous support and valuable guidance throughout my PhD life. Their patience, enthusiasm and knowledge have inspired me to go through this precious journey during the last four years. I am very thankful that they allowed me great freedom to think and develop ideas in my research and provided me with all I needed to improve my research skills and work. It was indeed my great honor doing research with them.

I am thankful to the other members of my dissertation committee: Dr. Bill Epling for providing his valuable insights and sharing the equipment in his lab, Dr. Stanko Brankovic, and Dr. Allan Jacobson, for accepting to be part of my dissertation committee.

I am thankful to BASF, especially Dr. C.Z. Wan, for supplying the catalyst samples used in this PhD research project, to DOE and NSF for funding my study. I also thank my former and current lab mates: Dr. Yi Liu and Dr. Mengting Yu for helping me in the lab especially in the beginning of my PhD work, Hoang Nguyen, Dr. Di Wang, Dr. Greg Bugosh, Dr. Sachi Shrestha, Aseem, Mengmeng Li, Yongjie Ren, Charles Perng, Dr. Richa Raj, Dr. Bijesh Shakya for being helpful in the lab, and my other lab mates: Dr. Vence Esterling, Wendy Lang, Po-Yu Peng, Tian Gu, and Dr. Arun Kota.

Finally, I would like to thank my family: my mother, father for their support and encouragement throughout my life. Very special thanks to my wife, Meng Wang, for her consistent love, support and encouragement. Without her understanding and company, my PhD work would have been impossible.

Applied and Fundamental Studies of LNT-SCR Dual-layer Monolithic Catalysts for Lean NO_x Emission Control

An Abstract

of a

Dissertation

Presented to

the Faculty of the Department of Chemical and Biomolecular Engineering

University of Houston

In Partial Fulfillment

of the Requirements for the Degree

Doctor of Philosophy

in Chemical Engineering

By

Yang Zheng

December 2015

Abstract

The increasingly stringent both greenhouse gas (GHG) and tailpipe NO_x emission standards have driven the continuous improvement of commercial deNO_x technologies, NO_x reduction & storage (NSR, also referred to as lean NO_x trap (LNT)) and selective catalytic reduction (SCR) technologies. This dissertation conducts applied and fundamental studies of coupled LNT-SCR dual-layer catalysts with the aim of expanding the operating temperature window of a conventional NSR system at lower cost. This is accomplished by a systems approach to identify the influencing factors such as catalyst composition and architecture, types of reducing agents, operating and regeneration strategies, as well as synergistic interactions between the LNT and SCR.

We start with performance evaluation of dual-layer catalysts under different regeneration conditions such as H₂ alone, CO/H₂ mixture and a simulated diesel exhaust containing the CO/H₂/C₃H₆ mixture. Spatial analyses of NH₃ yield and NO_x conversion along the LNT monolith identify the upstream zone as major NH₃ generator and NO_x reducer, especially at temperatures exceeding 300 °C. Zoning of either or both the SCR and LNT having a dual-layer structure enables an increase in the low-temperature (200-250 °C) NO_x conversion, and minimizes the high temperature (300-400 °C) conversion loss caused by the SCR diffusion resistance and undesired NH₃ oxidation by the LNT.

The hydrocarbon (HC) reductant leads to an alternative LNT-SCR synergy to classical NH₃-pathway; a LNT-assisted HC-SCR pathway. The LNT promotes the formation of partially oxidized HC intermediates during the rich purge which are otherwise difficult to be generated by the Cu-zeolite layer at low temperatures. These activated intermediates can be captured and utilized by the SCR catalyst via HC-SCR during the

ensuing lean phase. This pathway plays a major role at low temperatures (≤ 225 °C) using the simulated diesel exhaust feed.

We investigated the steady-state and transient effects of reductants (CO, H₂ and C₃H₆) on Cu-SSZ-13 catalyzed NH₃-SCR as the SCR component in the combined system is periodically exposed to a rich exhaust. The three reductants affect to different extent the NH₃-SCR reactions. Propylene is most effective in promoting NO₂ reduction to NO by formation of organic intermediates. CO effectively reduces nitrates to nitrites that react with NO₂, releasing NO. H₂ follows a similar pathway as CO but is less effective.

Finally, the effects of the lean/rich cycling frequency on both LNT and combined catalysts are investigated. Rapid C₃H₆ pulsing into a lean exhaust stream expands the operating temperature window of a conventional NSR system in both low and high-temperature regions. The combination of rapid propylene pulsing and the dual-layer catalyst architecture achieves the highest low-temperature NO_x conversion. The working mechanisms of rapid propylene pulsing on both LNT and LNT-SCR catalysts are elucidated. Optimization of top-layer material and catalyst configuration like SCR and PGM zoning can improve system performance at lower cost.

Table of Contents

Acknowledgments	v
Abstract	vii
Table of Contents	ix
List of Figures	xiii
List of Tables.....	xix
Nomenclature	xx
Chapter 1 Introduction	1
1.1 Fuel economy and emission challenges	1
1.2 Lean NO _x emission control technologies.....	3
1.3 Combined LNT + SCR systems	5
1.4 LNT-SCR dual-layer architecture	7
1.5 Di-Air system	9
1.6 Research objectives and thesis outline	10
Chapter 2 Lean NO _x reduction on LNT-SCR dual-layer catalysts by H ₂ and CO	14
2.1. Introduction	14
2.2. Experimental.....	16
2.2.1. Catalyst preparation	16
2.2.2. Reactor tests	18
2.3. Desired ceria level in LNT for dual-layer application.....	20
2.4. Spatial analysis of NH ₃ yield and NO _x conversion.....	22
2.5. Impact of top-layer diffusional resistance	25
2.6. Effects of zonal distribution of SCR and LNT washcoat	27

2.7. Conclusions	33
Chapter 3 NO _x reduction on LNT-SCR dual-layer catalysts under simulated diesel exhaust conditions	
3.1. Introduction	36
3.2. Experimental.....	37
3.3. NO _x reduction by a C ₃ H ₆ /CO/H ₂ mixture.....	39
3.4. LNT-assisted HC-SCR pathway.....	40
3.5. Impact of zoning SCR loading	49
3.6. PGM loading and zoning effects	52
3.7. Conclusions	55
Chapter 4 Effects of CO, H ₂ and C ₃ H ₆ on Cu-SSZ-13 Catalyzed NH ₃ -SCR	
4.1 Introduction	57
4.2 Experimental.....	59
4.2.1. Catalyst.....	59
4.2.2. Temperature ramp experiments.....	59
4.2.3. Lean/rich cycling experiments	60
4.2.4. Temperature-programmed desorption (TPD) experiments	61
4.3 NO and NO ₂ reactions with CO, H ₂ and C ₃ H ₆	62
4.4 The effects of CO, H ₂ and C ₃ H ₆ on NH ₃ oxidation and storage.....	68
4.5 Steady-state effects of CO, H ₂ and C ₃ H ₆ on NH ₃ -SCR reactions	71
4.5.1. Temperature ramp experiments.....	71
4.5.2. Step-response method	77
4.5.3. N ₂ O formation.....	80

4.6	Impact of CO, H ₂ and C ₃ H ₆ on cyclic NH ₃ -SCR reduction	82
4.7	Conclusions	85
Chapter 5 Rapid C ₃ H ₆ pulsing for enhanced low temperature NO _x conversion on combined LNT-SCR Catalysts.....		87
5.1	Introduction	87
5.2	Experimental.....	88
5.2.1.	Catalysts	88
5.2.2.	Reactor system	89
5.3	Effects of combining rapid propylene pulsing with SCR layer addition.....	92
5.3.1.	Effect of rapid propylene injection	95
5.3.2.	Effect of Cu-SAPO-34 top-layer.....	98
5.4	Effect of ceria in LNT layer	102
5.5	Effect of top-layer material	103
5.6	N ₂ O yield and selectivity.....	105
5.7	Working mechanism of rapid propylene pulsing	106
5.8	Effects of catalyst configuration.....	109
5.9	Conclusions	110
Chapter 6 Conclusions and recommendations for future study		112
6.1	Conclusions	112
6.1.1.	Catalyst formulation.....	112
6.1.2.	Catalyst configuration	113
6.1.3.	Rich feed composition.....	113
6.1.4.	Lean/rich timing	115

6.2	Recommendations for future study	116
	References	119

List of Figures

Fig. 1-1 Comparison of global CO ₂ regulations for passenger cars.....	1
Fig. 1-2 California LEVIII fleet average combined non-methane organic gas and NO standards (NMOG+NO _x) for cars and light-duty trucks (LDT1 up to 3750 lbs.; LDT2 3751-8500 lbs.).....	3
Fig. 1-3 Reaction scheme of dual-layer concept.....	8
Fig. 1-4 Critical parameter flow down for combined LNT-SCR system.....	11
Fig. 2-1 Impact of Ceria on NO _x conversion and NH ₃ yield from ceria-free LNT1 and ceria-rich LNT3 using (a) 2.5% H ₂ and (b) 1%CO+1.5% H ₂ as reductants	21
Fig. 2-2 Spatial NH ₃ , N ₂ yields and NO _x conversion along honeycomb catalysts of LNT1 and LNT3 with 1% CO+1.5% H ₂ as reductant at 250 °C	22
Fig. 2-3 NO _x conversion and NH ₃ yield at the middle and the end of the LNT3 honeycomb catalyst using (a) 2.5% H ₂ and (b) 1% CO+1.5% H ₂ as reductants	23
Fig. 2-4 Comparison of NO _x conversion using (a) 2.5% H ₂ and (b) 1% CO+1.5% H ₂ as reductants over L(4.6) and CuC(0.8)/L(4.6) catalysts	24
Fig. 2-5 NO _x conversion (a) and NH ₃ yield (b) from dual-layer catalysts by 2.5% H ₂ and GHSV=120,000 h ⁻¹ at fixed LNT3 loading but different NaZ loadings	26
Fig. 2-6 NO _x conversion from LNT3, CuC(0.8)/L(4.6) and L(4.6)+CuC(0.8)/L(4.6) catalysts using as reductants (a) 2.5% H ₂ and (b) 1% CO+1.5% H ₂	28
Fig. 2-7 Comparison of effluent concentrations of NO _x , NH ₃ , N ₂ O from L(4.6) and L(4.6)+CuC(0.8)/L(4.6) during cycling at 200 °C using 1% CO + 1.5% H ₂ as reductants	29

Fig. 2-8 Mechanism of NO _x decomposition by zoned dual-layer LNT-SCR catalyst at temperatures above 300 °C.....	30
Fig. 2-9 NO _x conversion by dual-layer catalysts with different zoned LNT and SCR loadings but the same total LNT loading using a) 2.5% H ₂ and b) 1% CO+1.5% H ₂	31
Fig. 2-10 NO _x conversion by dual-zone dual-layer catalysts with different downstream LNT loadings using a) 2.5% H ₂ and b) 1% CO+1.5% H ₂	33
Fig. 3-1 Comparison of cycle-averaged NO _x conversion for L(4.6) and CuC(0.8)/L(4.6) catalysts using 2.4% CO + 0.8% H ₂ + 1000 ppm C ₃ H ₆ as reductants (Rich #1)	40
Fig. 3-2 Comparison of effluent concentrations of a) NO _x , b) NH ₃ , c) C ₃ H ₆ and d) N ₂ O from L(4.6) and CuC(0.8)/L(4.6) during cycling at 200 °C using 2.4% CO + 0.8% H ₂ + 1000 ppm C ₃ H ₆ as reductants (Rich #1)	41
Fig. 3-3 Cycle-averaged (a) NH ₃ yield and (b) NO _x conversion at the 0.5, 1, 2 cm length of LNT monolithic catalyst using 2.4% CO + 0.8% H ₂ + 1000 ppm C ₃ H ₆ as reductants (Rich #1)	42
Fig. 3-4 Comparison of cycle-averaged NO _x conversion and NH ₃ yield for L(4.6) and CuC(0.8)/L(4.6) catalysts using 2.4% CO + 0.8% H ₂ as reductants (Rich #2)	43
Fig. 3-5 Comparison of cycle-averaged NO _x conversion and NH ₃ yield for L(4.6) using 1000 or 3550 ppm C ₃ H ₆ as reductant (Rich #3 or Rich #4) and CuC(0.8)/L(4.6) catalysts using 1000 ppm C ₃ H ₆ as reductant (Rich #3)	44
Fig. 3-6 a) NO _x conversion using 0.1% C ₃ H ₆ + 1% O ₂ with and without 2.4% CO + 0.8% H ₂ as reductants over the SCR only. b) Steady-state NO _x and C ₃ H ₆ conversions over CuC(2.4) under feeding 500 ppm NO, 500 ppm C ₃ H ₆ and 5% O ₂	45

Fig. 3-7 DRIFTS spectra over LNT catalyst taken at 200 °C after a 1h pre-conditioning by 500 ppm NO + 5% O ₂ and purge with He (a), subsequently exposed to a flow of 0.1% C ₃ H ₆ + 1% O ₂ for 5 min (b), 15 min (c), 30 min (d).....	47
Fig. 3-8 Comparison of cycle-averaged NO _x conversion from dual-layer catalysts with fixed LNT loading but different NaZ loadings using 2.4% CO + 0.8% H ₂ + 1000 ppm C ₃ H ₆ as reductants (Rich #1).....	50
Fig. 3-9 Cycle-averaged NO _x conversion from L(4.6), CuC(0.8)/L(4.6) and L(4.6) + CuC(0.8)/L(4.6) using 2.4% CO + 0.8% H ₂ + 1000 ppm C ₃ H ₆ as reductants (Rich #1)..	51
Fig. 3-10 Cycle-averaged NO _x conversion by LNT and two dual-layer catalysts having the same SCR loading but different LNT loadings using 2.4% CO + 0.8% H ₂ + 1000 ppm C ₃ H ₆ as reductants (Rich #1).....	52
Fig. 3-11 Cycle-averaged NO _x conversion from dual-layer catalysts with different zoned LNT and SCR loading but the same total LNT loading using 2.4% CO + 0.8% H ₂ + 1000 ppm C ₃ H ₆ as reductants (Rich #1)	53
Fig. 3-12 Cycle-averaged NO _x conversion by zoned dual-layer catalyst with different downstream LNT loading using 2.4% CO + 0.8% H ₂ + 1000 ppm C ₃ H ₆ as reductants (Rich #1)	54
Fig. 4-1 NO conversion (solid) and NH ₃ selectivity (dash) during reaction of NO (500 ppm) with three reductants (either 1% CO, 1% H ₂ , or 500 ppm C ₃ H ₆) in the absence of O ₂ (a) and in the presence of 5% O ₂ (b)	62
Fig. 4-2 a) NO ₂ (solid) and NO _x (dash) conversion; b) corresponding NO ₂ (solid) and NO (dash) effluent concentration during reaction of NO ₂ with either 1% CO, 1% H ₂ , or 500 ppm C ₃ H ₆) without O ₂ ; Baseline condition: 500 ppm NO ₂ in carrier gas	64

Fig. 4-3 Effluent species concentrations during a three-phase step-response protocol at 500 °C; (500 ppm NO ₂ , 1% H ₂ , 5% O ₂ if required, in carrier gas of 2.5% H ₂ O, 2% CO ₂ and balance Ar)	67
Fig. 4-4 NH ₃ -TPD profiles after saturating the catalyst with NH ₃ at 200 °C in the absence (baseline) or in the presence of a mixture of reductants, including 1% CO, 1% H ₂ , and 500 ppm C ₃ H ₆	69
Fig. 4-5 NH ₃ conversion during NH ₃ oxidation in the presence of 500 ppm C ₃ H ₆ or 1% CO+1% H ₂	70
Fig. 4-6 C ₃ H ₆ conversion and CO generation during C ₃ H ₆ oxidation experiment with 500 ppm C ₃ H ₆ and 5% O ₂ in carrier gas of 2.5% H ₂ O, 2% CO ₂ and balance Ar	71
Fig. 4-7 NO _x conversion of (a) standard SCR and (b) fast SCR in the presence of either 1% CO, 1% H ₂ , or 500 ppm C ₃ H ₆ . Baseline conditions: 5% O ₂ , 500 ppm NH ₃ and NO for standard SCR, while 500 ppm NH ₃ , 250 ppm NO and NO ₂ for fast SCR.....	72
Fig. 4-8 DRIFTS spectra over a Cu-SSZ-13 catalyst taken at 200 °C, after a 1h pre-conditioning by 500 ppm NO + 1% O ₂ and purge with He (0 min), subsequently exposed to a flow of 0.1% C ₃ H ₆ + 1% O ₂ for 2 min and 30 min	73
Fig. 4-9 NO _x conversion during slow SCR reaction in the presence of one reductant (either 1% CO, 1% H ₂ , or 500 ppm C ₃ H ₆)	76
Fig. 4-10 Effluent species concentrations during a five-phase step-response protocol at 400 °C; (500 ppm NO ₂ , 500 ppm NH ₃ , 500 ppm C ₃ H ₆ , 5% O ₂ if required, in carrier gas of 2.5% H ₂ O, 2% CO ₂ and balance Ar)	78

Fig. 4-11 Effluent species concentrations during a five-phase step-response protocol at 400 °C; (500 ppm NO ₂ , 500 ppm NH ₃ , 1% CO, 5% O ₂ if required, in carrier gas of 2.5% H ₂ O, 2% CO ₂ and balance Ar)	79
Fig. 4-12 N ₂ O effluent concentration during TPD of NH ₄ NO ₃ in the absence (baseline) or in the presence of either 500 ppm C ₃ H ₆ , 1% CO or 1% H ₂	80
Fig. 4-13 Cycle-averaged NO _x conversion of a) standard, b) fast and c) slow SCR reactions when NH ₃ and either C ₃ H ₆ or H ₂ +CO are present with in the rich phase.....	82
Fig. 4-14 Effluent gas concentration during (a) standard and (b) slow SCR reactions under cyclic condition at 350 °C when NH ₃ and either C ₃ H ₆ or H ₂ +CO are present in the rich phase.....	83
Fig. 5-1 Cycle-averaged NO _x as a function of (a) feed temperature and (b) temperature at the center of monolith, T _c , for LNT alone and dual-layer catalysts with different cycle times	93
Fig. 5-2 Effluent NO _x /C ₃ H ₆ concentration and catalyst temperature for a set of cycling experiments at 225 °C feed temperature over LNT and dual-layer catalysts.....	95
Fig. 5-3 Temporal DRIFTS spectra over SCR catalyst taken at 200 °C after a 1h pre-conditioning by 500 ppm NO + 5% O ₂ and purge with He, subsequently exposed to a flow of 0.1% C ₃ H ₆ + 1% O ₂	101
Fig. 5-4 Cycle-averaged NO _x as a function of feed temperature for dual-layer catalysts with and without ceria under fast cycling	102
Fig. 5-5 (a) NO _x conversions as a function of feed temperature for dual-layer catalysts with either Cu-SAPO-34 or γ-Al ₂ O ₃ or Ag/Al ₂ O ₃ . (b) Propene oxidation over LNT, LNT-Al ₂ O ₃ and LNT-Ag/Al ₂ O ₃ catalysts.....	103

Fig. 5-6 N ₂ O selectivity (a) and yield (b) as a function of feed temperature for LNT alone and dual-layer catalysts with different cycle times	106
Fig. 5-7 Working mechanism for fast propylene pulsing over dual-layer catalyst	108
Fig. 5-8 Cycle-averaged NO _x as a function of feed temperature by LNT, dual-layer and dual-brick catalysts under fast cycling	109
Fig. 5-9 Cycle-averaged NO _x as a function of feed temperature by (a) LNT, dual-layer catalysts with different PGM loading under the same fast cycling and (b) LNT alone with varied PGM loading and varied cycle times	109

List of Tables

Table 2-1 Composition of the monolith-supported LNT catalysts	17
Table 2-2 Composition of metal-exchanged zeolites	17
Table 2-3 Configuration and notation of zoned & layered catalysts	18
Table 3-1 Gas conditions for 60/5 cycling test	38
Table 4-1 Gas condition for baseline cycling test	61
Table 4-2 Accumulated N ₂ O release from TPD of NH ₄ NO ₃	81
Table 5-1 Gas condition for baseline cycling test	91

Nomenclature

CARB	California Air Resources Board
DOC	Diesel oxidation catalyst
DPF	Diesel particulate filter
DRIFTS	Diffuse reflectance infrared Fourier transform spectroscopy
EPA	Environmental Protection Agency
FTIR	Fourier transform infrared spectroscopy
GHG	Greenhouse gas
GHSV	Gas hourly space velocity
HC	Hydrocarbon
LEV	Low-emission vehicle
LNT	Lean NO _x trap
NEDC	New European Drive Cycle
NMOG	Non-methane organic gas
NO _x	Oxides of nitrogen, including NO and NO ₂
NSR	NO _x storage and reduction
OEM	Original equipment manufacturer
OSC	Oxygen storage compound
PGM	Platinum group metals
PM	Particulate matter
SCR	Selective catalytic reduction
T _c	Temperature at the center of the monolithic catalyst
TWC	Three-way catalytic convertor
WGS	Water-gas shift

Chapter 1 Introduction

1.1 Fuel economy and emission challenges

The automotive industry is currently facing a tremendous worldwide challenge posed by the public and regulatory agencies to decrease the emission of both greenhouse gas (GHS, including carbon dioxide, nitrous oxide and methane) and regulated toxic pollutants including carbon monoxide, nitrogen oxide (NO_x; NO+NO₂), hydrocarbons (HC) and particulate matter (PM). Fig. 1-1 summarizes recent and proposed fuel economy or CO₂ emission regulations around the world, normalized by the CO₂ emissions of the New European Drive Cycle (NEDC). Most large economies have specified decreasing CO₂ emission targets for new vehicles [1]. The US government recently announced new standards that will increase by 2025 the fuel economy to 54.5 mpg for cars and light-duty truck. An even stricter standard by EU legislation mandates fuel economy up to 4.1 L/ 100 km (57.4 mpg) by 2021. Other countries like Japan, China and India, etc. also implement similar regulations that demands much higher fuel efficiency.

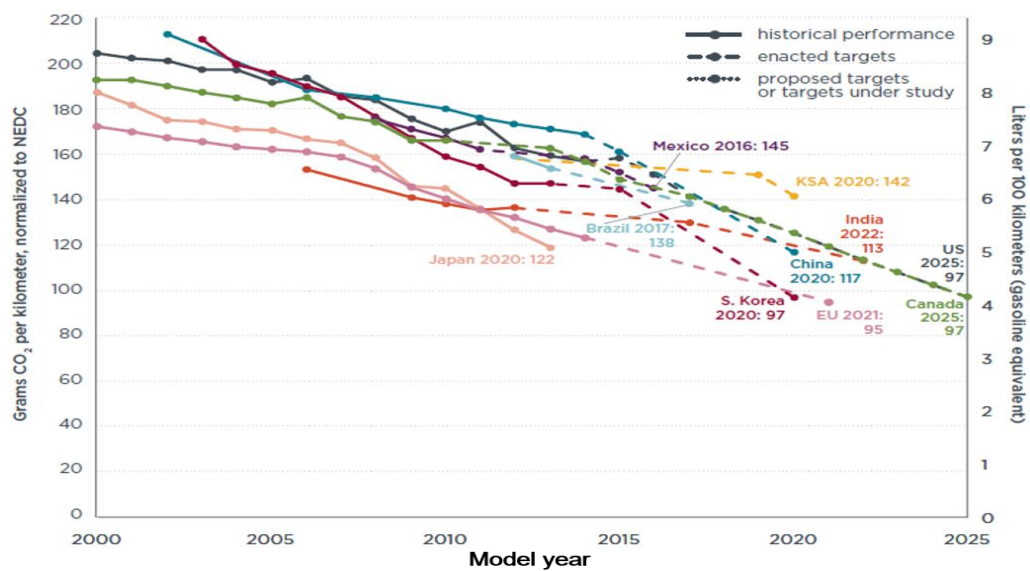


Fig. 1-1 Comparison of global CO₂ regulations for passenger cars [2].

To address the regulatory challenge, OEMs (original equipment manufacturers) have to resort to a combination of advanced engine combustion and powertrain technologies. Three main types of combustion strategies with higher fuel efficiency have attracted great interest: lean burn gasoline, clean diesel and low-temperature combustions [3]. Although each combustion technique produces a unique exhaust, lower temperature and oxygen-rich (lean) exhaust conditions are typically expected. This stems from the fact that lower exhaust enthalpy will be available as more fuel energy will be converted to mechanical work and the nature of the lean combustion. Powertrain strategies like hybrid, turbo charging and start/stop techniques further boost the fuel efficiency with far less heat energy available in the exhaust for the aftertreatment system. For example, typical turbo chargers can lower the temperature of the exhaust gas by more than 100 °C [3].

Technologies needed to increase the fuel economy inevitably complicate current state-of-art aftertreatment solutions by the challenging exhaust conditions of low temperature and excess oxygen [4]. In other words, there is a trade-off between fuel economy and emission control. For example, the three-way catalytic convertor (TWC) commonly used on most current gasoline-powered passenger cars can effectively satisfy regulated exhaust emission reduction. However, the lower exhaust temperature from lean-burn gasoline and diesel engines, would require catalysts with much lower light-off temperatures to efficiently remove pollutants, especially during cold start. Besides, even a little excess oxygen remaining in the exhaust can cause a failure to abate NO_x by TWC.

The fuel economy and emission challenges have been exacerbated by more stringent emission regulations implemented recently like LEV III, Tier 3 and Euro 6 [1]. For example, Fig. 1-2 shows that LEV III set by California Air Resources Board (CARB)

further tightens current NO_x + NMOG (Non-methane Organic Gas) tailpipe limit by 75% by 2025. In addition to more restrictive emission limits, new emission certification test procedures, like Worldwide Harmonized Light-duty Vehicles Test Procedure (WLTP), Real Driving Emissions (RDE), and Portable Emissions Measurement System (PEMS) expanded emission-relevant engine operation area [5]. This further challenges aftertreatment systems to provide a high performance over a wider range of operating conditions encountered in practice, especially during cold start, idling, high-speed and high-load driving conditions.

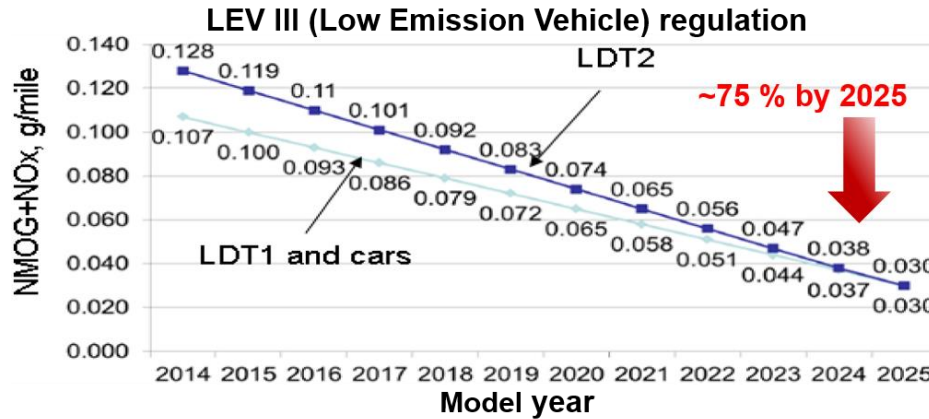
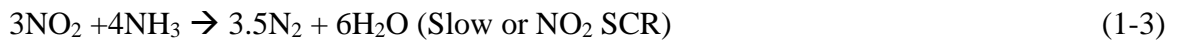
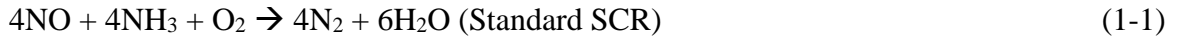


Fig. 1-2 California LEV III fleet average combined non-methane organic gas and NO standards (NMOG+NO_x) for cars and light-duty trucks (LDT1 up to 3750 lbs.; LDT2 3751-8500 lbs.).

1.2 Lean NO_x emission control technologies

To address fuel-economy and emissions trade-off, it is imperative to develop advanced lean NO_x emission control technologies that deliver higher NO_x conversion efficiency over a wider temperature range. Leading NO_x abatement technologies primarily include selective catalytic reduction of NO_x with NH₃ (NH₃-SCR) or HC (HC-SCR) and NO_x storage reduction (NSR) [6].

NH₃-SCR is a more mature technology that efficiently reduces NO_x to N₂ over vanadium-based or transition metal (Cu or Fe) exchanged zeolite catalysts by a reaction with NH₃ generated from urea thermal hydrolysis [7]. It is used mostly for heavy duty (HD) vehicles but it is recently considered as well for light duty vehicles. Urea-SCR system can achieve 90-95% deNO_x efficiency via the following three NH₃-SCR reactions.



But it requires a bulky and expensive urea injection system which causes packaging and cost issues for light-duty application. Besides, the minimum urea dosing temperature of ~ 200 °C limits the low-temperature functionality of the SCR, especially during cold start and idling.

To avoid the need of urea injection infrastructure, the use of hydrocarbons as reductants (HC-SCR) has received special interest because hydrocarbons from of incomplete combustion of fuels are readily available in the exhaust. A typical HC-SCR catalyst consists of Ag, Co or Cu for NO_x adsorption and alumina or zeolites for HC adsorption [6]. Among these, Ag/Al₂O₃ has received most attention, especially due to the promoting effect of H₂ (H₂-assisted HC-SCR) that enables a dramatic decrease of the light-off temperature by more than 100 °C [8]. Remaining problems that prevents its commercialization are unselective HC oxidation, efficient HC activation as well as catalyst hydrothermal stability, etc.

NSR, also referred as lean NO_x trap (LNT), technology is particularly suitable to light-duty passenger cars (i.e., engine displacement less than 2.0 L). LNT catalysts are

essentially TWC catalysts that contain precious group metals (PGM, like Pt and Rh) as well as alkali (like K) or alkaline-earth metals (like Ba), which serve as NO_x storage materials [9]. NSR involves cyclic operation by alternating a long lean phase (typically 30-90 s) with a short rich phase (3-10 s). The basic concept is that under lean-feed condition, NO is oxidized by the Pt to NO₂ that can be trapped by storage materials to form nitrates/nitrites. As NO_x storage sites fill up, the NO_x trapping efficiency drops. As this happens, the adsorbed NO_x species can be released and reduced to N₂ over the precious metals during the short regeneration by the introduction of a rich exhaust feed that contains CO, H₂ and hydrocarbons (HC). The operation temperature window for LNT catalysts is relatively narrow (typically 250-400 °C). The low-temperature performance is limited by incomplete purge, as well as by the low rate of NO oxidation. The high-temperature performance suffers from decreased NO_x storage capacity as nitrates/nitrites become thermally unstable. Compared with SCR, LNT is more vulnerable to sulfur poisoning and thermal aging, which raises durability concerns. In response to ever-tightening tailpipe limits and exhaust conditions, either SCR or NSR systems require further improvements are required in to provide high NO_x removal efficiency over a board range of operating conditions.

1.3 Combined LNT + SCR systems

The increasing demands on high performance, small-size and cost-effective aftertreatment systems have motivated the integration of existing complementary technologies, including LNT + SCR [10, 11], SCR on filter (SCRf) [12], and diesel particulate-NO_x reduction (DPNR) [13], etc. Among them, combined LNT + SCR systems have arose great interest in both industry and academia.

The concept of combining LNT and SCR together is based on the fact that LNT catalyst produces NH_3 as a by-product during the rich regeneration while SCR catalyst stores and utilizes it to reduce NO_x . Hence, combined LNT + passive SCR systems offer a potential of enhancing NO_x conversion, reducing NH_3 slip and PGM usage as well as eliminating the need for urea injection to the SCR catalyst [14, 15]. Several LNT+SCR configurations have been proposed, including zoned or layered configurations [14, 16]. Daimler commercialized in 2007 the first LNT + SCR system on Mercedes E320 Bluetec [17]. Chen et al. [18] enhanced the performance of LNT-SCR system by tuning OSC (oxygen storage component) loading in LNT and utilizing a SCR catalyst with excellent low temperature NH_3 -SCR activity and resistance to high temperature lean/rich aging. Xu et al. [14] from Ford demonstrated the ability of the LNT+SCR dual-zone approach to achieve the Tier 2 Bin 2 standard with up to 30% saving in PGM loading compared to the LNT alone. They also found out non- NH_3 reductants like HC derivatives produced from the reaction of HC and stored NO_x during LNT regeneration could be utilized by SCR for additional NO_x conversion.

The overall NO_x conversion of the combined system is still dominated by the performance of LNT component that is relatively low at both low and high temperatures. Several attempts have been made to improve LNT regeneration in order to achieve high NH_3 yield at minimum fuel penalty (< 2%). Wittka et al. [19] proposed a novel configuration for the LNT + passive SCR system featuring the use of an out-line fuel reformer and an exhaust bypass around the LNT. Fuel is converted in the reformer to H_2 and CO that are more efficient reductants than HC for NH_3 generation. During regeneration, the main exhaust stream flows around the LNT via the bypass while the LNT is locally

enriched by feeding the reformate gas at low space velocity, in order to achieve complete regeneration and high NH_3 yield for the downstream SCR. This configuration enables engine-independent LNT regeneration (no need for engine management like air throttling or post-injection to reach lambda below 1 in the LNT), resulting in high overall NO_x conversion at a low fuel penalty. Another approach proposed by researchers from SwRI [20] and Hyundai [21] is to combine the LNT with the SCR with urea dosing (LNT + active SCR). It uses a LNT to assist SCR to address cold-start NO_x emission, when the temperature is too low for urea dosing. The combined system has been demonstrated to meet the LEV III limits but at the price of large packaging space, high hardware cost and control complexity.

1.4 LNT-SCR dual-layer architecture

In order to minimize the size and the weight of aftertreatment devices, a more compact design for system integration of LNT + SCR is desired. Honda researchers first proposed a dual-layered LNT + SCR architecture comprising a solid acid on top of Pt/OSC that enabled a significant downsizing from that of a sequential configuration [10]. This is in favor of application in cars with limited space. Fig. 1-3 shows basic working principle of LNT-SCR dual-layer catalysts involve in-situ NH_3 production from the bottom LNT layer during the rich regeneration, followed by the capture and utilization of released NH_3 by the SCR top layer for incremental NO_x reduction via classic NH_3 -SCR pathway. Recently, Honda researchers further improved the dual-layer system by introducing a zirconia-based intermediate layer that minimized the negative interaction between the LNT and SCR layers of opposite acid-base properties [22]. The improved system had high NO_x reduction performance even for low exhaust gas temperature. In addition to system

downsizing, the intimate contact between LNT and SCR layers is expected to enhance the utilization efficiency of key intermediates like NH_3 . In the dual-zone configuration, a considerable amount of NH_3 released from the front LNT section could be oxidized by stored NO_x and oxygen in the LNT downstream before it can reach the SCR brick, limiting the NH_3 supply to the SCR reaction.

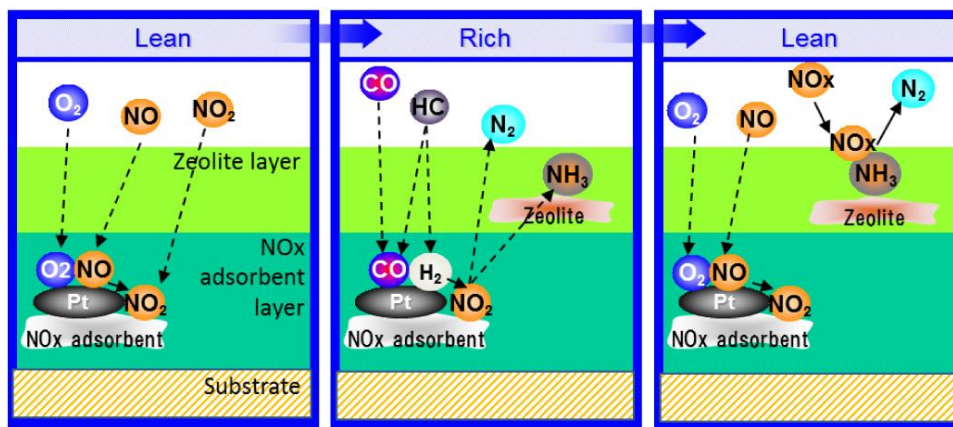


Fig. 1-3 Reaction scheme of dual-layer concept [22].

Inherent drawbacks are also associated with the dual-layer architecture. The foremost issue is the inevitable diffusion resistance by the SCR upper layer, which inhibits the effective transport of NO_x to the underlying LNT layer for storage during the lean feed and of reductants for regeneration during the rich feed. Thus, undesired diffusion limitation lowers the both NO_x conversion and NH_3 yield of LNT component. Koltsakis et al. [23] reported that at either high temperature or high space velocity, the dual-layer de NO_x efficiency was severely reduced by the additional resistance of the SCR layer and was lower than either LNT alone or a dual-bed system. Another deficiency is the undesired oxidation of stored NH_3 to NO_x by the adjacent LNT layer at high temperatures [24]. Another concern is SCR poisoning by reducing agents like HC, CO, H_2 encountered during the LNT

regeneration. Such detrimental effects may counterbalance or even outweigh the benefit of adding the SCR layer.

Hence, still lots of room is remained for improvement, especially in terms of catalyst design. There are a different set of requirements for LNT and SCR catalysts as components in combined system, compared to stand-alone system. High NH_3 selectivity during rich purge can be a desirable feature of the LNT component in a combined system, as opposed to a LNT only system that requires high N_2 selectivity. High NH_3 storage capacity for effective NH_3 trapping can significantly improve the overall NO_x reduction efficiency of the LNT-SCR systems, but may be undesirable for standalone SCR systems because it causes appreciable NH_3 slip during transient temperature excursion associated with certain drive cycles. More importantly, the SCR component must be able to withstand periodic rich exposure during regeneration and high-temperature desulfation of underlying LNT, which is a unique durability requirement for this system.

1.5 Di-Air system

Recently Toyota researchers observed a very interesting phenomenon that achieves high NO_x conversion at high temperatures over NSR catalysts [25, 26]. This increased conversion occurs when continuous short cycle injection of HC (cycle time $< \sim 5$ s) into a lean exhaust stream fed to an LNT catalyst. The enhanced performance was attributed to adsorbed HC intermediates, which are generated by a reaction between adsorbed NO_x and partially oxidized hydrocarbons during the high-frequency HC pulsing. These short-lived intermediates are rapidly converted through a reaction with surface and/or gas phase NO_x species to N_2 during the lean part of the cycle. Compared to NSR, Di-Air operation shifts the major N_2 formation from the rich to the lean. Thus, the process based on this concept

was named Di-Air (diesel NO_x aftertreatment by adsorbed intermediate reductants). This system significantly improved the deNO_x performance under high-temperature and high-SV operations, where conventional NSR (cycle time 1-2 min) performs unsatisfactorily. A recent study of our group found that fast cycling of propylene enhanced somewhat deNO_x activity of LNT catalysts even at low temperatures, but to a smaller extent than at high temperatures [27]. It is interesting to see if Di-Air concept with high-frequency HC pulsing can also benefit a combined LNT+ passive SCR system, especially at low temperatures.

1.6 Research objectives and thesis outline

Although Honda's pioneering work provoked great interest in layered architecture, they did neither provide complete information about the catalyst (formula, loading) nor propose detailed mechanism of the reactions on the dual-layer catalyst. Furthermore, in order to optimize this combined system, a deep insight into the complex nature of the combined systems is required, including what are critical system parameters, how critical parameters are measured and how they are interconnected. A simplified version of the critical parameter flow down for combined LNT-SCR system is shown in Fig. 1-4. Obviously, an optimal design of the combined system have to take into account all these influencing factors and their interactions one another. Thus, the primary objective of this dissertation is to investigate the application feasibility and fundament aspects of the combined LNT-SCR dual-layer system through experimental studies. Specifically, critical factors including impacts of reducing agents, catalyst composition and architecture, as well as operating strategies on the performance and reaction pathways of combined LNT-SCR system are elucidated. Optimized combined system is expected to have potential to meet

NO_x emission abatement target over a wide range of operating conditions for light duty application. This dissertation consists of the following parts:

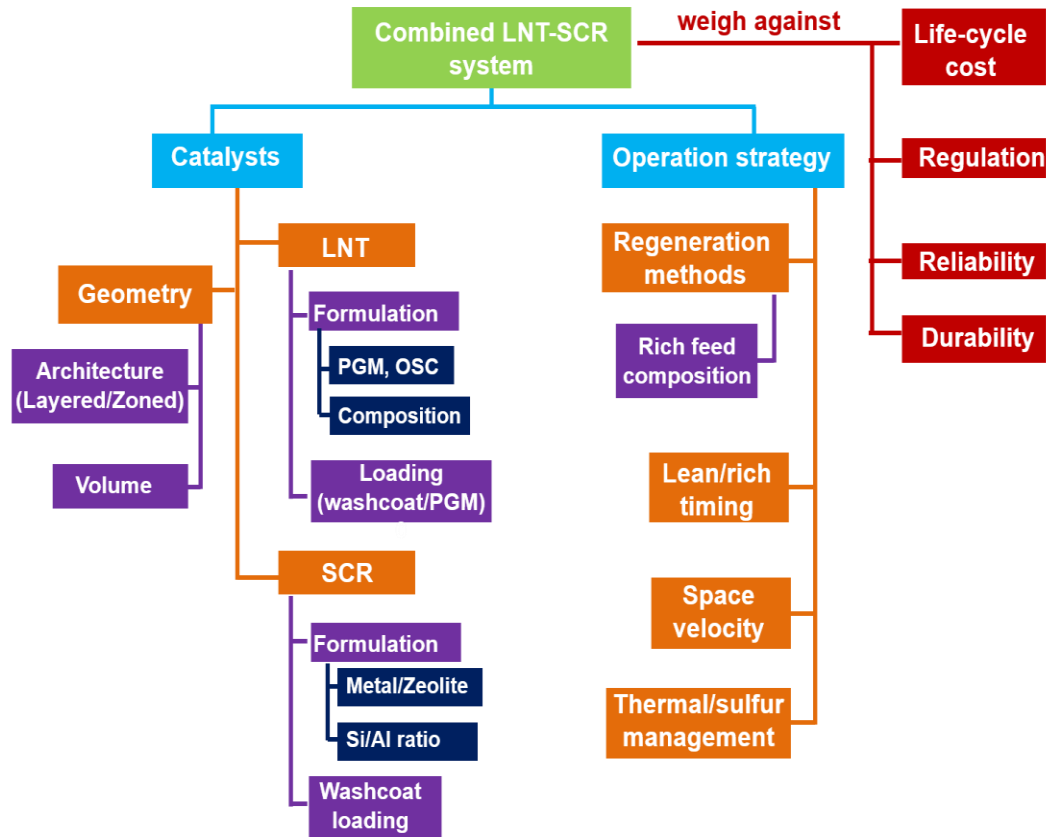


Fig. 1-4 Critical parameter flow down for combined LNT-SCR system

Chapter 2 investigates the performance of LNT-SCR dual-layer catalysts using H₂ and CO as reductants to simulate syngas when a fuel-reformer is applied for regeneration. H₂ and CO are major reducing agents for LNT regeneration especially involving the use of a fuel reformer. Spatial-temporal analyses of products distribution along the length of monolithic catalysts are conducted to elucidate the NO_x reduction pathways of dual-layer catalysts using H₂ and CO. Effects of catalyst design variables, including SCR and LNT

zoning, the ceria and PGM level in LNT, as well as SCR zeolite layer thickness, are accessed.

Chapter 3 furthers the performance study of dual-layer catalysts under simulated diesel exhaust conditions, especially when using in-cylinder enrichment method for regeneration. Addition NO_x reduction pathway associated with non-NH₃ intermediates is studied by both bench reactor and DTRIFTS (Diffuse reflectance infrared Fourier transform spectroscopy). The LNT-assisted HC-SCR pathway is proposed. The same optimization approach for dual-layer architecture as Chapter 2 is evaluated under this more realistic condition.

Chapter 4 explores the effects of different reducing agents (H₂, CO, C₃H₆) on Cu-SSZ-13 catalyzed NH₃-SCR reactions, given the periodic rich exposure of SCR component in the combined LNT + SCR system. This chapter elucidates the steady-state and transient effects of different reductants on NO₂ reduction, NH₃-SCR (selective catalytic reduction), NH₃ adsorption and oxidation, as well as N₂O production on a Cu-SSZ-13 monolithic catalyst.

Chapter 5 focuses on the application of Di-Air operation on combined LNT-SCR catalysts. Rapid propene pulsing effectively improves low-T NO_x conversion of dual-layer LNT-SCR catalysts over that of conventional NSR. We investigated the effects of cycle timing, exothermic heat, SCR catalyst types as well as loadings of ceria and PGM, on the deNO_x performance of combined catalysts. The fast cycling mechanism is discussed in comparison to the conventional NSR operation. The different dominant LNT-SCR synergy under fasting cycling was also investigated.

This dissertation finalizes with Chapter 6. This chapter includes conclusions from the preceding performance studies and makes several recommendations for further research.

Chapter 2 Lean NO_x reduction on LNT-SCR dual-layer catalysts by H₂ and CO

2.1 Introduction

In order to increase SCR contribution to the overall NO_x conversion of an LNT-SCR device, it is desirable to achieve high NH₃ yield from the LNT. Pihl et al. [28] reported that during the LNT regeneration, NH₃ was produced behind and at the reductant front due to the over-reduction of NO_x. The formed NH₃ that manages to slip past the reductant front rapidly reacts with the oxygen and NO_x species adsorbed on the catalyst surface downstream of the reductant front. Thus, no NH₃ is emitted from LNT outlet until the reductant front breaks through. Extensive studies regarding NH₃ selectivity over LNT have been carried out. Many factors affecting the NH₃ formation are identified, including the catalyst formulation [18, 29] (load, type, and dispersion of PGMs, NO_x adsorbent type and OSC load), reaction conditions [28] (temperature, space velocity, reductant species), and LNT regeneration strategy [9, 30] (regeneration method, frequency and duration, concentration of reductant species). To a certain extent, all these factors are correlated with each other, further complicating the predictability of NH₃ yield.

Reductant species have a direct impact on the NH₃ formation, with H₂ being the most effective reductant, especially at temperatures below 300 °C, followed by CO and then HC. The use of a reformer to promote H₂ and CO (syngas gas) production via steaming forming and partial oxidation of injected fuel, has been widely applied to combined LNT + SCR system [19]. Clayton et al. [29] reported that there are two primary competing routes for NO_x reduction to N₂ using H₂: a direct route via the reduction of stored NO_x by H₂ (H₂

+ NO_x → N₂) and a sequential route involving NH₃ as intermediate formed from the reaction of stored NO_x with H₂, followed by the reaction of the formed NH₃ with NO_x stored downstream to produce N₂ (H₂ + NO_x → NH₃; NH₃ + NO_x → N₂). This pathway was corroborated by Ribeiro et al. [31] who confirmed that the regeneration of a Pt/BaO/Al₂O₃ NO_x trap by H₂ occurs through the formation of NH₃ as an intermediate. When it comes to CO as reductants, the NO_x reduction pathway is more complicated. Peden et al. [32] used *in-situ* DRIFTS to observe stable isocyanates (NCO) formation over Pt–Ba/Al₂O₃ at low temperatures under dry conditions. The as-formed NCO species can readily react with NO_x to give N₂ and CO₂ (NCO + NO_x → N₂ + CO₂). Forzatti et al. [33] proposed that under dry conditions a consecutive reaction scheme with formation of NCO species from the reduction of nitrates by CO, followed by the reaction of these species with nitrates/nitrites or NO/O₂ to give N₂. However, different routes are active in the reduction of stored NO_x species by CO under wet conditions [34]. NCO can be readily hydrolyzed to NH₃ that reacts with NO_x to give N₂ similar to the indirect route for H₂ case. In addition, the water gas shift (WGS) reaction occurs between CO and H₂O to generate H₂. Therefore, it is concluded that in the presence of water H₂ formed through WGS and/or NH₃ formed by hydrolysis of NCO species could be involved in the reduction of stored NO_x by CO. Given the large content of H₂O present in the real exhaust, this pathway has more practical relevance. Studies on reaction pathways using H₂ and CO as reductants of the LNT under wet conditions, confirms that NH₃ is a key intermediate that acts as a chemical link between LNT and SCR in the combined system.

The goal of this chapter is to enhance our understanding of the performance of LNT-SCR dual-layer catalysts while using H₂ and CO as simulated reformer gas.

Specifically, we investigate the impact of ceria level in the LNT on the NH_3 formation, the H_2/CO ratio on the axial NH_3 and NO_x profiles, and of top-layer diffusion limitation on cycle-averaged NO_x conversion. Finally, we propose how to mitigate the negative impact of top-layer and to reduce required PGM load via zoning of SCR and LNT.

2.2 Experimental

2.2.1 Catalyst preparation

Monolithic LNT and SCR (Cu-SSZ-13) bricks were supplied by BASF Catalysts (Iselin, NJ). The LNT samples had a cell density of 400 cpsi and washcoat loading of 4.6 g/in^3 , corresponding to $60\sim 80 \text{ }\mu\text{m}$ in thickness. Cylindrical cores ($D=2.54 \text{ cm}$, $L=7.6 \text{ cm}$) were drilled out of the monolithic brick from which small monolithic pieces were prepared with a specific shape ($D=0.8 \text{ cm}$, $L=2.0 \text{ cm}$, 28 channels). The compositions of two LNT catalysts containing the same PGM, barium loading and varying ceria loadings are reported in Table 2-1. The metal-exchanged zeolites used in our study are described in Table. 2-2. The Cu-SSZ-13 catalyst has an 8-membered ring, chabazite (CHA) crystal structure, referred as CuC. The washcoat loading was estimated to be about 2.4 g/in^3 with ca. 2.5 wt% Cu loading. The in-house synthesized Cu-ZSM-5 catalyst powder with Si/Al ratio of 23, denoted as CuZ, was synthesized via a wet-ion exchange method. Its Cu content was about 2 wt% determined by inductive coupled plasma-atomic emission spectroscopy (ICP-AES) analysis.

Both commercial and in-house made LNT-SCR dual-layer monolithic catalysts were used. The in-house made dual-layer catalysts used CuZ as the SCR catalyst on top of a commercial LNT3 monolith. Briefly, an aqueous Cu-ZSM5 slurry was prepared and washcoated onto the LNT3 monolith by a dip-coating technique [15]. Washcoating was

repeated until the desired loading was obtained. The final step involved calcinations of the monolithic catalyst at 500 °C for 5 h to get a dual-layer catalyst. After washcoating, a uniform layer of CuZ (thickness of ca. 40 μm for 0.9 g/in³) was deposited on top of the LNT3 layer. We referred to this dual-layer catalyst as CuZ(Y)-L(X). The “Y” is the top-layer washcoat loading of the CuZ, while the “X” indicates the bottom-layer loading of LNT3 denoted by “L”. The other LNT3-SCR dual-layer monolithic catalysts, provided by BASF Catalysts (Iselin, NJ), comprised of LNT3 as the bottom layer and Cu-exchanged chabazite (CuC) as the top layer, and is referred to as CuC(Y)-L(X), using the same notation principle as above. A series of CuC-L dual-layer catalysts with varying LNT3 (2.3, 3.45, 4.6 g/in³) and SCR (0.8, 1.6 g/in³) loadings were prepared for our study. Catalyst notation and configurations used in our experiment are reported in Table 2-3.

Table 2-1 Composition of the monolith-supported LNT catalysts

	LNT1	LNT3
Formula	Pt/Rh/BaO/Al ₂ O ₃	Pt/Rh/BaO/CeO ₂ /Al ₂ O ₃
PGM(g/ft ³)	90	90
BaO(wt%)	14	14
CeO ₂ (wt%)	0	34



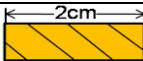

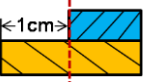
Table 2-2 Composition of metal-exchanged zeolites

	Metal(wt%)	Si/Al ratio
Cu-CHA	2.5 est.	20-30
Cu-ZSM-5	ca. 2	23
Na-ZSM-5	0.2 est.	280

In order to investigate the impact of the top-layer washcoat diffusion resistance, an inert Na-ZSM-5 (NaZ) with a high Si/Al ratio was deposited on the LNT3 monolith instead

of Cu-zeolite to form, NaZ(Y)-L(X), dual-layer catalysts. The synthesis of Na-ZSM-5 is similar to Cu-ZSM-5 except for the final ion-exchange with copper ion. The as-prepared Na-ZSM-5 powder was washcoated onto the blank cordierite or LNT3 monoliths for testing. The high Si/Al ratio minimized the adsorptive or catalytic properties of the zeolite catalyst.

Table 2-3 Configuration and notation of zoned & layered catalysts

Catalysts	Configurations	LNT3,g/in ³	CuC*,g/in ³
			
L(X)		X	—
CuC*(Y)/L(X)		X	Y
L(X ₁) + CuC*(Y)/L(X ₂)		X ₁ /X ₂	Y

* CuC may be also CuZ or NaZ in study.
CuC, CuZ, NaZ represent Cu-CHA, Cu-ZSM-5, Na-ZSM-5, respectively.
X₁ is the washcoat load of the front zone of the LNT, while X₂ the washcoat load of the rear LNT zone.

2.2.2 Reactor tests

The bench-scale reactor set-up comprised a gas supply, a reactor, an analytical and a data acquisition systems. Water was fed by a syringe pump (ISCO Model 500D) and vaporized in a heated line. The reactor gaseous effluents of NO, NO₂, N₂O, NH₃, CO, CO₂ and H₂O were measured by a FT-IR spectrometer (Thermo-Nicolet, Nexus 470). A quadrupole mass spectroscopy (QMS; Cirrus LM99, MKS Inc.) monitored the concentrations of H₂ and O₂ if needed. In the presence of CO, having the same *m/e* of 28 as N₂, the cycle-averaged formed N₂ was determined by closing an overall nitrogen balance.

A typical cyclic operation was conducted by use of 60s-lean and 5s-rich feed. The fixed lean/rich cycling times simplifies the study of the impact of different catalyst design variables. The carrier gas contained 2.5% H₂O and 2.0 % CO₂ in Ar. The lean feed contained 500 ppm NO and 5% O₂ in the carrier gas mixture. The rich feed contained 2.5% reductant but no NO and O₂ in the same carrier gas. Two types of reductant feeds were used: 2.5% H₂ for simulating ideal rich condition and 1.5% H₂/1.0% CO. The cycle-average H₂/NO feed ratio was 1.04 times the stoichiometric ratio needed for NH₃ formation by the reaction to promote the effective NH₃ production but minimize reductant slip: $16\text{H}_2 + 4\text{NO} + 3\text{O}_2 \leftrightarrow 4\text{NH}_3 + 10\text{H}_2\text{O}$. The real rich exhaust is a complex mixture of HC/CO/H₂ with a CO:H₂ ratio of about 3:1. A similar study but using simulated diesel exhaust is discussed in Chapter 3. Before measurements, each catalyst was exposed to 5% O₂ in Ar continuously at 500 °C for 30 min and then to the lean/rich cycling at 500 °C for another 30 min, using 2.5% H₂ as reductant.

The total flow rate was 1000 sccm. Unless specifically stated, the GHSV was 60,000 h⁻¹ (based on the total monolith volume, 2 cm long). In some cases, shorter pieces of LNT1 & LNT3 were prepared to construct spatial profiles. The feed temperature was increased from 150 to 400 °C in steps of 50 °C. The time needed to reach a cyclic state varies with temperature, reductant feed, flow rate, cycling frequency, the nature and loading of the catalysts. It usually takes 10 cycles for CuC/L and 5 cycles for CuZ/L at low temperatures and 3~4 cycles at high temperatures for both dual-layer catalysts. At each temperature the final ten cycles were averaged after a cyclic state was reached to determine the cycle-averaged NO_x conversion, product selectivity and NH₃ yield for a particular operating condition.

The fractional NO_x conversion was calculated by

$$X_{NO_x} = 1 - \frac{\int_0^{\tau_T} [F_{NO}(t) + F_{NO_2}(t)] dt}{\int_0^{\tau_l} F_{NO}^i(t) dt} \quad (2-1)$$

The fractional NH₃ yield was calculated by

$$Y_{NH_3} = \frac{\int_0^{\tau_T} F_{NH_3}(t) dt}{\int_0^{\tau_l} F_{NO}^i(t) dt} \quad (2-2)$$

Here τ_l and τ_T are the duration of lean phase feed and a lean-rich total cycle (s). $F_{NO}^i(t)$ is the NO feed rate and $F_{NO}(t)$, $F_{NO_2}(t)$, $F_{NH_3}(t)$, are the corresponding effluent molar flow rates (mole/s).

2.3 Desired ceria level in LNT for dual-layer application

Ceria, an effective oxygen storage component, is typically incorporated into LNT catalysts to improve their overall activity, durability and desulfation properties [35]. The impact of ceria on NH₃ formation during the regeneration of LNT catalysts is quite complex. It is widely accepted that NH₃ is produced only when the catalyst is under a net reducing condition. Oxygen stored on ceria consumes reductants to lower the reductant/NO_x ratio and delays the time at which the catalyst reaches a net reducing state. Both effects inhibit NH₃ formation, especially at high temperatures. On the other hand, ceria increases NH₃ formation at low temperature by providing additional NO_x storage sites and promoting the WGS reaction and NO_x reduction. The ceria level in the LNT layer must be tuned to match the targeted temperature window to achieve optimum performance of a dual-layer catalyst.

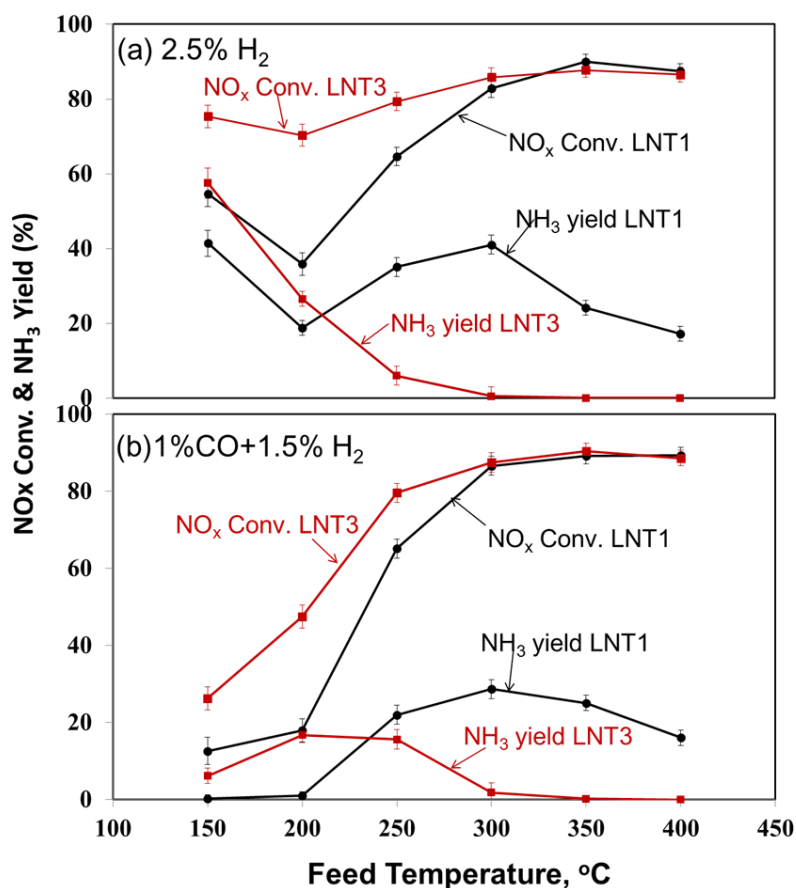


Fig. 2-1 Impact of Ceria on NO_x conversion and NH₃ yield from ceria-free LNT1 and ceria-rich LNT3 using (a) 2.5% H₂ and (b) 1% CO+1.5% H₂ as reductants.

Fig. 2-1 compares the NO_x conversion and NH₃ yield using ceria-free LNT1 and ceria-rich LNT3 catalysts. The addition of ceria to the LNT significantly increased NO_x conversion at low temperatures for either pure H₂ or CO/H₂ feed case mainly due to increased NO_x storage capacity combined with enhanced NO oxidation and mitigated CO poisoning (for CO/H₂ feed case) by ceria-supported Pt. The difference in NO_x conversion decreases as the temperature increases. The NO_x conversion for LNT1 and LNT3 are similar above 300 °C. Effluent NH₃ yield from LNT3 is higher than that from LNT1 at temperatures below 250 °C. The difference is more pronounced when introducing CO into the rich feed. Ceria-supported precious metal catalysts exhibit several orders of magnitude

higher rate of WGS reaction than precious metal alone [35], significantly promoting H_2 and NH_3 generation at low temperatures. On the other hand, at high temperatures almost no NH_3 breakthrough from LNT3 is observed due to intensified NH_3 oxidation by the oxygen in the ceria while still appreciable amounts of NH_3 are emitted by the LNT1.

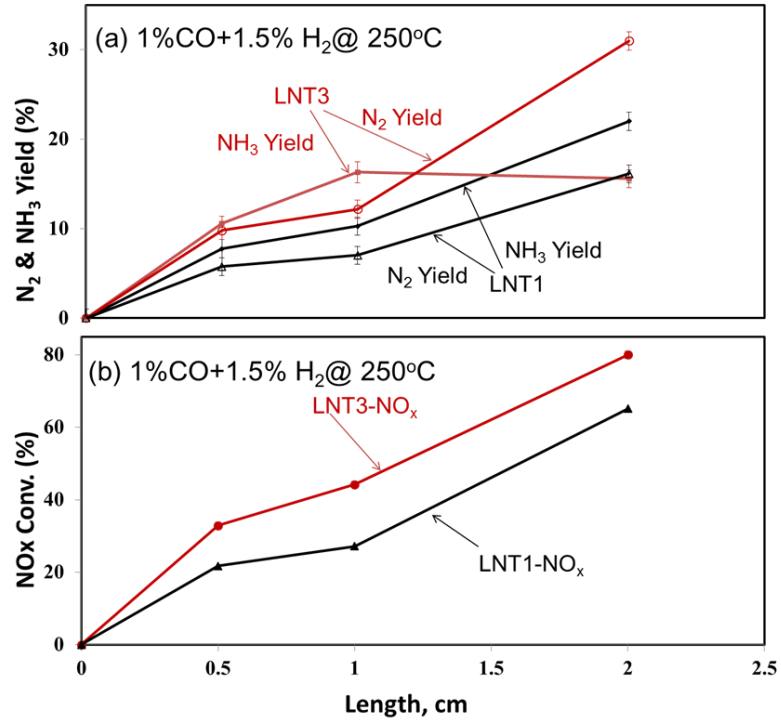


Fig. 2-2 Spatial NH_3 , N_2 yields and NO_x conversion along honeycomb catalysts of LNT1 and LNT3 with 1% CO+1.5% H_2 as reductant at 250 °C.

2.4 Spatial analysis of NH_3 yield and NO_x conversion

Fig. 2-2 compares the spatially-resolved NH_3 and N_2 yields and NO_x conversion along the LNT1 and LNT3 catalysts at 250 °C for a feed of 1% CO + 1.5% H_2 . The spatial data was achieved by cutting the monoliths into several different length. The LNT3 generates higher upstream NH_3 yield than LNT1 but slightly lower downstream NH_3 yield combined with significantly higher downstream N_2 yield. This trend is consistent with downstream NH_3 oxidation by stored NO_x and by oxygen in ceria. An added SCR top layer can minimize the

downstream NH_3 consumption by effectively capturing the released NH_3 for additional NO_x reduction. Thus, ceria-rich LNT3 is more effective than ceria-free LNT1 in NH_3 generation and NO_x adsorption for dual-layer application over the low temperature window (150-250 °C). For these reasons, LNT3 was chosen as the LNT layer in the dual-layer study.

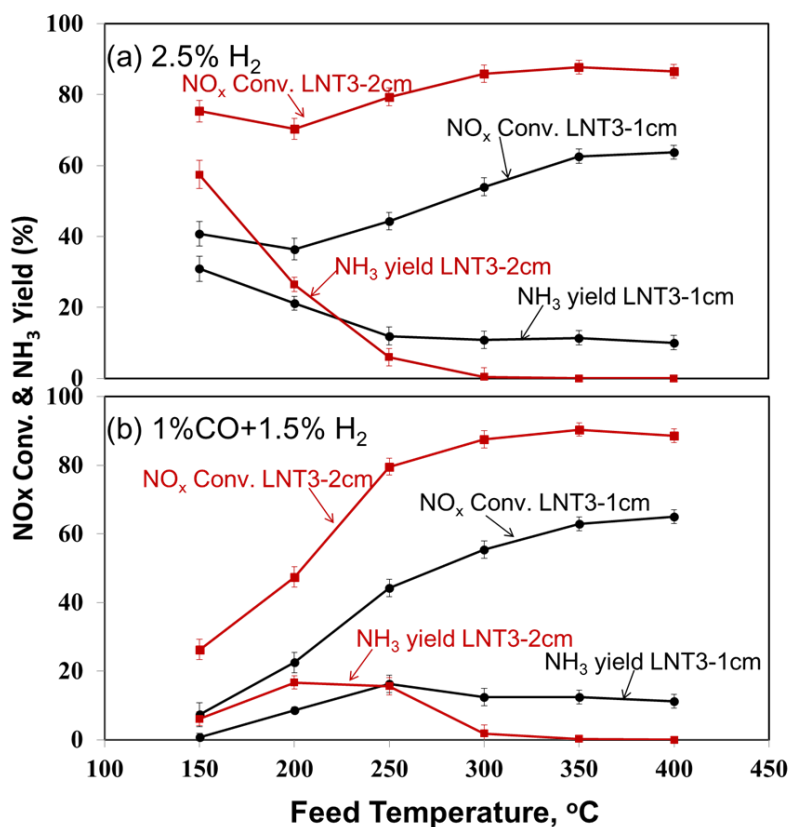


Fig. 2-3 NO_x conversion and NH_3 yield at the middle and the end of the LNT3 honeycomb catalyst using (a) 2.5% H_2 and (b) 1% CO +1.5% H_2 as reductants

Fig. 2-3 compares the NO_x conversion and NH_3 yield at the middle point (1 cm) and the end (2 cm) of the LNT3. Below 250 °C, both upstream and downstream LNT3 zones have comparable de NO_x contribution while the exit NH_3 yield is higher than that at the middle point. But at high temperatures (above 300 °C), the front half zone converts about 75% of the overall NO_x and almost the entire NH_3 yield under either pure H_2 or CO/H_2 feed. Almost no NH_3 is emitted at the downstream due to its oxidation by

downstream stored NO_x and oxygen. In other words, the upstream LNT3 is the major NO_x reducer and NH_3 generator at high temperatures, which primarily determines the high-temperature performance.

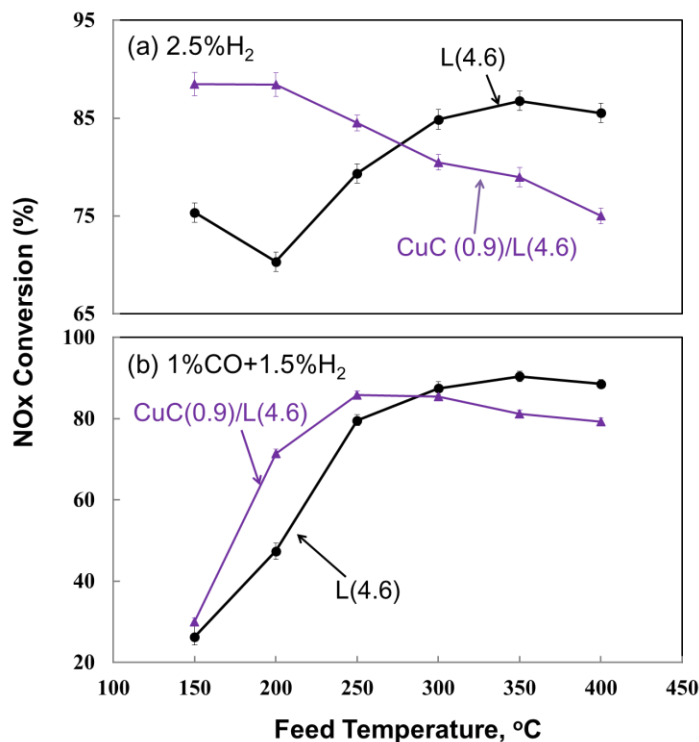


Fig. 2-4 Comparison of NO_x conversion using (a) 2.5% H_2 and (b) 1% $\text{CO}+1.5\% \text{H}_2$ as reductants over L(4.6) and CuC(0.8)/L(4.6) catalysts.

Fig. 2-4 compares the performance of CuC(0.8)/L(4.6) and LNT3 only catalysts. The CuC layer leads to significantly higher low-temperature NO_x conversion than LNT3 only due to effective NH_3 production and active NH_3 -SCR reaction. Almost no NH_3 slip is detected from CuC/L over the entire temperature range for both rich feeds. Using pure H_2 as reductant, the NO_x conversion from the CuC/L decreases monotonically as the temperature increases. This can be attributed to decreased NH_3 yield and intensified adverse effects by the SCR layer as the temperature increases. As shown in Fig. 2-1a, the NH_3 yield drops dramatically from 57% at 150 °C to 6% at 250 °C. For CO/H_2 feed, NO_x conversion

from CuC/L reaches a maximum at 250 °C and then decreases as the temperature rises. The increasing conversion to the left of the maxima is due to the decreased CO inhibition and increased NH₃-SCR activity, while the decreasing conversion to the right of the maxima is due to intensified diffusion limitation and lower NH₃ yield above 250 °C.

For both rich feed cases, CuC/L has the lowest NO_x conversion above 300 °C, probably due to higher washcoat diffusion resistance caused by the small-pore CHA structure. At high temperatures the effluent lean-phase NO_x slips from dual-layer catalysts are higher than that from LNT3-only catalyst, while lower NO_x spikes are observed from dual-layer catalysts (data not shown). The higher lean-phase NO_x slip from dual-layer catalysts at high temperature indicate that at high temperatures, SCR top-layer simply act as diffusional barrier that inhibits effective NO_x trapping. It is concluded that dual-layer architecture benefit the low-temperature NO_x conversion but compromise the high-temperature performance.

2.5 Impact of top-layer diffusional resistance

Diffusion resistance caused by the top SCR layer is arguably the most serious detriment for dual-layer application under high temperature and high flow rate. The thicker the SCR layer, the more severe is the washcoat diffusion limitation. However, a minimal thickness of SCR layer is required to guarantee the effective adsorption of NH₃. Thus, there is a trade-off between high NH₃ storage capacity and low diffusion limitation. In order to determine the optimal SCR loading for dual-layer application, it is necessary to know the effect of the diffusional resistance of the SCR top layer on the overall performance. Unfortunately, the impacts of NH₃-SCR and undesired NH₃ oxidation on overall NO_x conversion to NO_x complicate the assessment of top-layer diffusion limitation. One

approach is to replace the active Cu-CHA layer by a top layer containing inert zeolite crystallites. This minimizes the interference from NH_3 -SCR and NH_3 oxidation and focuses only on the diffusional resistance effect. We accomplished this by a Na-ZSM-5 layer with Si/Al ratio of up to 280 containing few Brønsted acid sites to minimize NH_3 adsorption and SCR activity.

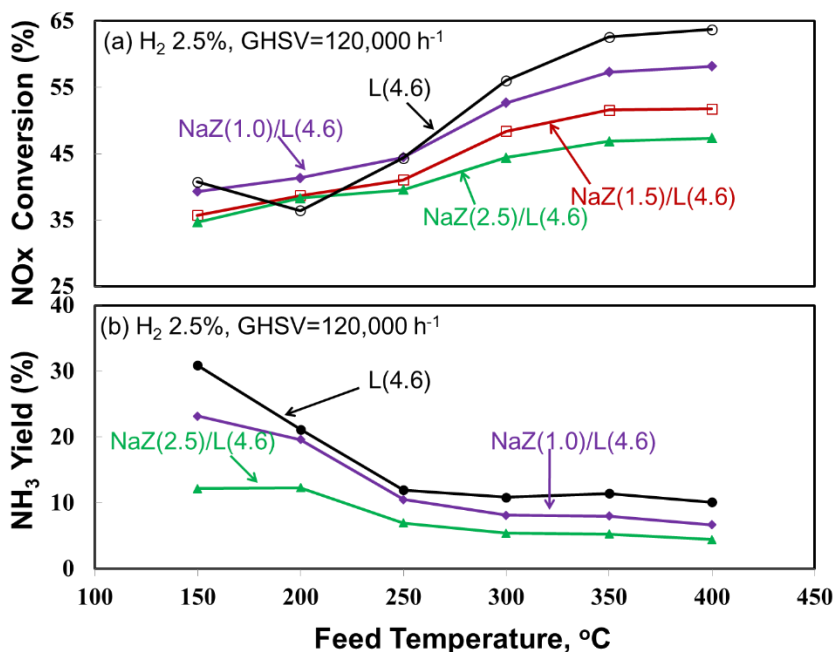


Fig. 2-5 NO_x conversion (a) and NH_3 yield (b) from dual-layer catalysts by 2.5% H_2 and $\text{GHSV}=120,000 \text{ h}^{-1}$ at fixed LNT3 loading but different NaZ loadings.

A series of NaZ/L with fixed LNT loading and different NaZ loading was prepared and tested with different reductant mixtures at a GHSV of $120,000 \text{ h}^{-1}$. Fig. 2-5a shows that increasing the upper layer loading from 1.0 to 1.5 and 2.5 g/in^3 lowers the NO_x conversion over the entire temperature range under pure H_2 feed. A similar trend is also observed under CO/H_2 feed, which is not shown here. The impact of additional diffusion resistance starts at 150°C for pure H_2 feed and 200°C for CO/H_2 feed when the top layer loading is 1.0 g/in^3 .

or higher. Compared to the LNT3-only catalyst, the additional diffusion resistance starts to decrease the overall NO_x conversions of the three dual-layer catalysts at 250 °C. Fig. 2-5b compares the NH_3 yield from LNT3, NaZ(1.0)/L(4.6), NaZ(2.5)/L(4.6). NH_3 slip from two NaZ/L catalysts is always present over the entire temperature range, even with up to 2.5 g/in³ top-layer loading at high temperatures. Increasing NaZ loading from 1.0 to 2.5 g/in³ decreases the NH_3 yield over the entire temperature, likely due to increased diffusion resistance limiting the transport of NO_x and reductants to the underlying LNT layer for NO_x reduction and NH_3 generation. The performance loss due to top-layer diffusion resistance can be quantitatively determined. For example, at 350 °C for either pure H_2 or CO/H_2 feed, the loss of overall NO_x conversion due to diffusion resistance is approximately 5%, 10% and 15% for a top layer loading of 1.0, 1.5 and 2.5 g/in³, respectively. Obviously, top-layer diffusion limitation needs to be minimized to get an optimum performance of the LNT–SCR dual-layer catalyst

2.6 Effects of zonal distribution of SCR and LNT washcoat

SCR zoning is expected to minimize the adverse high-temperature effects of SCR top layer while maintaining the improved low-temperature performance to strike a better balance between low- and high- temperature performance. Compared to a typical dual-layer architecture, consider a catalyst in which the first half has a LNT3 layer without SCR deposited on top, and SCR is deposited only on the second half of the LNT3 layer. This catalyst was prepared by linking a 1 cm L(X₁) single-layer catalyst with a 1 cm CuC(Y)/L(X₂) dual-layer catalyst to get the dual-zone dual-layer catalyst, named L(X₁)+CuC(Y)/L(X₂) in

Table 3. The “X₁” and “X₂” represents the LNT3 loading in the first and second half bottom layer, while “Y” denotes the downstream SCR top layer loading.

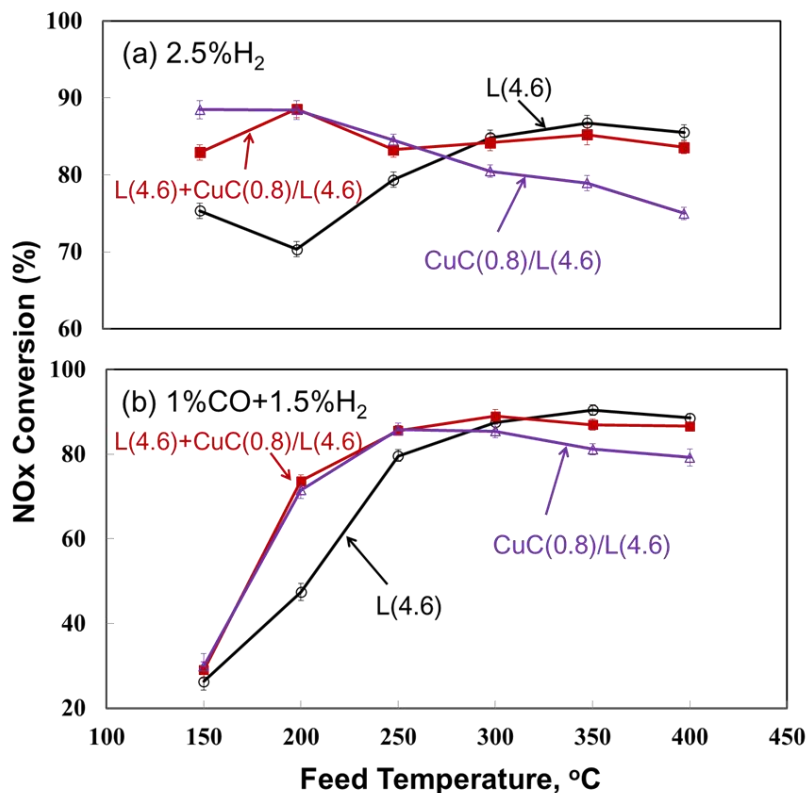


Fig. 2-6 NO_x conversion from LNT3, CuC(0.8)/L(4.6) and L(4.6)+CuC(0.8)/L(4.6) catalysts using as reductants (a) 2.5% H₂ and (b) 1% CO+1.5% H₂.

Fig. 2-6 compares the performance of L(4.6)+CuC(0.8)/L(4.6), CuC(0.8)/L(4.6) and LNT3 only catalysts. The three catalysts have the same total PGM loading but the SCR loading of L+CuC/L is only half that of CuC/L in order to reduce diffusion resistance over the downstream of the LNT. The dual-layer catalyst with downstream SCR loading has similar low-temperature NO_x conversion as the CuC/L, especially under CO/H₂ feed, and better high-temperature deNO_x performance. Fig. 2-7 compares NO_x, NH₃ and N₂O effluent concentrations from the LNT3 and zoned dual-layer catalyst. It reveals that the effluent lean-phase NO_x slip from the zoned dual-layer catalyst is clearly lower than that from the

LNT3, while only a slight decrease is observed in the rich-phase NO_x puff. The added CuC layer with high NH_3 storage capacity captures almost all the NH_3 . Thus, the incremental NO_x reduction by SCR layer mainly comes from the lean mode, where the NH_3 stored in the SCR layer can react with NO_x in the lean phase to reduce the NO_x slip. These results confirm that SCR zoning of dual-layer configuration can improve the low-temperature performance without compromising high-temperature performance. The CuC/L dual-layer catalyst with downstream SCR loading is the best dual-layer catalyst design of those examined.

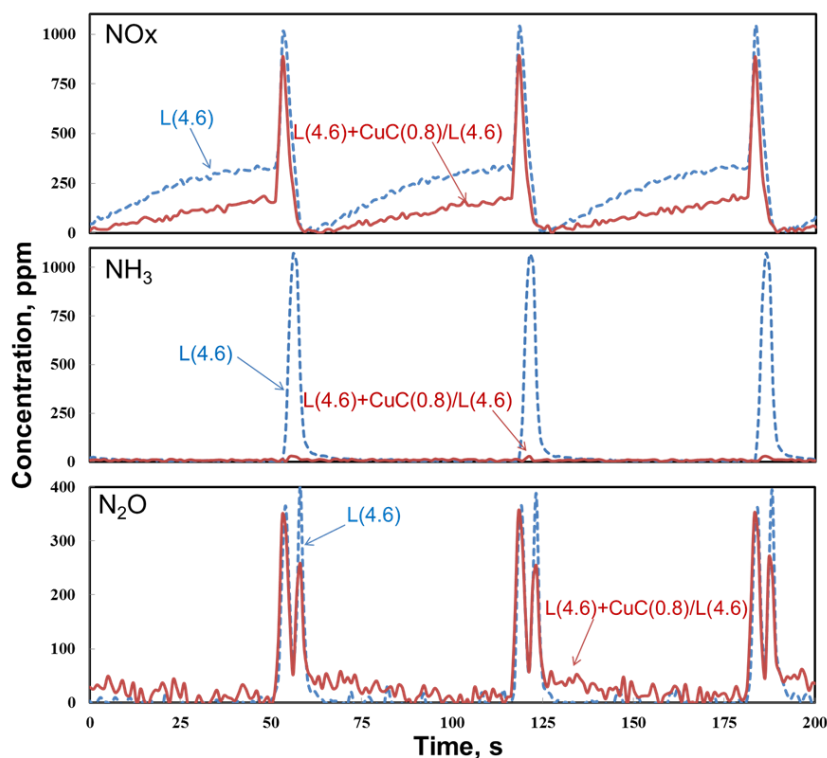


Fig. 2-7 Comparison of effluent concentrations of NO_x , NH_3 , N_2O from L(4.6) and L(4.6)+CuC(0.8)/L(4.6) during cycling at 200 °C using 1% CO + 1.5% H_2 as reductants

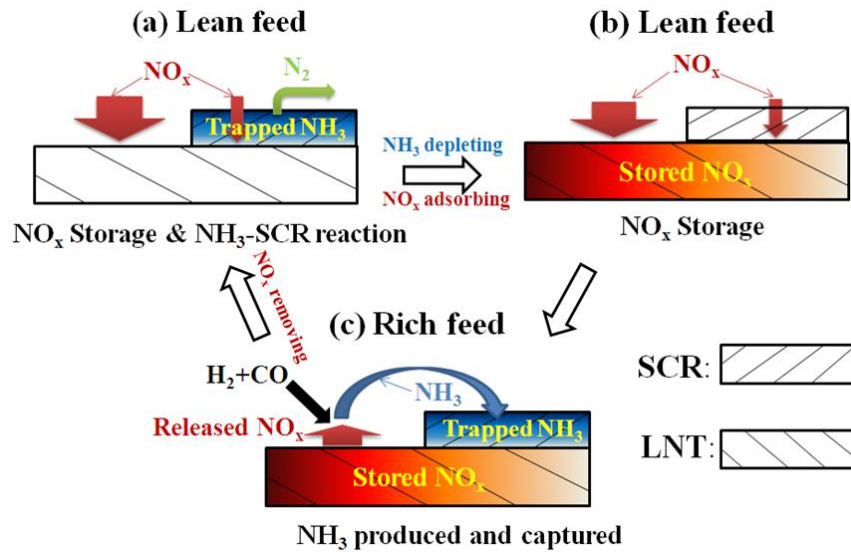


Fig. 2-8 Mechanism of NO_x decomposition by zoned dual-layer LNT-SCR catalyst at temperatures above 300°C .

Fig. 2-8 schematically illustrates the advantages of applying SCR zoning over conventional dual-layer architecture at high temperatures exceeding 300°C . The downstream SCR layer enables the effective capture of NH_3 either from the upstream or underlying LNT catalyst for additional NO_x reduction, which improves the low-temperature performance. As mentioned above with respect to Fig. 2-3, the upstream LNT3 is the major NO_x reducer and NH_3 generator at high temperature, which primarily determines the high-temperature performance. Hence, the removal of upstream SCR layer minimizes the adverse impact of additional diffusion resistance on the overall NO_x conversion. Moreover, in conventional dual-layer catalysts most formed NH_3 is adsorbed by the SCR top layer at sites close to the LNT. The stored NH_3 proximal to LNT/SCR interface is likely to diffuse back to the adjacent LNT layer and be oxidized to NO_x at high temperatures during the lean phase. The zoned dual-layer catalyst can mitigate such undesired NH_3 oxidation by removing upstream SCR. The NH_3 released from the upstream

LNT is then adsorbed by the surface of the downstream SCR layer and then reacts with NO_x/O_2 with high selectivity towards N_2 .

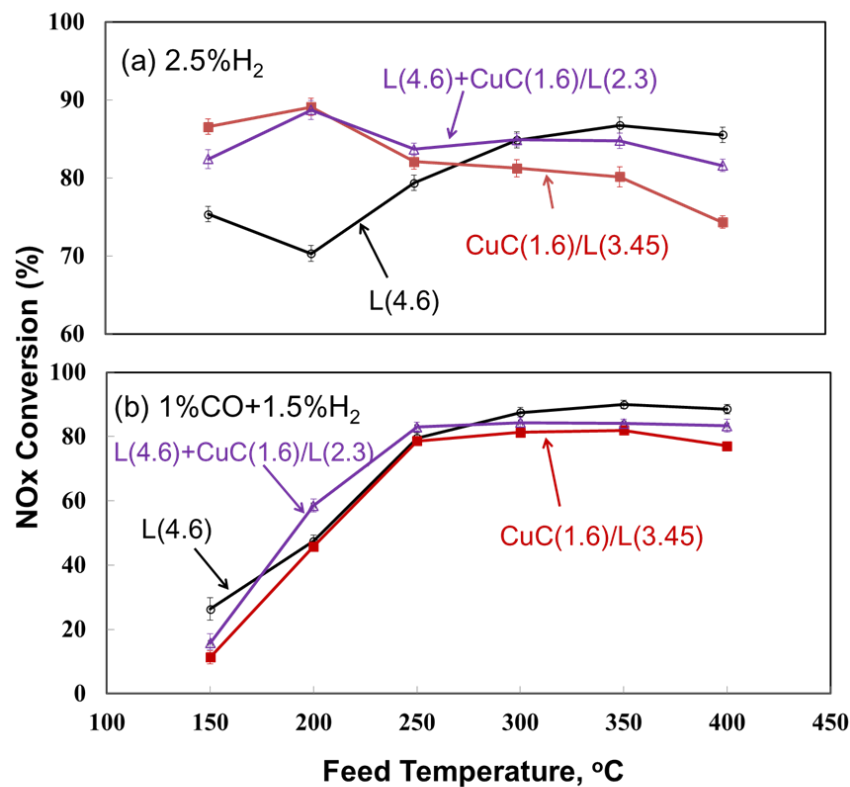


Fig. 2-9 NO_x conversion by dual-layer catalysts with different zoned LNT and SCR loadings but the same total LNT loading using a) 2.5% H₂ and b) 1% CO+1.5% H₂.

Fig. 2-9 compares the NO_x conversion from LNT3 only, CuC(1.6)/L(3.45) and L(4.6)+CuC(1.6)/L(2.3). Both dual-layer catalysts have the same total LNT3 loading, which is lowered by 25% from that of LNT3 only catalyst. The SCR loading on the CuC/L is twice that of the L+CuC/L catalyst. Compared to the CuC/L catalyst, the L+CuC/L catalyst exhibits higher high-temperature NO_x conversion for both rich feeds, and also a better low-temperature performance for the CO/H₂ feed. The higher low-temperature conversion is due to LNT & SCR zoning. Higher upstream LNT loading, which is free of

any top-layer diffusion resistance, makes the front zone an effective NO_x reducer and NH₃ generator over the entire temperature range. Compared with LNT3 only catalyst, L+CuC/L with less 25% LNT loading shows similar performance at high temperatures, but better performance at low temperatures under both feeds except for 150 °C with CO. Thus, SCR & LNT zoning in dual-layer catalyst improves the deNO_x performance relative to normal dual-layer catalyst over the entire temperature range. This enables better compensation for activity loss by decreased LNT loading.

Fig. 2-10 compares the NO_x conversion of three zoned dual-layer catalysts with different downstream LNT loadings. Compared to L(4.6), the LNT3 loading is reduced by 12.5%, 25% and 37.5% for L(4.6)+CuC(1.6)/L(3.45), L(4.6)+CuC(1.6)/L(2.3) and L(4.6)+CuC(1.6)/L(1.15), respectively. Higher downstream LNT loading increases low- and high-temperature NO_x conversion. Zoned dual-layer catalyst with 37.5% lower LNT loading still has a comparable deNO_x efficiency to L(4.6), ~ 5% lower in average, over the entire temperature range for both rich feeds. Note that the commercial LNT3 catalyst used in our study is not optimized for dual-layer application. It is desirable to reduce the expensive PGM loading at constant barium and ceria loading to maintain the NO_x storage capacity, rather than decreasing total LNT loading.

The lean/rich duration in our study is fixed to 60s/5s. Optimization of lean/rich cycling timing and rich regeneration control is expected to yield higher deNO_x performance. Thus, it would be helpful to explore the minimum feasible PGM loading based on the optimized LNT catalyst and operating conditions. According to a cost assessment of Tier 2 Bin-5 compliant deNO_x aftertreatment systems by Posada et al. [36], the Cu-zeolite cost per liter of SCR brick is about \$2.40-\$6, compared to the PGM cost of ca. \$154 per liter of

LNT brick based on precious metal price at that time. In other words, the LNT catalyst cost per liter is about 25-60 times higher than that of Cu-zeolite. This preliminary study demonstrates that the zoned LNT-SCR dual-layer catalyst has the potential to reduce PGM loading up to 37.5% under our laboratory test conditions used in this study. This will enable the LNT-based system to be more cost competitive with the urea-SCR system for application in passenger cars.

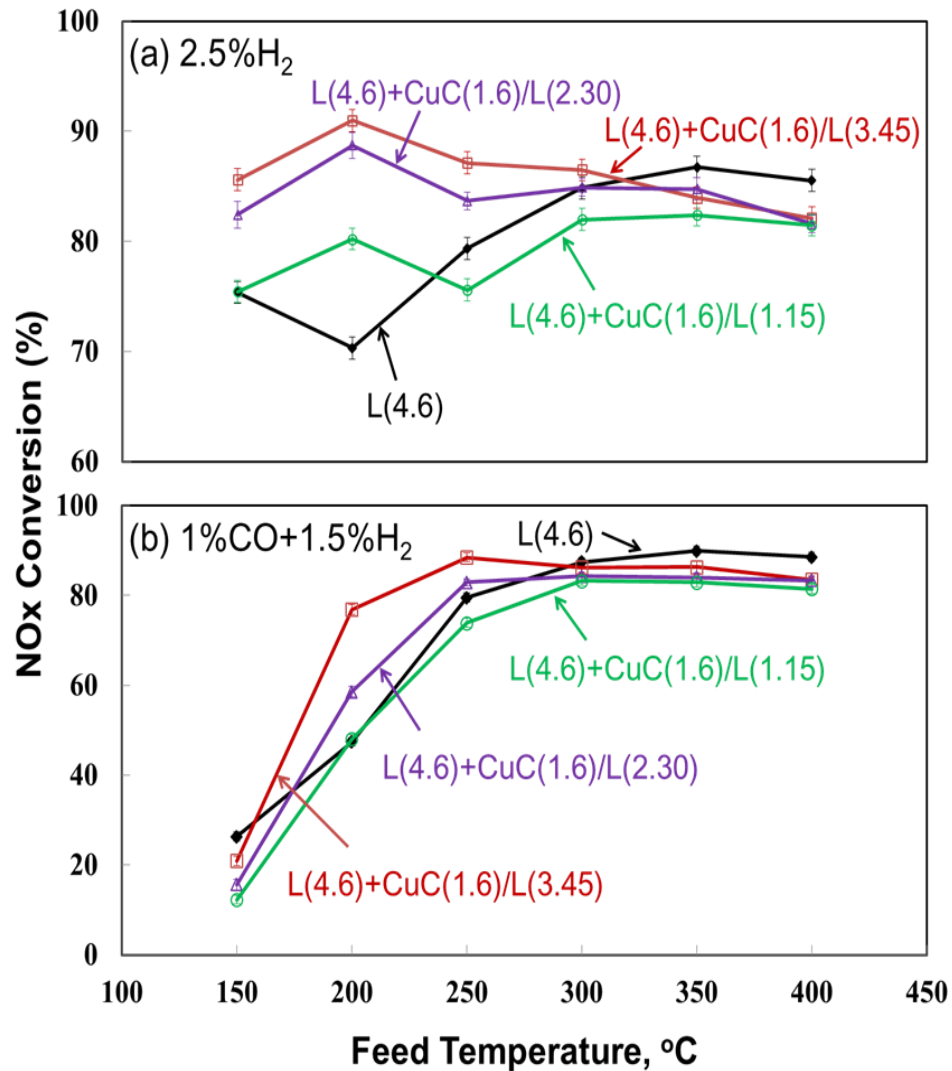


Fig. 2-10 NO_x conversion by dual-zone dual-layer catalysts with different downstream LNT loadings using a) 2.5% H₂ and b) 1% CO+1.5% H₂.

2.7 Conclusions

The main findings of this chapter are:

- High ceria level (34 wt.%) in LNT improves the low-temperature performance of the dual-layer catalysts, due to enhanced NO_x adsorption and NH_3 generation at low temperatures (150-250 °C).
- Depositing an inert Na-ZSM-5 with a high Si/Al ratio of 280 instead of the active Cu-zeolite layer allows decoupling the impact of the NH_3 -SCR reaction and NH_3 oxidation from that of the additional diffusion resistance on NO_x conversion. A zeolite top-layer of 1.0 g/in³ causes diffusion limitation at temperatures exceeding 150 °C for pure H_2 feed and 250 °C for CO/H_2 feed at a GHSV of 120,000 h⁻¹.
- Zoned dual-layer catalyst with downstream SCR loading can maintain the enhanced de NO_x efficiency at low temperature, while minimizing the high-temperature performance loss caused by the additional diffusion resistance and undesired NH_3 oxidation.
- Zoning of both SCR & LNT in dual-layer catalyst increases the de NO_x performance over that of a conventional dual-layer catalyst over the entire temperature range. This enables a large reduction of the PGM loading.
- Zoning of both SCR & LNT in dual-layer catalyst increases the de NO_x performance over that of a conventional dual-layer catalyst over the entire temperature range. This enables a large reduction of the PGM loading.

Finally, the operating conditions adopted by this study aims to simulate the regeneration strategy with the use of a fuel-reform to favor NH_3 generation and NH_3 is the sole reductant for the SCR top-layer as the rich reductants was a either pure H_2 or CO/H_2

mixture. However, in a real exhaust, the CO/H₂ ratio would be closer to 3:1, which would probably further increase the role of CO. The presence of HC might affect some of the conclusions, which is discussed in next chapter.

Chapter 3 NO_x reduction on LNT-SCR dual-layer catalysts under simulated diesel exhaust conditions

3.1 Introduction

Three general strategies for reductant delivery to the LNT have been adopted in practice [9]. The first strategy is the direct injection of fuel into the exhaust feed to the LNT catalyst during the regeneration. A very broad range of complex hydrocarbon products attributed to the reforming, cracking and partial oxidation of the fuel over the catalyst was reported by Partridge et al. [37]. The second strategy is based on the introduction of reformed gas that is generated by either a continuous or periodic processing of injected fuel over an upstream reformer or partial oxidation catalyst. The so-formed reformer gas consists of CO, H₂ and light HC species that are more efficient reductants for the release and conversion of stored NO_x, in comparison to diesel fuel directly used on the catalyst. In the third strategy, the engine control is adapted via post-injection, throttling, etc., so that the lean-burn engine periodically operates in a mode where the exhaust gas becomes rich. The intermittent pulses of rich exhausts either directly contain the reductant or are processed by the NSR catalyst or by an upstream catalyst to form the reductants. Therefore, different regeneration strategies result in different types and composition of reductants.

Although H₂ and CO are preferable reductants and NH₃-formation agents, in a real exhaust hydrocarbons always exist. This complicates the NO_x reduction pathway on the LNT. When using HCs as reductants, two general mechanisms have been reported [38]. One mechanism is based on the NO decomposition on reduced Pt sites enabled by HC that acts as oxygen scavenger. The other mechanism is based on the formation of surface HC

intermediates ($C_xH_yO_zN_t$, $C_xH_yO_z$), resulting from the reaction of NO_x/O_2 with HC. These intermediates may either directly decompose to N_2 or evolve to other intermediates that react with NO_x to give N_2 . Since different hydrocarbons species could go through different mechanism, it is difficult to distinguish between the two mechanisms, given the extreme complexity of HC species derived from the fuel. Burch et al. [38] reported that even the subtle changes in the operating conditions could affect the NO_x reduction mechanism. For example, the same HC species may follow different pathways under different temperatures.

No matter through which mechanism NO_x is reduced by the HC, the generation of large amount of HC intermediates from LNT imply that a HC-SCR pathway potentially is available in the SCR component of the combined catalyst. The focus of this chapter is to verify the existence of non- NH_3 pathway for the combined system using simulated rich exhaust gas of a $C_3H_6/CO/H_2$ mixture. The different roles of NH_3 and non- NH_3 pathways in the incremental NO_x conversion are elucidated. The versatility of zoning strategy to improve dual-layer architecture is demonstrated under simulated diesel exhaust conditions.

3.2 Experimental

Monolithic LNT (Pt/Rh/BaO/CeO₂/Al₂O₃) and SCR (Cu-SSZ-13) bricks were supplied by BASF Catalysts (Iselin, NJ). The LNT sample had a cell density of 400 cpsi and a washcoat loading of 4.6 g/in³, corresponding to 60~80 μm in thickness. It contained a PGM loading of 90 g/ft³, 14 wt% BaO and 34 wt% CeO₂ in the washcoat. The Cu-SSZ-13 catalyst, referred to as CuC, has an 8-membered ring, small-pore chabazite (CHA) crystal structure. Its cell density was 400 cpsi and the washcoat loading was about 2.4 g/in³. Cylindrical cores (D=2.54 cm, L=7.6 cm) were drilled out of a monolithic brick. Then small monolithic pieces were prepared with a specific shape (D=0.8 cm, L=2.0 cm, 28 channels).

LNT-SCR dual-layer monolithic catalysts, provided by BASF Catalysts (Iselin, NJ), comprised a Cu-SSZ-13 layer deposited on top of the LNT catalyst. We refer to these dual-layer catalysts as CuC(Y)/L(X), in which the “Y” is the top-layer washcoat loading of the CuC while the “X” indicates the bottom-layer loading of the LNT denoted by “L”. The compositions of the LNT and SCR in the dual-layer catalysts are the same as above. A series of CuC-L dual-layer catalysts with varying LNT (1.15, 2.3, 3.45, 4.6 g/in³) and SCR (0.8, 1.6 g/in³) loadings were prepared for our study. Catalyst notation and configurations used are described in Table 2-3.

Table 3-1 Gas conditions for 60/5 cycling test.

Gas	Lean	Rich #1	Rich #2	Rich #3	Rich#4
NO	300 ppm	300 ppm	300 ppm	300 ppm	300 ppm
CO	—	2.4%	2.4%	—	—
H ₂	—	0.8%	0.8%	—	—
C ₃ H ₆	—	1000 ppm	—	1000 ppm	3550 ppm
O ₂	5%	1%	—	—	—
CO ₂	2%	2%	2%	2%	2%
H ₂ O	2.5%	2.5%	2.5%	2.5%	2.5%

The reactor testing system is the same as described in Chapter 2. Lean-rich cycling experiments were conducted over either LNT-only or SCR-only or dual-layer catalysts. Table 3-1 describes the 60s-lean and 5s-rich cycling conditions. These gas compositions are not entirely representative of diesel exhaust. A 3:1 ratio of CO:H₂ was used. We utilized propylene (C₃H₆) as our HC - typical of light cracked hydrocarbons in a diesel exhaust but not representative of larger unburned fuel species. A fixed operating condition makes it easy to focus on the impact of different catalyst design variables. The same lean phase

conditions were used in all the experiments. Unless otherwise mentioned, the standard set of gas compositions with a lean gas feed and a rich gas feed #1 described in Table 1 was used for the majority of the tests to simulate real diesel exhaust gas. A 3:1 ratio of CO:H₂ was used and propylene (C₃H₆) was chosen as the model HC reductant typical of light cracked hydrocarbons in a diesel exhaust. Prior to the measurements, each catalyst was degreened by exposing it to 5% O₂ in Ar at 500 °C for 30 min and then to lean/rich cycling conditions with rich feed #1 at 500 °C for another 90 min.

The total flow rate was 1000 sccm. Unless specifically stated, the GHSV was 60,000 h⁻¹ (based on monolith volume, 2 cm long). In some cases, a series of shorter LNT pieces were used to construct spatial concentration profiles. The feed temperature was increased from 150 to 250 °C in steps of 25 °C, and then up to 400 °C in steps of 50 °C. It took approximately 5~10 min to reach a periodic state. At each temperature the final ten cycles were averaged after a cyclic state was reached to determine the cycle-averaged NO_x conversion and NH₃ yield for a particular operating condition.

3.3 NO_x reduction by a C₃H₆/CO/H₂ mixture.

Fig. 3-1 compares the cycle-averaged NO_x conversion under simulated diesel exhaust conditions (rich feed #1 in Table 3-1) for a high-loaded LNT catalyst, L(4.6), and one with a top SCR layer, CuC(0.8)/L(4.6). The added SCR layer improves the NO_x conversion in the low- and mid- temperature range (below 300 °C). Above 300 °C, the NO_x conversion from the dual-layer catalyst is slightly lower than that of the LNT-only catalyst. Hence, addition of a SCR top layer is beneficial for temperatures below 300 °C but somewhat detrimental above 300 °C. Fig. 3-2 shows the transient concentration profiles of NO_x (NO+NO₂), N₂O, NH₃, and C₃H₆ after cyclic behavior was achieved at 200 °C for the

same LNT catalysts with and without a SCR top layer. The effluent lean-phase NO_x slip from the dual-layer catalyst is slightly lower than that from the LNT and a slight decrease is also observed in the rich-phase NO_x puff. This suggests that the reductants stored in the SCR layer can react with NO_x in the lean phase to reduce its slip. Note that only a small amount of NH_3 is emitted from the LNT at 200 °C and slightly less C_3H_6 slip from the dual-layer catalyst is observed, apparently due to the HC adsorption by the SCR layer.

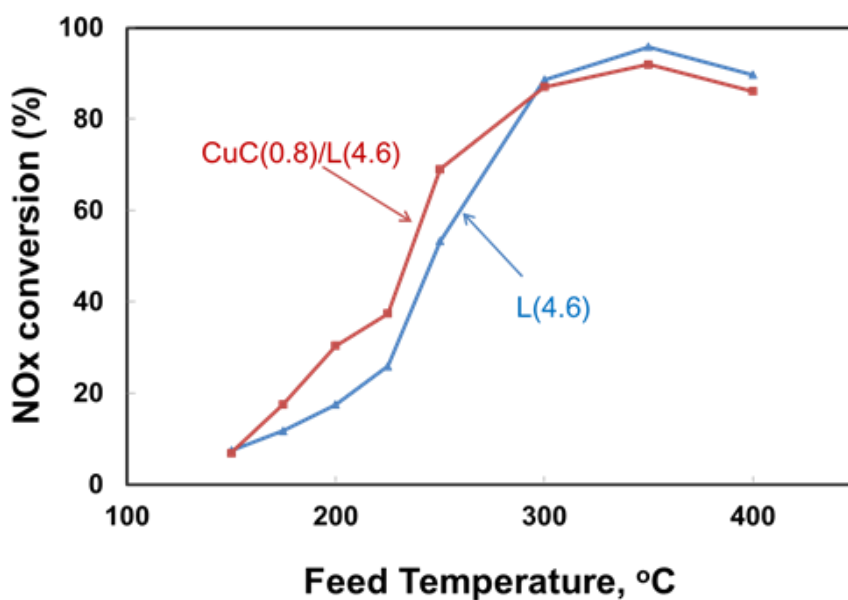


Fig. 3-1 Comparison of cycle-averaged NO_x conversion for L(4.6) and CuC(0.8)/L(4.6) catalysts using 2.4% CO + 0.8% H_2 + 1000 ppm C_3H_6 as reductants (Rich #1).

3.4 LNT-assisted HC-SCR pathway

NH_3 is generally considered as the primary reductant of NO_x reduction in the SCR component of the combined catalyst. The contribution of the SCR towards overall NO_x

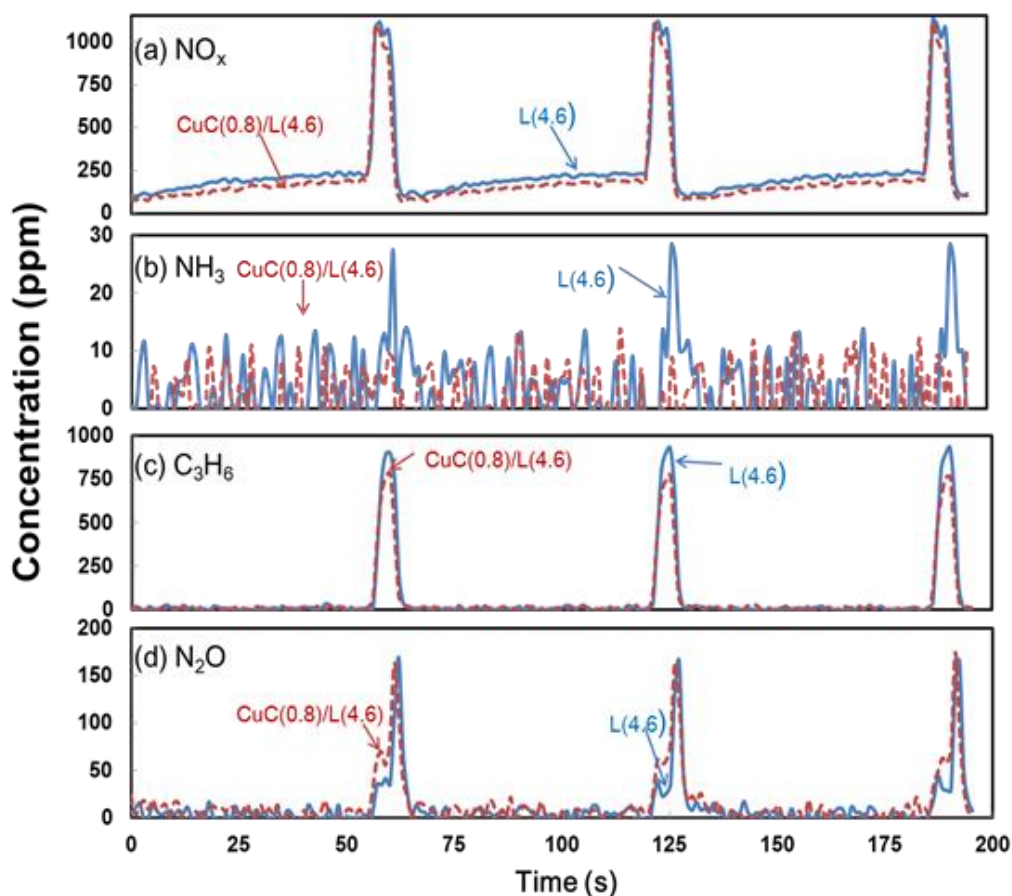


Fig. 3-2 Comparison of effluent concentrations of a) NO_x , b) NH_3 , c) C_3H_6 and d) N_2O from L(4.6) and CuC(0.8)/L(4.6) during cycling at 200 °C using 2.4% CO + 0.8% H_2 + 1000 ppm C_3H_6 as reductants (Rich #1).

conversion strongly depends on the in-situ NH_3 supply from the LNT. Fig. 3-3a describes the spatially-resolved NH_3 yield along the LNT monolith under the same feed gas conditions. An increasing amount of NH_3 is produced in the upstream LNT at temperatures higher than 225 °C and reaches a maximum at 300 °C. Almost no NH_3 is formed along the LNT at 200 °C or below. However, since there is an obvious increase in the NO_x conversion in this temperature range (150-200 °C) due to the addition of the SCR layer, this means an NH_3 reduction pathway cannot alone be responsible. The data indicates the existence of non- NH_3 reductants that participate in the NO_x reduction in the SCR layer. The spatial

distribution shows that NH_3 yield at the upstream (0.5 cm) are highest and then decreases with distance. For example, at 300 °C, the NH_3 yield decreased from 14.5% at the 0.5 cm distance from the inlet, to ~11% at a 1 cm distance and to ~5% at the 2 cm distance (i.e., the exit of the LNT). Fig. 3-3b compares the NO_x conversion at the points of 0.5, 1.0 and 2.0 cm along the LNT. Above 225 °C, the first half of the catalyst contributes the majority (~75%) of the overall NO_x conversion. In other words, the upstream LNT is the major NO_x reducer and NH_3 generator at temperature exceeding 225 °C, which primarily determines the high-temperature performance.

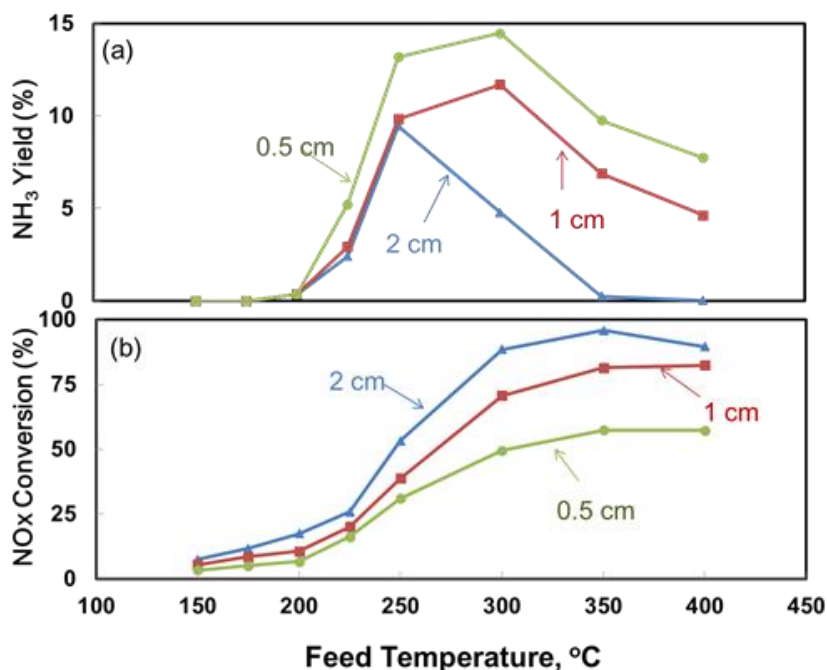


Fig. 3-3 Cycle-averaged (a) NH_3 yield and (b) NO_x conversion at the 0.5, 1, 2 cm length of LNT monolithic catalyst using 2.4% CO + 0.8% H_2 + 1000 ppm C_3H_6 as reductants (Rich #1).

Fig. 3-4 compares the NO_x conversion and NH_3 yield during cycling for LNT only, L(4.6), and dual-layer catalysts, $\text{CuC}(0.8)/\text{L}(4.6)$, using an anaerobic reductant mixture containing 2.4% CO + 0.8% H_2 (without C_3H_6 , corresponding to rich phase #2 in Table 2). Adding the SCR layer increases the NO_x conversion only in temperatures exceeding 200

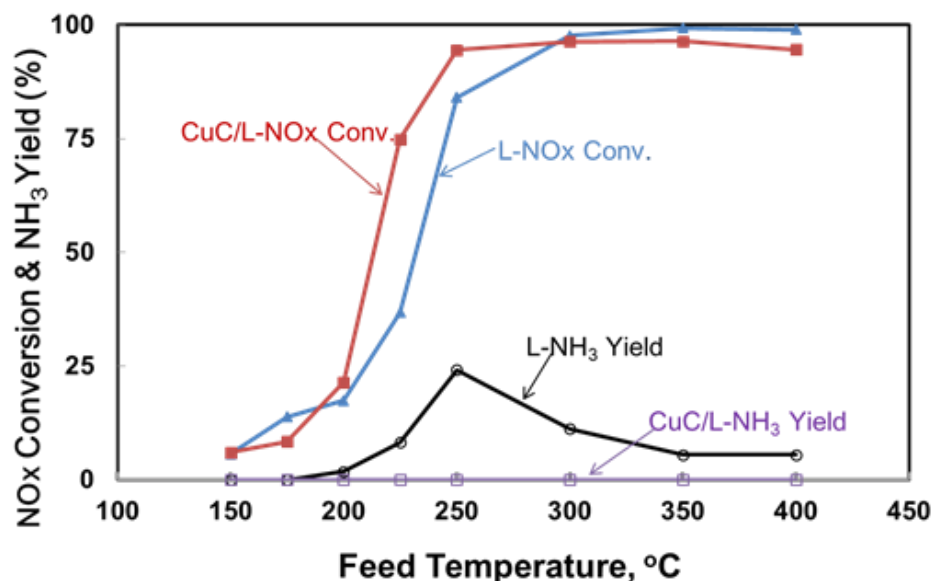


Fig. 3-4 Comparison of cycle-averaged NO_x conversion and NH₃ yield for L(4.6) and CuC(0.8)/L(4.6) catalysts using 2.4% CO + 0.8% H₂ as reductants (Rich #2).

°C, which coincides with the temperatures for NH₃ slip from the LNT-only catalyst. Unlike the results shown in Fig. 3-1 in which the reactant mixture contains C₃H₆, the dual-layer catalyst does not improve the NO_x conversion using a CO/H₂ reductant mixture below 200 °C. This indicates that the non-NH₃ reductant species under simulated exhaust conditions are not derived from the CO/H₂ reaction with NO_x. A comparison of Figs. 3-1 and 3-4 reveals that the addition of C₃H₆ to the CO/H₂ reductant mixture decreases both the NO_x conversion and NH₃ yield above 200 °C over the LNT-only catalyst. This is due in part to the inhibition by the C₃H₆, i.e., Pt site poisoning and slower NO_x reduction rate by C₃H₆ [39]. Another factor is the absence of O₂ in the Fig. 3-4 (Rich #2) results, i.e., the reductant mixture is richer.

Fig. 3-5 compares cycle-averaged NO_x conversion for the LNT only using 1000 or 3550 ppm C₃H₆ as the reductant (rich condition #3 and #4 in Table 2) with CuC(0.8)/L(4.6) using rich feed #3. Increasing the C₃H₆ concentration to 3550 ppm for LNT alone, the same

S_N value as for Rich #2, only improves NO_x conversion at temperatures exceeding 250°C . This indicates that at low temperatures the LNT catalyst suffers from severe propene poisoning. No NH_3 breakthrough from LNT alone is observed over the entire temperature range for Rich #3 and below 350°C for Rich #4 (data not shown). Enhanced NO_x conversion in the presence of the SCR layer is obtained in the low temperature range (150 - 250°C). The similar low-temperature improvement by the added SCR layer occurs for either C_3H_6 only (Rich #3) or the simulated exhaust condition (Rich #1) but not for CO/H_2 (Rich #2). This confirms that propene itself, or its derivatives, serve as the non- NH_3 reductants, which enable additional NO_x reduction by the SCR catalyst. Xu et al. [14] first reported the existence of the non- NH_3 pathway for a LNT+SCR dual-zone system and speculated that the key species for this non- NH_3 reduction are organo-nitrogen derivatives formed over the LNT via the reaction between HC and stored NO_x during the rich purge. However, the non- NH_3 intermediates were not identified.

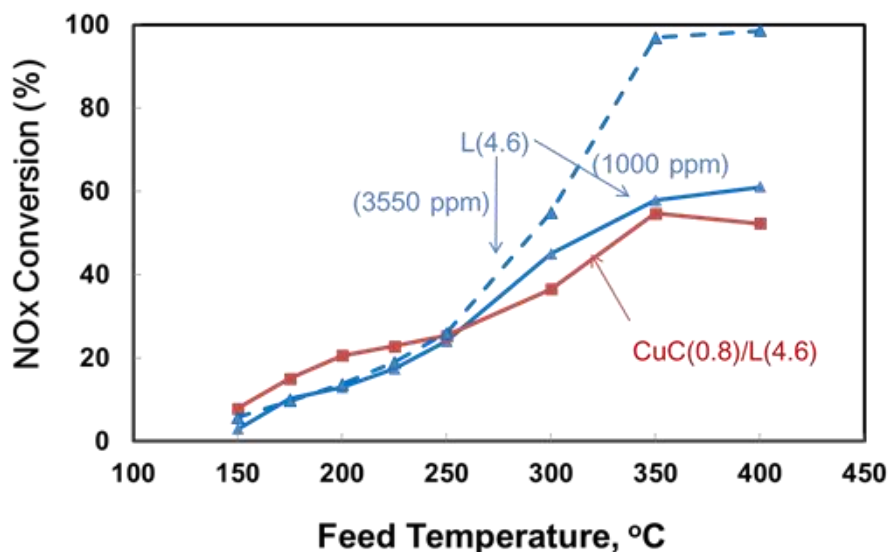


Fig. 3-5 Comparison of cycle-averaged NO_x conversion and NH_3 yield for L(4.6) using 1000 or 3550 ppm C_3H_6 as reductant (Rich #3 or Rich #4) and $\text{CuC}(0.8)/\text{L}(4.6)$ catalysts using 1000 ppm C_3H_6 as reductant (Rich #3).

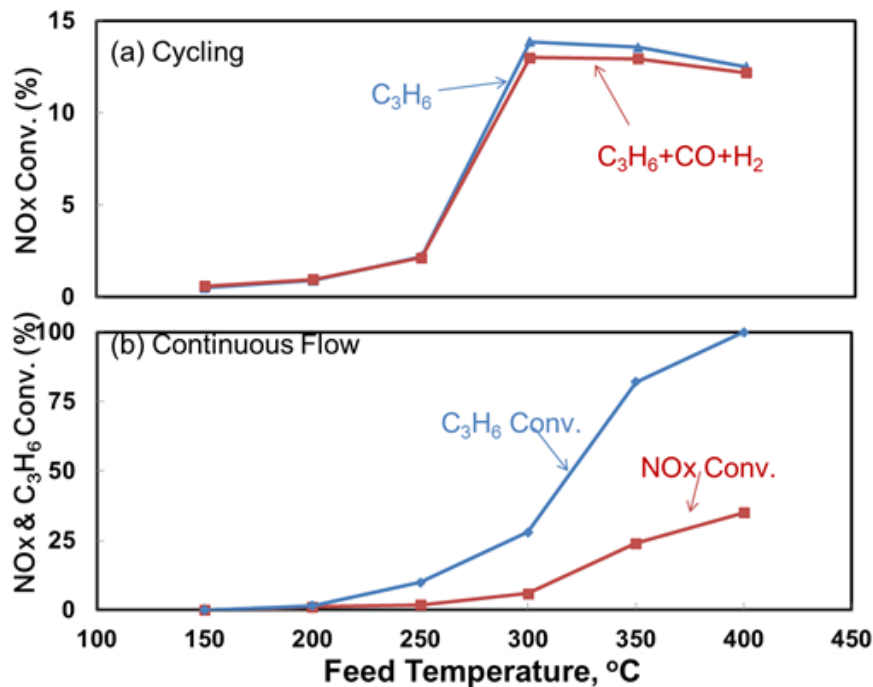


Fig. 3-6 a) NO_x conversion using 0.1% C₃H₆ + 1% O₂ with and without 2.4% CO + 0.8% H₂ as reductants over the SCR only. b) Steady-state NO_x and C₃H₆ conversions over CuC(2.4) under feeding 500 ppm NO, 500 ppm C₃H₆ and 5% O₂.

In an attempt to determine whether propene or its oxygenated derivatives plays the primary role in non-NH₃ reduction pathway, we studied NO_x reduction over the SCR catalyst under both periodic and stationary conditions. Fig. 3-6a shows the cycle-averaged NO_x conversion using 1000 ppm C₃H₆ + 1% O₂ with and without CO/H₂ in the rich feed. Fig. 3-6b shows the stationary NO_x and C₃H₆ conversions when continuously feeding a mixture of 500 ppm NO, 500 ppm C₃H₆ and 5% O₂ in a carrier gas. A very low NO_x conversion is observed across the SCR catalyst below 250 °C under either periodic or stationary conditions. Fig. 3-6a indicates a negligible impact of the CO/H₂ on the HC-SCR reaction over Cu-zeolite SCR catalyst. Comparing Fig. 3-6a and b, under periodic operation the light-off temperature for the HC-SCR is shifted by 50 °C towards lower temperature due to the mitigated inhibitive effect of propene and its derivatives, which can be flushed

away during the lean phase. This is consistent with reported results by Crocker et al. [40]. Given the rather limited activity of Cu-zeolite catalyst towards NO_x reduction with propene at low temperatures, it is unlikely that propene itself is the primary non- NH_3 reductant of NO_x reduction in the SCR catalyst, especially at low temperatures ($\leq 200^\circ\text{C}$). The C_3H_6 conversion in Fig. 3-6b indicates that oxygenated propene derivatives cannot be effectively produced by the SCR itself at low temperatures ($150\text{--}200^\circ\text{C}$) due to the negligible C_3H_6 conversion in that temperature range. In contrast, due to the higher activity of Pt, C_3H_6 can react with NO_x over the LNT at much lower temperatures, as shown in Fig. 3-5. Therefore, the key non- NH_3 reductant species, oxygenated propene derivatives, are primarily produced over the underlying LNT layer during the rich purge and then are stored and react in the upper SCR layer.

DRIFTS (diffuse reflectance infrared Fourier transform spectroscopy) measurements were conducted to identify and monitor the evolution of surface organic intermediates over a powder LNT catalyst. Fig. 3-7 shows the temporal changes of the in situ DRIFTS spectra when exposing a NO_x pre-adsorbed LNT to a feed of $0.1\% \text{ C}_3\text{H}_6 + 1\% \text{ O}_2$ at 200°C . After 1h of pre-conditioning the catalyst by $500 \text{ ppm NO} + 5\% \text{ O}_2$, three intense peaks were observed at 1270 , 1300 and 1575 cm^{-1} , which can be assigned to the bulk nitrates, surface nitrites and surface nitrates, respectively [32, 41]. After feeding propene the spectra shows a temporal decrease in the intensity of the surface nitrates peaks at 1300 and 1575 cm^{-1} , and an almost simultaneous evolution of four new bands at 1650 , 1680 , 2190 and 2215 cm^{-1} . Compared to the nearly constant peak at 1270 cm^{-1} corresponding to bulk nitrates, the dramatic decreased spectral intensity of the surface

nitrates peak suggests that NO_x stored at surfaces sites close to the Pt are more prone to be converted at low

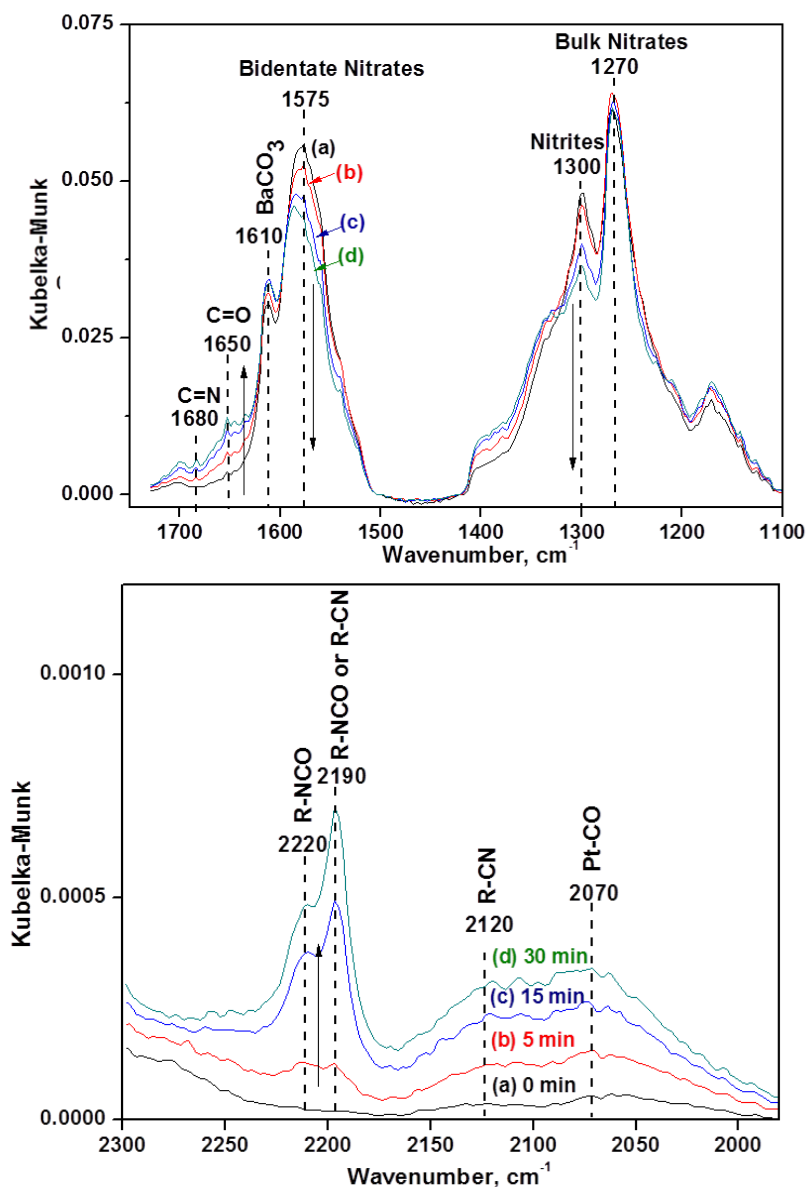


Fig. 3-7 DRIFTS spectra over LNT catalyst taken at 200 °C after a 1h pre-conditioning by 500 ppm NO + 5% O₂ and purge with He (a), subsequently exposed to a flow of 0.1% C₃H₆ + 1% O₂ for 5 min (b), 15 min (c), 30 min (d)

temperatures. This indicates NO_x stored in close proximity to Pt is easier to be reduced.

The band at 1650 cm⁻¹ is most likely a C=O group of aldehydes (R-CHO) like acrolein [42].

The bands at 1680, 2190 and 2215 cm^{-1} can be assigned to C=N stretching vibration of either acetone oxime [43], isocyanate (R-NCO) over barium [44] or cyanide species (R-CN) over alumina [45], and surface isocyanate over alumina [44], respectively.

Although the deNO_x mechanism of HC-SCR over various types of catalysts, such as zeolites, metal oxides or platinum group metals, is still under debate, the role of organic nitrogen-containing species ($\text{C}_x\text{H}_y\text{N}_t\text{O}_z$) as key intermediates formed through interaction of HC and NO_x and/or O₂ has been widely recognized [46]. Sachtler and co-workers [43] proposed that for NO_x reduction by light hydrocarbons (propane, propylene, i- or n- butane, etc.) over Fe/ZSM-5 catalysts, active N-containing organic deposits are first formed at the catalyst surface by the reaction of the hydrocarbon with adsorbed nitro/nitrate group, which further react with gas-phase NO₂ (or NO+O₂) to release N₂. They provided direct evidence by isotopic labeling to prove that one N atom in every N₂ molecule comes from the N-containing deposit and the second from NO₂. The formation of the active organo-nitrogen species is believed to be the rate-determining step in the NO_x reduction [38]. Therefore, for the SCR of NO_x by HC over LNT-SCR dual-layer catalyst, a synergic effect between LNT and SCR layers is expected. The Pt-based layer serves to promote the formation of active N-containing species during the rich purge, which are otherwise difficult to produce by Cu-zeolite layer itself at low temperatures. The activated intermediates can be stored and reacted with NO_x in the SCR catalyst during the ensuing lean phase.

In summary, under simulated exhaust conditions, the non-NH₃ reduction pathway by propene derivatives plays a major role in the incremental NO_x conversion over SCR layer at low temperatures ($\leq 225\text{ }^\circ\text{C}$) where these intermediates are relatively stable. The impact of NH₃ and C₃H₆ as reductants for NO_x conversion over the SCR catalyst increases

with temperature ($> 225\text{ }^{\circ}\text{C}$). The relative roles of NH_3 and C_3H_6 and its organo-nitrogen derivatives in NO_x reduction over the SCR varies with the rich purge control, temperature.

3.5 Impact of zoning SCR loading

As mentioned in Chapter 2, one approach to assess the effect of washcoat diffusion limitation is to replace the active Cu-SSZ-13 top-layer with inert Na-ZSM-5 (NaZ). Thus, a series of dual-layer NaZ/L catalysts with fixed LNT loading of 4.6 g/in^3 and different NaZ loading were prepared to study the diffusion limitation of top-layer under simulated diesel exhaust conditions. To intensify the diffusion limitations, the tests were carried out at high GHSV of $120,000\text{ h}^{-1}$ by shortening the catalyst length from 2cm to 1cm. The increase of space velocity decreases the residence time during which the gas species can diffuse through the SCR top layer to the LNT layer. Fig. 3-8 shows that above $250\text{ }^{\circ}\text{C}$ depositing an upper layer loading of 1.0 g/in^3 starts to decrease the overall cycle-averaged NO_x conversion. Increasing the top layer loading to 1.5 g/in^3 further lowers the high-temperature NO_x conversion. Thus, the effect of the diffusion resistance starts at $250\text{ }^{\circ}\text{C}$ under simulated exhaust condition at a GHSV of $120,000\text{ h}^{-1}$. The performance loss due to top-layer diffusion resistance can be quantitatively determined. For example, at $350\text{ }^{\circ}\text{C}$ the loss of overall NO_x conversion due to diffusion resistance is ca. 16 % for 1.0 g/in^3 and ca. 24 % for 1.5 g/in^3 top-layer loading. Compared to the diffusional loss over the same NaZ/L catalysts using only CO/H_2 reductant mixture shown in Chapter 2, the impact of diffusion limitation when adding C_3H_6 as the rich reductant is more severe. This is likely due to the relative larger kinetic diameter of C_3H_6 than that of CO or H_2 , which hinders its effective diffusion through the top layer and thus intensifies the diffusion limitation. In addition, given the low NH_3 yield shown in Fig. 3-3, the diffusion resistance at high temperatures

causes a larger loss than the undesired NH_3 oxidation and needs to be minimized to optimize the performance of the LNT-SCR dual-layer catalyst.

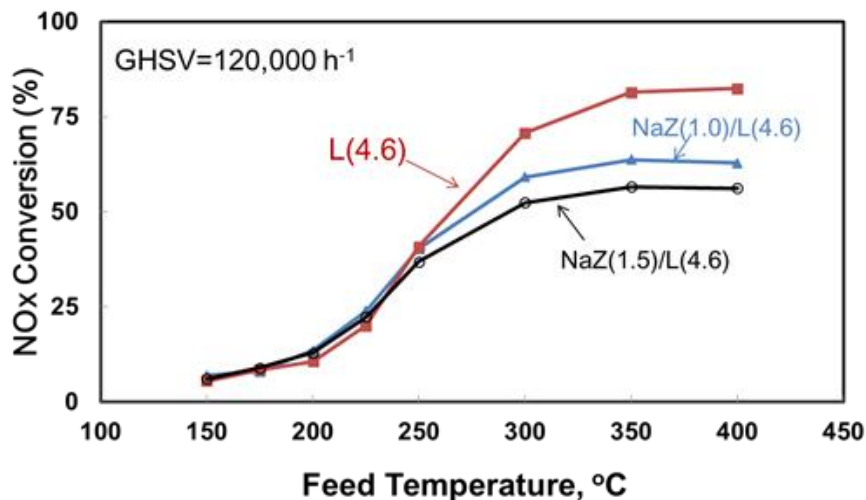


Fig. 3-8 Comparison of cycle-averaged NO_x conversion from dual-layer catalysts with fixed LNT loading but different NaZ loadings using 2.4% CO + 0.8% H_2 + 1000 ppm C_3H_6 as reductants (Rich #1).

SCR catalyst zoning can minimize the adverse effects of the SCR top layer while maximizing the improved low-temperature deNO_x performance when using CO/H_2 as reductants, as demonstrated in Chapter 2. Fig. 3-9 compares the performance of $\text{L}(4.6)+\text{CuC}(0.8)/\text{L}(4.6)$, $\text{CuC}(0.8)/\text{L}(4.6)$ and $\text{L}(4.6)$ catalysts under simulated exhaust conditions. The three catalysts have the same total PGM loading but the SCR loading of $\text{L}+\text{CuC}/\text{L}$ is only half that of CuC/L . The dual-layer catalyst with downstream SCR loading has better deNO_x performance than a catalyst with uniform SCR loading over the entire temperature range. SCR zoning moderately enhances the NO_x conversion in the temperature range from 175 to 300 °C, and slightly improves it at high temperatures.

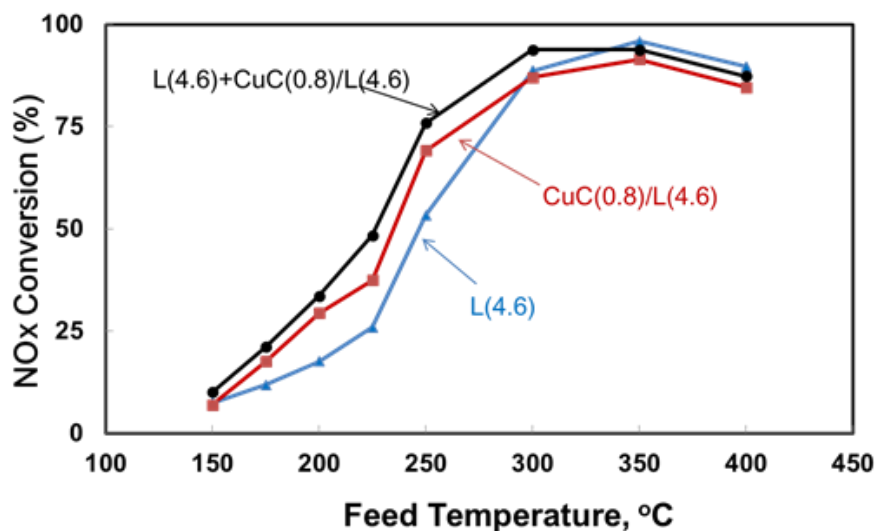


Fig. 3-9 Cycle-averaged NO_x conversion from L(4.6), CuC(0.8)/L(4.6) and L(4.6) + CuC(0.8)/L(4.6) using 2.4% CO + 0.8% H₂ + 1000 ppm C₃H₆ as reductants (Rich #1)

Below 250 °C the NH₃ yield across the LNT catalyst is rather limited and N-containing organic intermediates are the likely primary reductants for NO_x reduction in the SCR layer. The effective formation of such intermediates requires the interaction of hydrocarbon and adsorbed NO_x over the LNT. Removing the SCR layer from the upstream enables easier access of propene to the active sites in the front LNT zone. This enables a more effective generation of these active intermediates for the downstream SCR layer. Since above 250 °C the reaction begins to be subjected to diffusion limitations, minimizing the diffusion resistance by not depositing a SCR layer in the upstream further enhances the deNO_x performance above 250 °C. The propene becomes an active NO_x reductant over the SCR at temperatures higher than 350 °C. This offsets to a certain extent the adverse impact of the top-layer diffusion resistance since propene can be directly utilized in the SCR layer without having to diffuse through it and react in the LNT layer. This probably explains why

above 350 °C the diffusion resistance of a reductant mixture with propene is less pronounced with respect to that of a mixture without propene in Chapter 2.

3.6 PGM loading and zoning effects

Fig. 3-10 shows the impact of reducing the LNT loading by half from 4.6 to 2.3 g/in³ in a dual-layer catalyst with fixed SCR loading of 0.8 g/in³ on its performance. Reducing the LNT loading by 50% causes the NO_x conversion to drop by 6% to 12% relative to that of a LNT-only catalyst over almost the entire temperature range. This occurs due to the decreased formation of NH₃ and non-NH₃ reductants at low temperatures caused by a 50% reduction in the Pt sites. This restricts the ability of the SCR layer to compensate for the performance loss caused by reduced LNT loading. Therefore, the reduction of the LNT loading in dual-layer catalysts is limited by inefficient reductant generation at low temperatures.

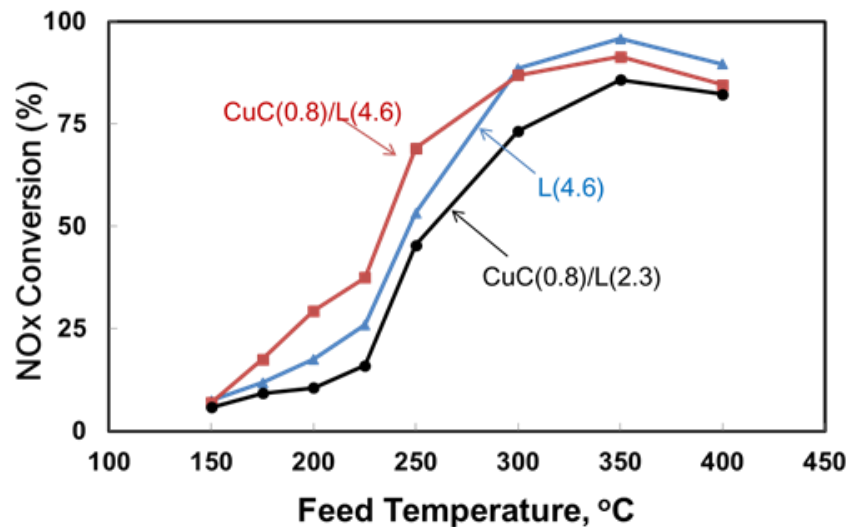


Fig. 3-10 Cycle-averaged NO_x conversion by LNT and two dual-layer catalysts having the same SCR loading but different LNT loadings using 2.4% CO + 0.8% H₂ + 1000 ppm C₃H₆ as reductants (Rich #1)

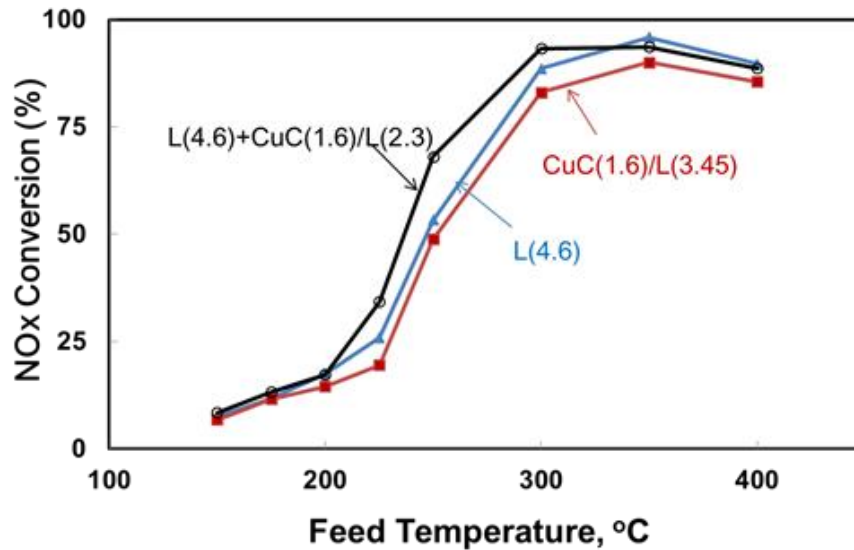


Fig. 3-11 Cycle-averaged NO_x conversion from dual-layer catalysts with different zoned LNT and SCR loading but the same total LNT loading using 2.4% CO + 0.8% H₂ + 1000 ppm C₃H₆ as reductants (Rich #1)

Fig. 3-11 compares the NO_x conversion from the LNT-only L(4.6), CuC(1.6)/L(3.45) and L(4.6)+CuC(1.6)/L(2.3) catalysts. Both dual-layer catalysts have the same total LNT loading, which is lowered by 25% from that of the LNT-only catalyst. The SCR loading on the CuC/L is twice that of the L+CuC/L catalyst. The L+CuC/L catalyst exhibits higher NO_x conversion than the CuC/L catalyst over the entire temperature range. The enhanced NO_x conversion at both low and high temperatures is due to the LNT and SCR zoning. Higher upstream LNT loading, which is free of any top-layer diffusion resistance, makes the front zone a more effective NO_x converter and NH₃ and non-NH₃ reductant generator over the entire temperature range. PGM zoning has been used for years in three way catalyst (TWC), where high PGM loading is applied in the front zone to provide fast light-off performance and low PGM loading in the rear zone to minimize the cost while providing good warm-up performance [47]. The L+CuC/L with 25% less LNT

loading shows better performance than the LNT-only catalyst over the entire temperature range, especially below 300 °C. The experiments reveal that SCR and LNT zoning in dual-layer catalyst increases the deNO_x performance relative to conventional dual-layer catalyst over the entire temperature range. This compensates for the activity loss by decreased LNT loading.

Based on the optimized design of zoned SCR and LNT dual-layer catalyst, we studied the extent to which the LNT loading can be reduced under simulated exhaust conditions. Fig. 3-12 shows that the LNT loading of L(4.6)+CuC(1.6)/L(2.3) and L(4.6)+CuC(1.6)/L(1.15), is reduced by 25% and 37.5% from that of L(4.6) only catalyst. Both zoned dual-layer catalyst exhibited improved NO_x conversion at low- and mid-temperatures (≤ 300 °C) and comparable performance at high temperatures (> 300 °C). Higher downstream LNT loading of L(4.6)+CuC(1.6)/L(2.3) over that of L(4.6)+CuC(1.6)/L(1.15) increases NO_x conversion slightly.

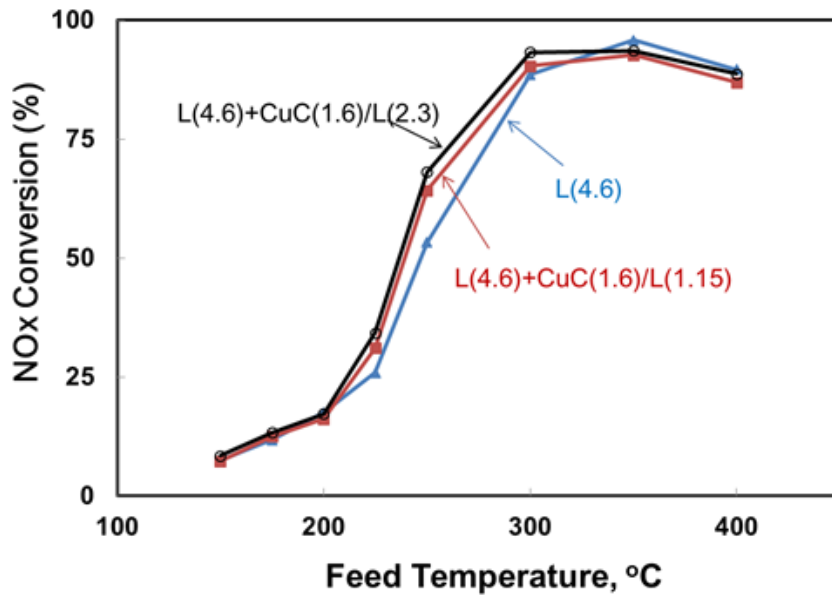


Fig. 3-12 Cycle-averaged NO_x conversion by zoned dual-layer catalyst with different downstream LNT loading using 2.4% CO + 0.8% H₂ + 1000 ppm C₃H₆ as reductants (Rich #1)

The commercial LNT catalyst used in our study is not optimized for dual-layer applications. It is desirable to reduce the expensive PGM loading at constant barium and ceria loading to maintain the NO_x storage capacity, rather than decreasing total LNT loading. The lean/rich duration was fixed to typical 60s/5s during the whole lab study. The optimization of lean/rich cycling timing and rich regeneration control is expected to yield higher deNO_x performance. Therefore, it would be helpful to determine the minimum feasible PGM loading via the optimized LNT catalyst and operating conditions. Nevertheless, our results demonstrate that the optimized LNT-SCR dual-layer catalyst has the potential to reduce PGM loading by up to 37.5% under such lab test conditions as shown in Table 3-1. This will make the dual-layer system less expensive than LNT alone for applications in passenger cars.

3.7 Conclusions

The main findings of this study are:

- A zeolite layer of 1.0 g/in³ on top of an LNT layer causes diffusion limitation at temperatures over 250 °C under simulated exhaust conditions at a GHSV of 120,000 h⁻¹.
- The non-NH₃ reduction pathway via propene derivatives, inferred as organic N-containing intermediates, plays a major role in the incremental NO_x conversion over the SCR of dual-layer catalysts at low temperatures (<= 225 °C) in laboratory tests. The importance of NH₃ and C₃H₆ as NO_x reductants over the SCR catalyst increases with temperature (> 225 °C).
- LNT-assisted HC-SCR pathway for the combined system is proposed, wherein the LNT layer promotes the formation of active N-containing species during the rich

purge which are otherwise difficult to produce by the Cu-zeolite layer at low temperatures. These activated intermediates can be stored and reacted with NO_x in the SCR catalyst during the ensuing lean phase.

- Zoning of both SCR & LNT in dual-layer catalysts increases the deNO_x performance over that of a conventional dual-layer catalyst at the entire temperature range. The optimized dual-zone dual-layer catalyst exhibited a potential PGM loading reduction of up to 37.5% over that of LNT only catalyst in a laboratory test.

Chapter 4 Effects of CO, H₂ and C₃H₆ on Cu-SSZ-13 Catalyzed NH₃-SCR

4.1 Introduction

In contrast to the stand-alone urea-SCR system designed to operate with a lean exhaust, the combined LNT+SCR is inevitably exposed to a rich exhaust condition during the LNT regeneration. Prolonged rich purges are preferred to promote NH₃ generation by the LNT. This may generate relatively high slippage levels of CO, H₂ and HC to the SCR catalyst. A recently-commercialized SCR on-filter (SCRF) technology comprises a diesel particulate filter (DPF) that is coated with SCR catalyst and is positioned in close proximity to the engine to enable fast SCR light-off [12]. The SCR component encounters a rich environment during the periodic DPF regeneration. Even the SCR-only system may be exposed to a rich feed under certain conditions such as cold-start period, extended vehicle idling, engine malfunction, or degraded upstream diesel oxidation catalysts (DOC) [48]. These scenarios raise questions about the potential impact of rich reducing agents on the performance of the SCR catalyst.

Previous studies of the impact of various reductants on NH₃-SCR performance over metal-exchanged zeolites have mainly focused on HC species poisoning. It is well known that stored HC on zeolites can have a detrimental effect on both the SCR catalyst performance and its durability. He et al. reported a negative effect of C₃H₆ due to carbon deposits during standard SCR (NO + NH₃ + O₂) over a Fe-beta zeolite [49]. Heo et al. [50] attributed the competitive adsorption of NH₃ and C₃H₆ on the catalyst as well as undesired NH₃ consumption by side reactions to the decreased NH₃-SCR activities of Fe- or Cu-

ZSM-5. Epling et al. [51] compared the effects of C_3H_6 and dodecane ($n-C_{12}H_{26}$) exposure over two Cu-exchanged zeolite catalysts; one was a small-pore zeolite (Chabazite framework, CHA) while the second was a standard large-pore Cu-BEA zeolite. The Cu-CHA had a much higher resistance to HC poisoning than the Cu-BEA by effectively suppressing HC adsorption and coke formation. A slightly decreased standard SCR activity was observed when adding C_3H_6 to the gas fed to the Cu-CHA. This was attributed to formation of partial oxidation intermediates. In a follow-up study, Kumar et al. found that even a small-pore zeolite could store non-negligible amounts of carbonaceous deposits from either short- or long-chain HCs via an oxygen-dependent, thermally-activated storage process [48]. All the above studies were conducted with continuous exposure of the SCR catalysts to a HC. Wang et al. [40] and Kim et al. [52] reported that under lean/rich cyclic conditions, the enhanced cycle-averaged NO_x conversion over a Cu-CHA catalyst by C_3H_6 , was attributed to the mitigation of HC poisoning and HC-SCR reactions.

The factors affecting the impact of HC on NH_3 -SCR over SCR zeolite catalysts include competitive adsorption, undesired NH_3 consumption, formation of partially oxidized intermediates and operating conditions (continuous or cyclic). A clear elucidation requires a systematic analysis. To date only a few studies investigated the effects of other reducing reagents like CO and H_2 on NH_3 -SCR zeolite catalysts. Huang et al. studied the deactivation of Cu-zeolites by reductive hydrothermal aging [53]. They found that extended exposure to a CO/ H_2 mixture at 650 °C resulted in permanent catalyst deactivation due to the sintering of Cu^0 from the reduction of isolated Cu^{2+} cations. Exposure to C_3H_6 under the same conditions resulted in a reversible deactivation after coke removal. Smith et al. [54] recently reported that compared to C_3H_6 , CO and H_2 had a negligible effect on the

NH₃-SCR chemistry over an Fe-zeolite catalyst, with the main contribution being a slight promotion of NO₂ reduction to NO.

The aim of this chapter is to systematically study the effects of different reducing agents including CO, H₂ and C₃H₆ on the NH₃-SCR performance of a small-pore Cu-chabazite catalyst under either steady-state or cyclic operations. To this end, we examine the effect of each reductant through temperature ramp, step-response and cyclic experiments. The results help the interpretation of NH₃-SCR on Cu-CHA catalysts when subjected to rich exhaust exposure.

4.2 Experimental

4.2.1 Catalyst

A Cu-SSZ-13 SCR catalyst having a CHA framework was provided by BASF (Iselin, NJ). The SCR sample had a cell density of 400 cpsi and an estimated washcoat loading of about 2.4 g/in³ with ca. 2.5 wt.% Cu loading. For bench reactor evaluation, a core sample was prepared (D=0.8 cm, L=1.0 cm, 28 channels). Prior to the reactor tests, the catalyst was de-greened at 500 °C for 5 hours in a feed mixture containing 5% O₂, 2.5% H₂O, 2% CO₂, and the balance Ar.

4.2.2 Temperature ramp experiments

The SCR catalyst was exposed to a constant feed composition at 500 °C to establish a steady state before the temperature ramp experiments. The downward temperature ramp to 200 °C was conducted at a rate of -2 °C/min to minimize the complicating effect of NH₄NO₃ formation. The ramp rate was sufficiently slow to avoid thermal hysteresis effects and to obtain essentially steady-state results. [Comment: The downward ramp was found to be more effective in this regard than an upward ramp. For example, the NO₂ SCR

reaction ($\text{NO}_2 + \text{NH}_3$) is difficult to reach a steady-state at low temperature ($\sim 200^\circ\text{C}$) due to the gradual accumulation of NH_4NO_3 on the catalyst. This process deactivates the catalyst and makes it difficult to differentiate among the effects of different reducing agents. In some experiments, a step-response method was employed in order to evaluate both the transient and long-term response to gas concentration changes.

The feed gas composition for the baseline NH_3 -SCR reactions comprised 500 ppm NH_3 and 500 ppm NO for standard SCR ($\text{NO}/\text{NO}_x=1$; $4\text{NO} + 4\text{NH}_3 + \text{O}_2 \rightarrow 4\text{N}_2 + 6\text{H}_2\text{O}$), 250 ppm NO and NO_2 for fast SCR ($\text{NO}/\text{NO}_x=0.5$; $\text{NO} + \text{NO}_2 + 2\text{NH}_3 \rightarrow 2\text{N}_2 + 3\text{H}_2\text{O}$) and 500 ppm NO_2 for slow SCR ($\text{NO}/\text{NO}_x=0$; $3\text{NO}_2 + 4\text{NH}_3 \rightarrow 3.5\text{N}_2 + 6\text{H}_2\text{O}$), in 0% or 5% O_2 (as specified) in a carrier gas of 2.5% H_2O , 2% CO_2 and balance of Ar, at a space velocity of $120,000\text{ hr}^{-1}$. A reductant feed of either 1% CO or 1% H_2 or 500 ppm C_3H_6 was introduced as specified. The amount of C_3H_6 (500 ppm) was lower than that of CO (1 %) or H_2 (1%) on a total reductant basis (the amount of O species that can be consumed by reductants); i.e., 500 ppm C_3H_6 can consume 4500 ppm O species, while 1% of either CO or H_2 can consume 1% O species.

4.2.3 Lean/rich cycling experiments

Lean/rich (30/5s) cycling experiments were conducted over the SCR catalyst. Table 4-1 describes the baseline cycling conditions. A reductant of either 1% CO or 1% H_2 or 500 ppm C_3H_6 was added to the baseline rich phase. The feed temperature was increased from 200 to 450°C in steps of 50°C . It typically took approximately ~ 10 min to reach a periodic steady state at each temperature. The cycle-averaged NO_x ($\text{NO} + \text{NO}_2$) conversion for a particular operating condition was determined from the average of the final ten periodic cycles.

Table 4-1 Gas condition for baseline cycling test

Gas	Lean (30s)	Rich (5s)
NO _x *	300 ppm	300 ppm
NH ₃	—	500 ppm
O ₂	5%	1%
CO ₂	2%	2%
H ₂ O	2.5%	2.5%

* NO/NO_x=1 for standard, 0.5 for fast and 0 for slow SCR reactions

4.2.4 Temperature-programmed desorption (TPD) experiments

Two types of TPD experiments were performed. The first evaluated the effects of the three reductants on the NH₃ storage capacity. The catalyst was exposed to 500 ppm NH₃ in a carrier gas with and without the presence of a reductant mixture containing 1% CO, 1% H₂ and 500 ppm C₃H₆ at 200 °C for 30 mins, followed by another 30-min flush with carrier gas. The sample was then heated in carrier gas at a rate of 7.5 °C/min up to 500 °C. The second type studied the surface reactions between NH₄NO₃ and reducing agents. An equal amount of NH₄NO₃ was first loaded by co-feeding 500 ppm NH₃ and 500 ppm NO₂ to the SCR catalyst at 200 °C for 30 mins, followed by a 30-min purge with carrier gas. The sample was then heated at 15 °C/min to 400 °C in a carrier gas (baseline), or in a mixture with either 1% CO or 1% H₂ or 500 ppm C₃H₆. Prior to each experiment, the catalyst was exposed to 5% O₂ in a carrier gas at 500 °C for 1h.

4.3 NO and NO₂ reactions with CO, H₂ and C₃H₆

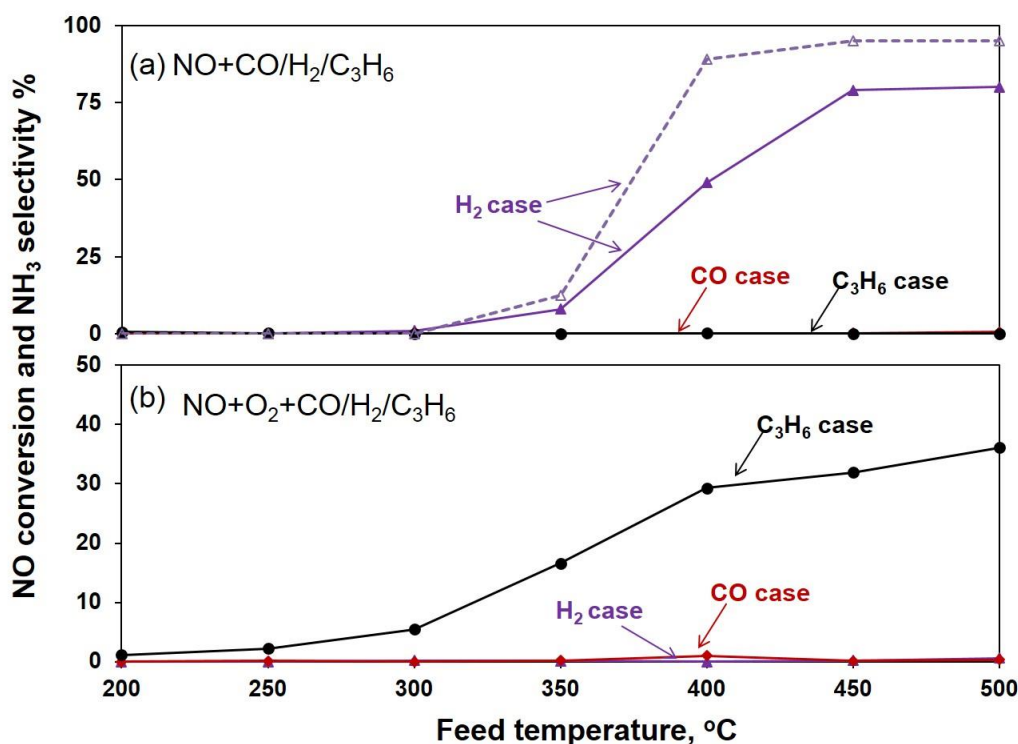


Fig. 4-1 NO conversion (solid) and NH₃ selectivity (dash) during reaction of NO (500 ppm) with three reductants (either 1% CO, 1% H₂, or 500 ppm C₃H₆) in the absence of O₂ (a) and in the presence of 5% O₂ (b).

Fig. 4-1 compares the temperature dependence of NO conversion during the reaction of NO with CO, H₂ or C₃H₆ under both anaerobic and aerobic conditions. CO has negligible NO conversion over the temperature range of 200 to 500 °C, regardless of the presence of O₂. Although C₃H₆ is inert to NO under anaerobic conditions, the presence of O₂ enables the reduction of NO to N₂ via a HC-SCR pathway, which involves reaction of propene partial oxidation intermediates with NO. On the other hand under anaerobic condition, H₂ begins to effectively reduce NO above 350 °C, with over 90% NH₃ selectivity. Copper-based catalysts have been reported to catalyze H₂-SCR reaction with metallic copper (Cu⁰) as the catalytically active site [55]. Cu-exchanged SSZ-13 is considered to

contain isolated Cu cations as active centers. Thus, the first step in H₂-SCR by Cu-SSZ-13 likely involves the reduction of Cu ions to Cu⁰. H₂-TPR method has been widely utilized to assess the reducibility of various copper species on Cu-CHA catalysts. For example, H₂ is capable of reducing Cu ions like Cu-dimers to Cu⁰ at temperatures above ~350 °C [56], which coincides with the light-off temperature of NO reduction by H₂ in Fig. 4-1a. This supports the speculation of a stepwise mechanism involving Cu⁰ formation followed by NO hydrogenation to NH₃.

The addition of O₂ inhibits the reaction of NO with H₂ as seen in Fig. 4-1b. This is attributed to two factors. First, Cu⁰ catalyzes the oxidation of H₂ by O₂ which reduces the H₂ available for NO reduction. Second, the excess O₂ inhibits the formation of Cu⁰ by oxidizing Cu⁰ to either Cu cations or CuO cluster [53], both of which result in less Cu⁰ available for NO adsorption and/or reduction.

Fig. 4-2a compares the NO₂ and NO_x conversions over a wide temperature range during the reaction of NO₂ with CO, H₂ or C₃H₆ in the absence of O₂. Fig. 4-2b shows the corresponding effluent NO and NO₂ concentrations over the same temperature range. C₃H₆ exhibits the highest reactivity with NO₂, leading to the lowest light-off temperature (defined as the temperature at which NO_x conversion is 50% of the maximum). NO₂ reduction by C₃H₆ begins at 200 °C and increases up to ~300 °C where it levels off at 100% NO₂ conversion and ~35% NO_x conversion. CO starts to reduce NO₂ at ~225 °C and plateaus at 100% NO₂ conversion and ~23% NO_x conversion at 350 °C. Although NO₂ reduction by H₂ is the least effective on the basis of having the highest light-off temperature, the NO_x conversion increases up to ~ 85% at 500 °C, in contrast to the plateaus observed for C₃H₆ and CO.

The NO and NO₂ effluent concentrations shown in Fig. 4-2b provide additional insights into the reactions of NO₂ with CO, H₂ or C₃H₆. NO₂ reduction to NO promoted by either CO or C₃H₆ occurs with concomitant and near-stoichiometric formation of NO. This is seen clearly at low temperatures; i.e., moles NO₂ consumed are equal to the moles NO produced. Both C₃H₆- and CO-assisted NO₂ conversion begin at 200 °C and reach 100% NO₂ conversion above 350 °C. Note that the N-balance is not closed at high temperatures in the baseline case. This is most likely due to the formation of some undetected gaseous HNO₃ that leaves the reactor.

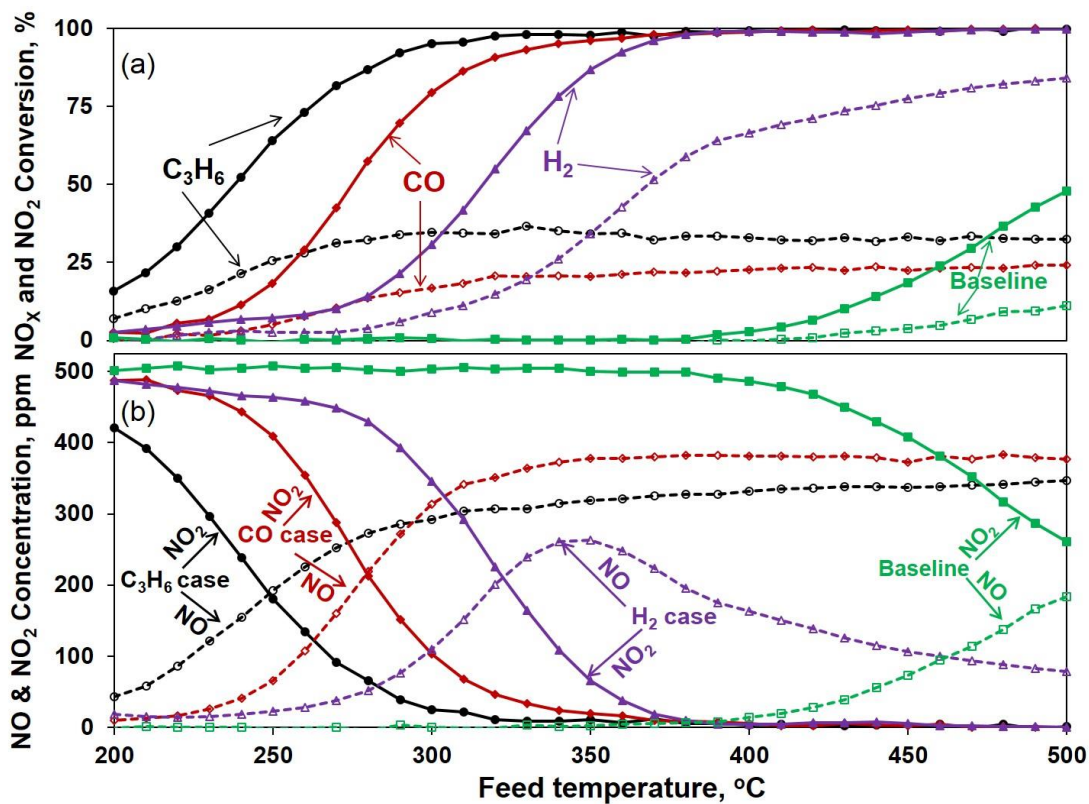
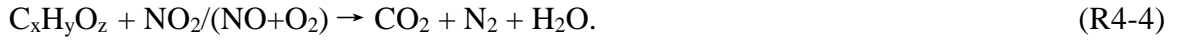


Fig. 4-2 a) NO₂ (solid) and NO_x (dash) conversion; b) corresponding NO₂ (solid) and NO (dash) effluent concentration during reaction of NO₂ with either 1% CO, 1% H₂, or 500 ppm C₃H₆) without O₂; Baseline condition: 500 ppm NO₂ in carrier gas.

The reaction of NO₂ with C₃H₆ was previously reported as part of the following HC-SCR pathway:



The overall HC-SCR reaction is given by:



Gorce et al. [46] proposed that organic nitro intermediates (denoted by R-NO₂) formed by the reaction of C₃H₆ and ad-NO_x species (R4-1), decompose to NO and oxygenates (C_xH_yO_z, such as acrolein) (R4-2). In turn, the oxygenates serve as active intermediates that further react with NO₂ or NO+O₂ to proceed the HC-SCR pathway (R4-4).

Overall reaction (R4-3) accounts for the stoichiometric conversion of NO₂ to NO. It also explains the appearance of the plateau in the NO_x conversion for C₃H₆ in Fig. 4-2a, which coincides with the complete conversion of NO₂. That is, a lack of NO₂, which is needed for reaction with oxygenates (R4-4), limits further NO_x conversion and results in the plateau.

We propose the following nitrate-related mechanism for CO:



The overall reaction (R7+R8) is



Nitrates formed by NO_2 disproportionation (R6) are reduced to nitrites by CO (R4-7), followed by their rapid reaction with NO_2 , generating NO (R4-8). This reaction pathway was verified in a separate experiment when pulsing CO to the SCR catalyst initially contacted with NO_2 for 1 h at 300 °C (data not shown here). The instantaneous CO_2 release upon the feed of CO confirms the reactivity between nitrates and CO. This is discussed further below. Forzatti et al. [33] proposed a similar reduction of nitrates over a LNT catalyst by CO to form nitrites with evolution of CO_2 .

Compared to CO and C_3H_6 , H_2 is not as effective in the reduction of NO_2 to NO. For example, 95% NO_2 conversion is achieved at ~380 °C, somewhat higher than that for C_3H_6 (~300 °C) and CO (~350 °C). Note that a peak in the effluent NO concentration occurs at ~350 °C. The increasing NO concentration to the left of the peak is likely due to a similar NO_2 reduction pathway as for CO, with H_2 reducing nitrates to nitrites (R4-10) that can further reduce NO_2 to NO (R4-8). This reaction pathway was verified by introducing H_2 to a pre-nitrated SCR catalyst at 300 °C. The nearly instantaneous production of H_2O , NO_2 and NO at the admission of H_2 agrees with the following proposed nitrate-related pathway:



The decreasing NO concentration above 350 °C, at which point the H_2 -SCR of NO begins to light off as shown in Fig. 4-1a, is attributed to increased H_2 -SCR activity. Based on the established mechanism for H_2 -SCR, which involve the adsorption and dissociation of H_2 and NO_x over metallic metal sites [57], we expect that the following H_2 -SCR pathway is favored over the above nitrate-related pathway at higher temperature range:

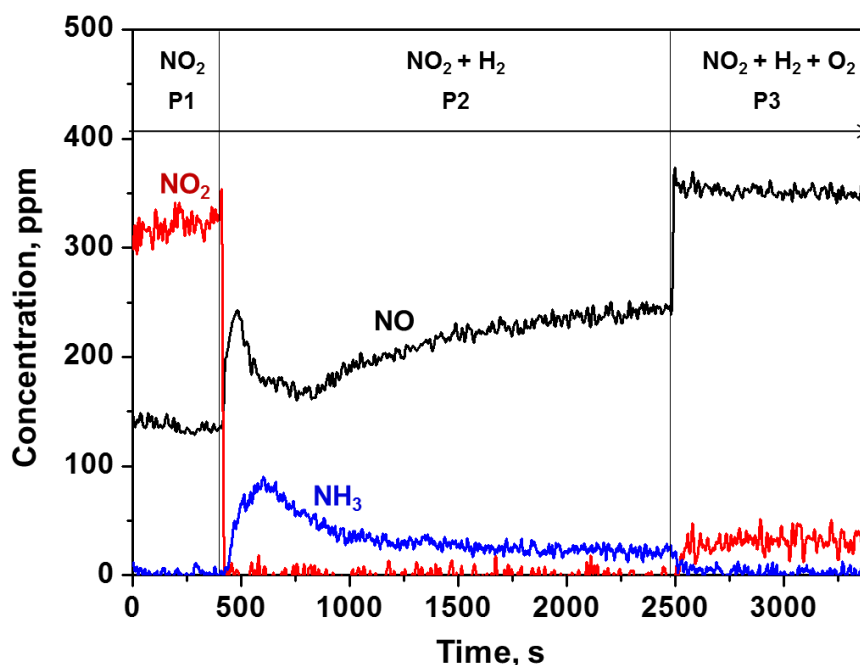
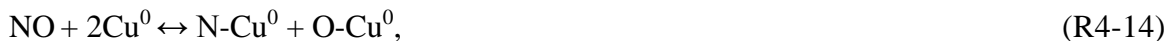


Fig. 4-3 Effluent species concentrations during a three-phase step-response protocol at 500 °C; (500 ppm NO₂, 1% H₂, 5% O₂ if required, in carrier gas of 2.5% H₂O, 2% CO₂ and balance Ar).

To examine the above pathways, a three-phase step response protocol was employed. As shown in Fig. 4-3, the protocol consisted of a NO₂ feed (500 ppm NO₂, Phase 1), followed by the addition of 1% H₂ in the absence (Phase 2) and presence (Phase 3) of 5% O₂ at 500 °C. During the Phase 1, NO₂ undergoes thermal decomposition, producing NO. A sharp decrease in NO₂ concentration to nil with a corresponding steep increase in

NO concentration occur upon the introduction of H_2 in Phase 2. The NO rapidly peaks and then decreases to a local minima at ~ 250 s entering Phase 2, followed by a gradual increase up to the 2450 s mark. The NO peak is attributed to the rapid reduction of accumulated surface nitrates to nitrites (R4-10) that reduces NO_2 to NO (R4-8). Meanwhile, the formation of metallic copper sites which catalyze the H_2 -SCR reaction, reduces the NO_x to N_2 and NH_3 (R4-11-4-16). The prolonged H_2 exposure results in sintering of metallic copper that is responsible for a gradual decrease in NO conversion from 750 to 2450 s. Huang et al. [53] reported that a high-temperature reducing treatment of Cu-zeolite catalysts by H_2 caused an irreversible sintering of Cu metals and thus the catalyst deactivation. Subsequent O_2 introduction in Phase 3, leads to a sharp increase in NO concentration. This confirms that the presence of O_2 inhibits H_2 -SCR reaction as was shown by in Fig. 4-1b. In addition, NO_2 disproportionation (R4-6) is favored by the presence of O_2 to produce nitrates for the nitrate-related pathway. The inhibition of H_2 -SCR pathway and the promotion of the alternative nitrate pathway results in a higher NO level under aerobic conditions.

4.4 The effects of CO , H_2 and C_3H_6 on NH_3 oxidation and storage

NH_3 storage plays a crucial role in the NH_3 -SCR performance, especially at low temperatures. Thus, it is important to assess the effects of reducing agents on the NH_3 storage. Heo et al. reported that C_3H_6 competes with NH_3 for storage sites over Cu-ZSM-5, inhibiting NO_x reduction [50]. Epling et al. [42] reported negligible C_3H_6 adsorption on Cu-SAPO-34 under anaerobic conditions, indicating that C_3H_6 may not compete with NH_3 for adsorption on the active sites. Kumar et al. [48] showed that extended exposure of Cu-SAPO-34 to C_3H_6 in the presence of O_2 at temperatures between 200 and 400 $^{\circ}C$ deceased

NH₃ storage capacity. This was attributed to the formation of carbonaceous deposits which block the storage sites. Wang et al. reported the co-adsorption of C₃H₆ and NH₃ on Cu-SSZ-13 under anaerobic conditions exhibited no apparent coupling between the two adsorbates [40]. Finally, no studies of the effect of CO or H₂ on NH₃ storage on Cu-CHA have been reported. H₂ and CO are considered as effective molecular probes in the characterization of various copper species over Cu-zeolite catalysts. For example, H₂ can reduce the oxidation state of Cu ions, while CO can strongly adsorb onto Cu⁺ to form carbonyls [58]. Thus, they may affect the NH₃ adsorption on Cu cations.

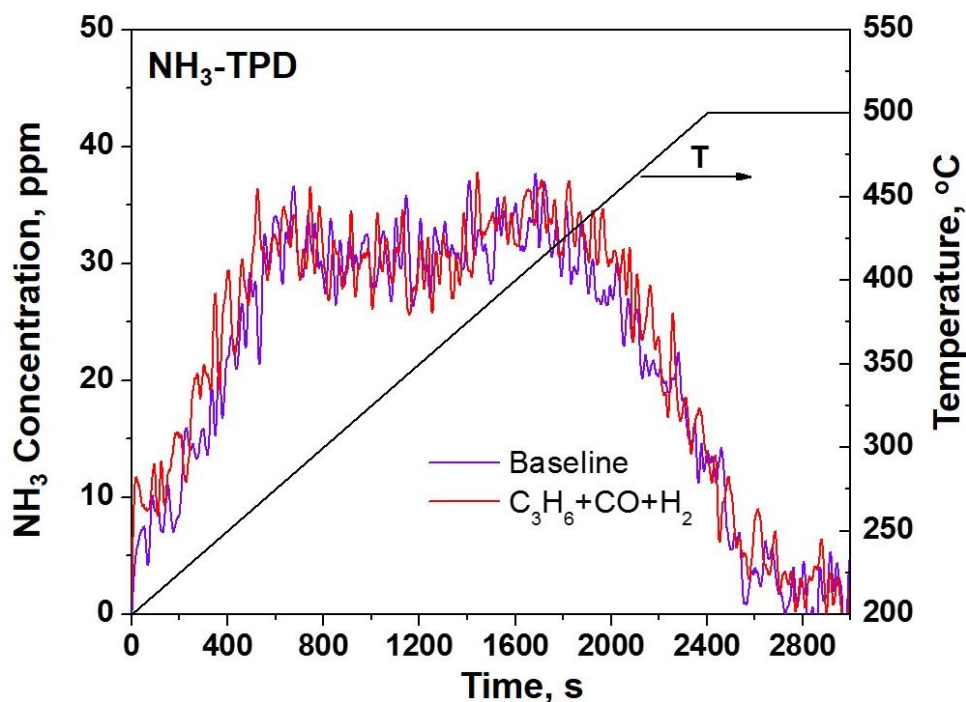


Fig. 4-4 NH₃-TPD profiles after saturating the catalyst with NH₃ at 200 °C in the absence (baseline) or in the presence of a mixture of reductants, including 1% CO, 1% H₂, and 500 ppm C₃H₆.

Fig. 4-4 shows NH₃ TPD profiles on Cu-SSZ-13 after being saturated at 200 °C with NH₃ in the presence and absence of CO, H₂ and C₃H₆. Two desorption peaks, one at ~275 °C and a second at ~400 °C, were observed during the temperature ramp; these can

be assigned to NH_3 adsorbed on weak acid sites (Cu cation or extra-framework Al Lewis sites) and stronger acid sites (Brønsted sites), respectively [59]. The near overlap of the two NH_3 desorption profiles indicates that addition of CO, H_2 and C_3H_6 has a negligible impact on both NH_3 storage capacity and the strength of different acid sites. These data suggests that none of the three reductants competes with NH_3 for the acid storage sites of the Cu-chabazite catalyst.

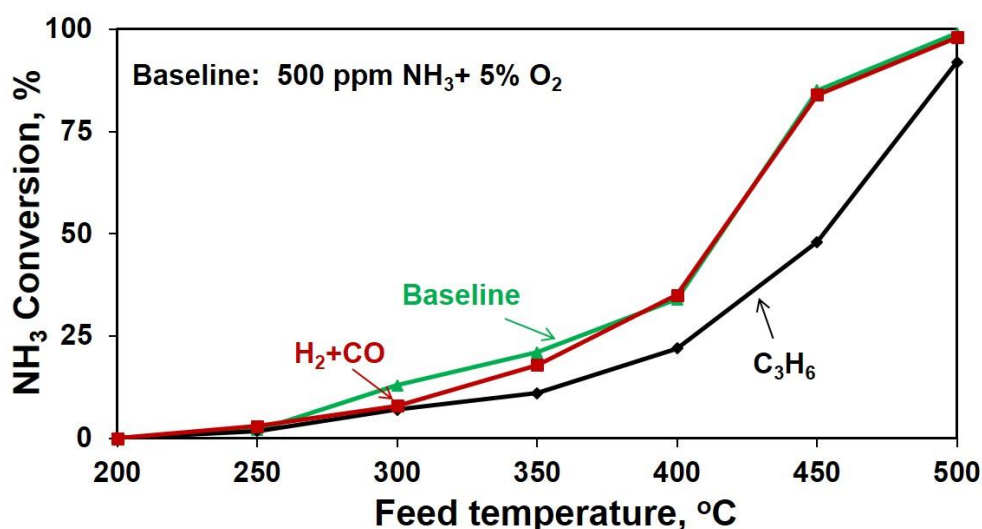


Fig. 4-5 NH_3 conversion during NH_3 oxidation in the presence of 500 ppm C_3H_6 or 1% CO+1% H_2 .

Ammonia oxidation is an undesired side reaction among the NH_3 -SCR reactions. It decreases the NH_3 available for NO_x reduction and can generate undesired byproducts, such as N_2O . Fig. 4-5 compares the NH_3 conversion in the presence of CO + H_2 and C_3H_6 . The data show that C_3H_6 inhibits the NH_3 oxidation by increasing the light-off temperature by about 50 °C. This is attributed to the formation of partial oxidation intermediates that block the active sites; this is evidenced by concomitant CO release above 300 °C during a separate propene oxidation experiment shown in Fig. 4-6. CO and H_2 , slightly decrease NH_3 conversion between 300 and 350 °C. This is probably due to the reduced copper

oxidation state by CO and H₂. For all NH₃ oxidation experiments, Cu-SSZ-13 exhibits very high N₂ selectivity (> 98%) during the entire temperature range.

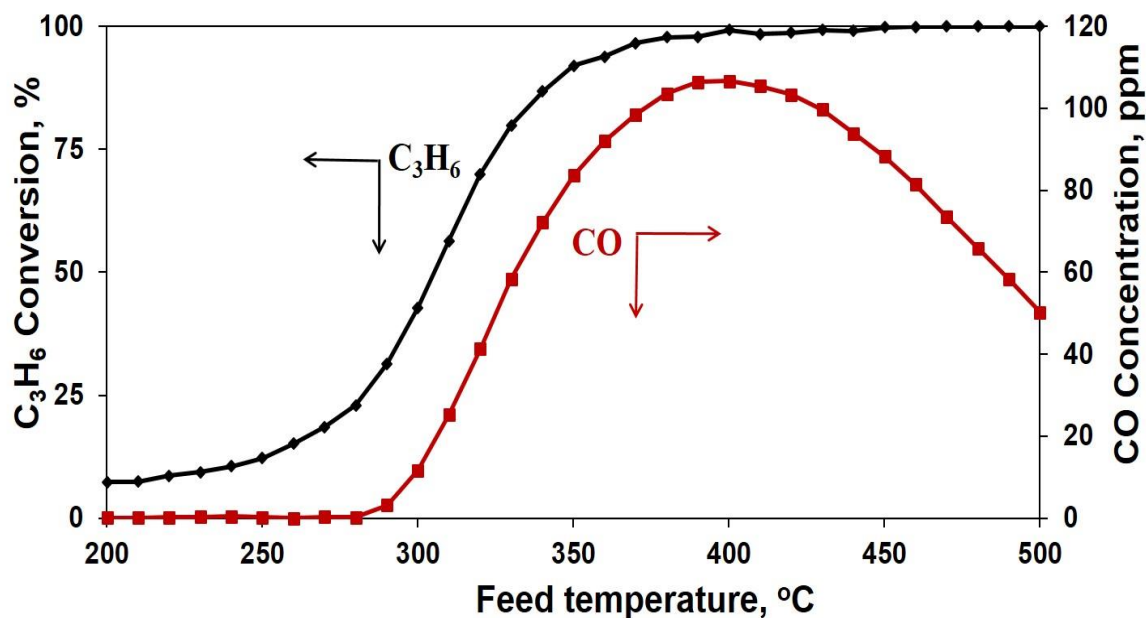


Fig. 4-6 C₃H₆ conversion and CO generation during C₃H₆ oxidation experiment with 500 ppm C₃H₆ and 5% O₂ in carrier gas of 2.5% H₂O, 2% CO₂ and balance Ar.

4.5 Steady-state effects of CO, H₂ and C₃H₆ on NH₃-SCR reactions

4.5.1 Temperature ramp experiments

In LNT+SCR applications, the SCR catalyst encounters a NO_x stream with widely varying NO₂/NO_x ratio. As shown earlier, C₃H₆, CO and H₂ promote the conversion of NO₂ to NO to different extents and thus affect the NO/NO₂ ratio. It is well known that the deNO_x efficiency of SCR catalysts is sensitive to the NO/NO₂ ratio, especially at low temperatures, with the highest NO_x conversion and/or N₂ yield achieved at an equimolar ratio of NO to NO₂ [7]. Thus, it is important to determine the effects of these reductants on SCR performance and the reaction mechanism.

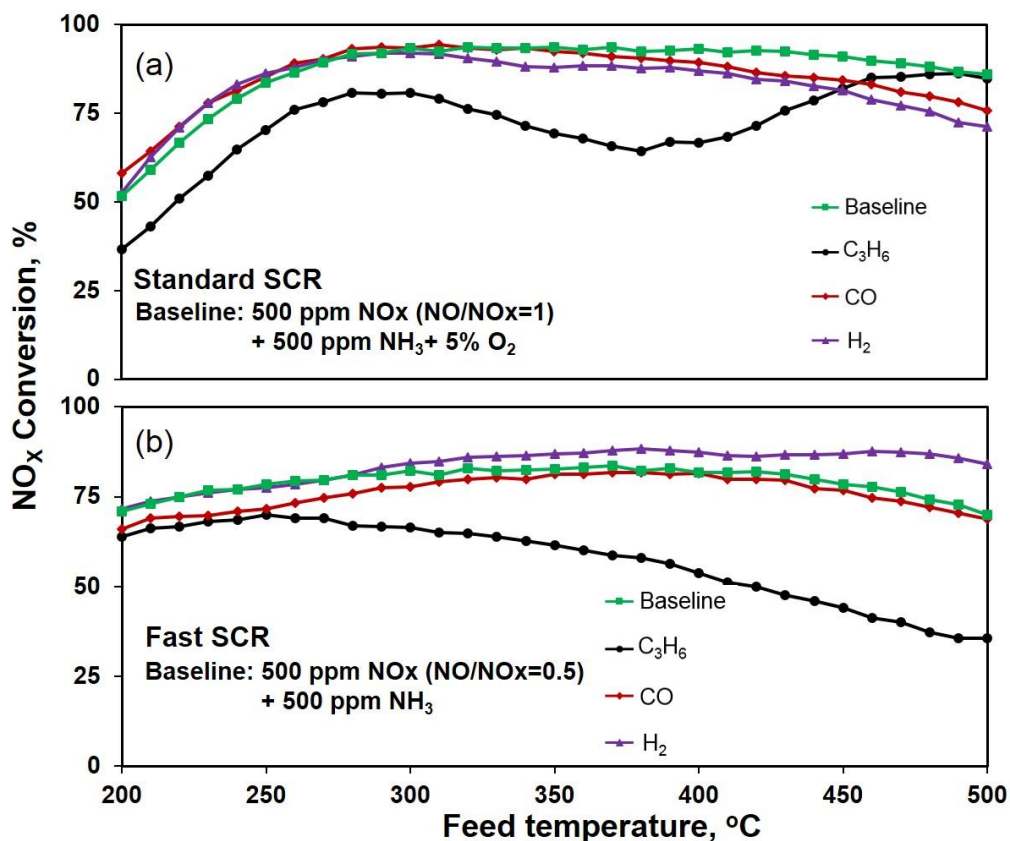


Fig. 4-7 NO_x conversion of (a) standard SCR and (b) fast SCR in the presence of either 1% CO, 1% H₂, or 500 ppm C₃H₆. Baseline conditions: 5% O₂, 500 ppm NH₃ and NO for standard SCR, while 500 ppm NH₃, 250 ppm NO and NO₂ for fast SCR.

Fig. 4-7a shows steady-state NO_x conversion during the standard SCR reaction in the presence of CO, H₂, or C₃H₆ for temperatures between 200 and 500 °C. The addition of either CO or H₂ has a negligible effect on baseline NO_x conversion in the low and intermediate temperatures, while slightly decreasing the high-temperature NO_x conversion. The inhibitory effect at high temperature may be due to the interference by either H₂ or CO with the redox cycling between Cu²⁺ and Cu⁺ that is critical for standard SCR reaction on Cu/CHA catalysts [7]. C₃H₆ inhibits the NO_x conversion with the most pronounced negative effect in the medium temperature range (~350 °C). The small pore structure of the Cu-CHA catalyst restricts the oligomerization of the propene oxidation intermediates inside

the channels of the zeolite, as reported by Epling et al. [51]. Thus, organic intermediates ($C_xH_yO_z$ or $C_xH_yO_zN_t$) instead of coke play an important role in the blocking of active sites.

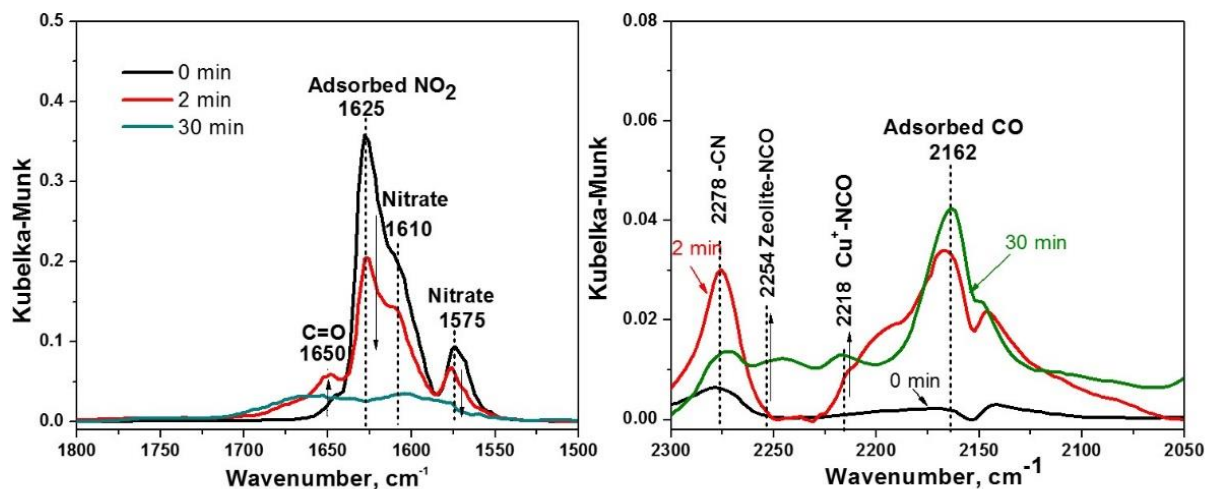


Fig. 4-8 DRIFTS spectra over a Cu-SSZ-13 catalyst taken at 200 °C, after a 1h pre-conditioning by 500 ppm NO + 1% O₂ and purge with He (0 min), subsequently exposed to a flow of 0.1% C₃H₆ + 1% O₂ for 2 min and 30 min.

In situ DRIFTS (diffuse reflectance infrared Fourier transform spectroscopy) measurements were conducted to identify surface intermediates species over a Cu-SSZ-13 powder catalyst. Fig. 4-8 shows the temporal DRIFTS spectra when exposing a NO_x pre-adsorbed SCR catalyst to a feed of 0.1% C₃H₆ + 1% O₂ at 200 °C. After 1h of pre-conditioning the catalyst by 500 ppm NO + 5% O₂, three intense bands were observed at 1575, 1610 and 1625 cm⁻¹. These can be assigned to the adsorbed NO₂ species, monodentate nitrates, and bidentate nitrates, respectively [60]. After feeding propene a temporal decrease in the intensity of the adsorbed NO₂ and surface nitrates peaks occurred, and four new bands at 1650, 2218, 2254 and 2278 cm⁻¹ gradually evolved. The dramatic spectral intensity of the surface NO_x species indicates a rapid reaction of surface NO_x species with propene. The band at 1650 cm⁻¹ may be assigned to a C=O bond vibration of

acrolein [42]. But it may also be the C=C stretch band of propene or other intermediates bands that are close to 1650 cm^{-1} . The bands at 2218 , 2254 and 2278 cm^{-1} can be assigned to $\text{Cu}^+\text{-NCO}$ [61], R-NCO over zeolites [61] and R-CN [62], respectively. The appearance of these bands confirms the formation of organic intermediates from the reaction between surface NO_x species and propene. In addition, a broad band formation at around 2168 cm^{-1} is assigned to CO adsorption on Cu cation [63]. This is consistent with CO being an incomplete oxidation product. The local minimum in NO_x conversion at $\sim 380^\circ\text{C}$ in Fig. 4-7a is attributed to the increasing formation of partial oxidation intermediates, as evidenced by the CO release peak at a similar temperature region for C_3H_6 oxidation in Fig. 4-6. At temperatures above 420°C , the poisoning effect of C_3H_6 is gradually reduced, since either intermediates or coke, if formed, may be burned off. Reaction at high temperatures gradually becomes controlled by the supply of reductant since oxygen competes with NO_x for NH_3 .

Fig. 4-7b shows that for the fast SCR reaction, H_2 has negligible effect on the baseline NO_x conversion at low temperatures. It moderately increases NO_x conversion at temperatures exceeding 350°C , due to the contribution by the $\text{H}_2\text{-SCR}$. Both CO and C_3H_6 slightly decrease the NO_x conversion (by $\sim 5\%$) for temperatures below 250°C . At temperatures above 250°C , CO has little effect while C_3H_6 decreases the NO_x conversion monotonically with temperature. In the absence of O_2 in the feed, the oxidation of C_3H_6 is minimal so the decreasing NO_x conversion cannot be attributed to the inhibitory effect of partial oxidation intermediates as for the standard SCR case, especially at high temperatures. To explain the decreasing NO_x conversion trend, consider the fast SCR pathway proposed by Tronconi et al. [64]:



As mentioned previously, surface-bound NO_2 rapidly reacts with C_3H_6 which produces oxygenates and NO (R4-3). The consumption of NO_2 by C_3H_6 decreases the rate of NO_2 disproportionation (R4-13). This decreases the production of nitrates (NO_3^-) and thus a lower consumption of NO is encountered (R4-14). The net effect is to increase the NO/NO_x ratio. Thus, from a global reaction standpoint, C_3H_6 competes with NH_3 for NO_2 , increasing the NO/NO_x ratio towards 1 and shifting the feed ratio from fast SCR to standard SCR. The absence of O_2 impedes the commencement of either standard SCR or HC-SCR pathway, thereby decreasing the NO_x conversion with increasing temperature.

In contrast, a NO_x conversion decrease is not observed when CO (or H_2) is present. This supports our conjecture that CO -assisted NO_2 reduction occurs through the nitrates to nitrites reaction (R4-7) rather than through the reaction of CO with gas-phase NO_2 , which would generate NO . If the latter were the case, the increased NO/NO_x ratio would lead to the same inhibitory effect that was encountered for the C_3H_6 feed. Thus, CO affects the fast SCR mechanism by competing with NO for nitrate reduction to nitrites (R4-14), which rapidly react with NH_3 , producing N_2 . Smith et al. observed a similar effect of CO on fast SCR reaction over an Fe-zeolite catalyst, but attributed it to the much higher fast SCR reaction rate than the rate of CO -assisted NO_2 reduction [54]. Their explanation is plausible from a global reaction perspective without looking more deeply into the underlying reaction mechanism. NO is known to effectively reduce nitrates at much lower temperature, even at 100°C over Cu-CHA catalysts as reported by Di et al. [60], while CO requires 200°C as

shown in Fig. 4-2b. It is reasonable to presume that NO is more competitive than CO in terms of nitrate reduction, thereby limiting the impact of CO on the fast SCR reaction.

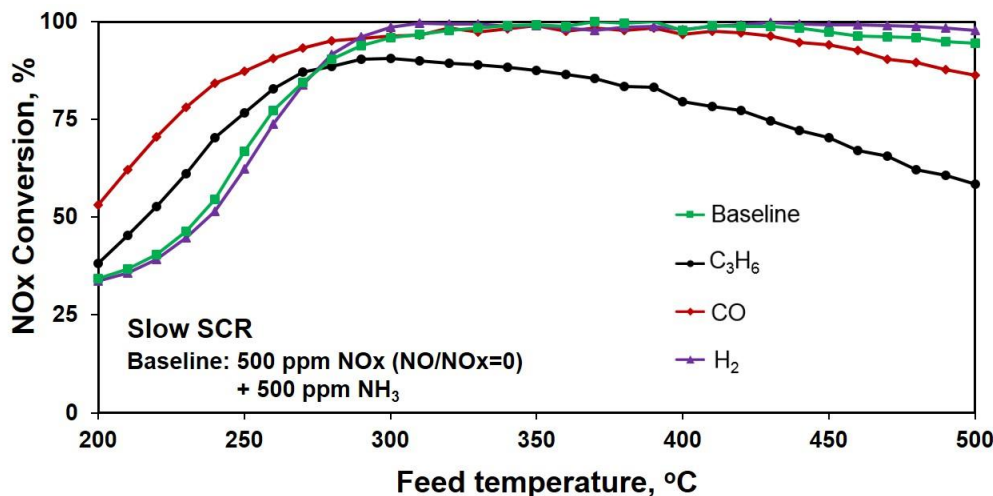


Fig. 4-9 NO_x conversion during slow SCR reaction in the presence of one reductant (either 1% CO, 1% H₂, or 500 ppm C₃H₆).

Fig. 4-9 shows that for the slow SCR reaction (NO₂-only NO_x feed), the addition of C₃H₆ or CO below 270 °C, enhances NO_x conversion while H₂ exerts a negligible impact. The ineffective reduction of NO₂ to NO by H₂ at low temperatures, shown in Fig. 4-2b, explains the negligible increase in low-temperature NO_x conversion for the H₂ case. In contrast, the effectively promoted NO₂ reduction to NO by either C₃H₆ or CO creates a mixture of fast and slow SCR feed conditions at low temperatures. The organic intermediates formed from the reaction between C₃H₆ and NO₂ somewhat offset the benefits of the additional fast SCR pathway, decreasing the NO_x conversion relative to that observed for the CO case. At temperatures exceeding 270 °C, C₃H₆ has an increasingly negative effect due to the increasing extent of the standard SCR pathway, while CO again has a slightly negative effect in terms of NO_x conversion. This is similar to the trend for fast SCR reaction. The same explanation for the effects of CO and C₃H₆ on the fast SCR

reaction can be applied for the slow SCR reaction. This will be discussed next based on step-response experiments.

4.5.2 Step-response method

A step-response was employed to examine both the transient and steady state behaviors to further elucidate the effects of C_3H_6 and CO on the NH_3 -SCR reaction mechanism. The five-phase protocol depicted in Figs. 4-10 and 4-11 included slow SCR reactions (500 ppm NO_2 + 500 ppm NH_3 ; Phase 1), addition of a reducing agent (500 ppm C_3H_6 or 1% CO) to the slow SCR feed in the absence (Phase 2) or presence (Phase 3) of 5% O_2 , followed by the reaction of these reductants with NO_2 in the absence of NH_3 with O_2 either present (Phase 4) or absent (Phase 5).

Fig. 4-10 describes the evolution of the effluent concentrations of NO, NO_2 , C_3H_6 , N_2O and NH_3 , during the five-phase protocol at 400 °C. A sudden increase in NO concentration occurs upon the introduction of C_3H_6 in Phase 2. This is followed by a slow decrease of the NO concentration, approaching a new steady state after an extended C_3H_6 exposure. The sharp increase in NO concentration suggests an active C_3H_6 -assisted NO_2 conversion to NO (R4-3). Along with increased NO concentration, the NH_3 concentration increases at a somewhat slower rate presumably due to its continued adsorption on the downstream catalyst. The NH_3 concentration stabilizes at twice the NO steady-state concentration. This confirms that in addition to the NH_3 -SCR pathway, a fraction of the NO_x is reduced via HC-SCR. Subsequent O_2 introduction in Phase 3, leads to a sharp drop in both NH_3 and NO concentrations to the same lower level, indicating that the standard SCR pathway is the primary pathway for NO_x reduction based on the 1:1 $NO_x:NH_3$ stoichiometry. The results confirm that lack of O_2 during Phase 2 hinders the standard SCR

reaction and thus limits the NO_x reduction. There is a minor performance loss relative to Phase 1 due to the poisoning by oxidation intermediates. Switching off NH₃ in Phase 4 increases the NO concentration and decreases the C₃H₆ concentration. HC-SCR is less effective for NO_x reduction than NH₃-SCR, and only achieves about 50% NO_x conversion. Further removal of oxygen during Phase 5 confirms that the activity of HC-SCR depends on the oxygen content.

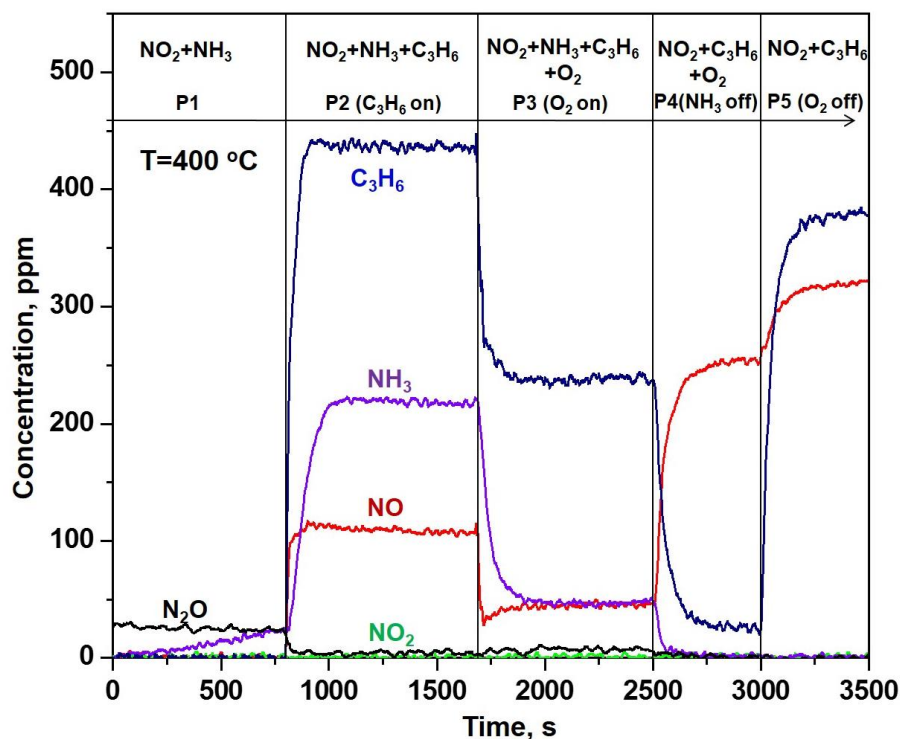


Fig. 4-10 Effluent species concentrations during a five-phase step-response protocol at 400 °C; (500 ppm NO₂, 500 ppm NH₃, 500 ppm C₃H₆, 5% O₂ if required, in carrier gas of 2.5% H₂O, 2% CO₂ and balance Ar).

Fig. 4-11 shows the effluent NO, NO₂, CO, N₂O, and NH₃ concentrations following the five-phase protocol at 400 °C. Compared to the significant jump in NO output upon C₃H₆ introduction in Fig. 4-10, a slight increase in NO concentration (less than 20 ppm) occurs following CO addition. This indicates that the mechanisms of CO and C₃H₆

interaction with NO_x are different. The proposed CO-assisted nitrate reduction to nitrite enables a fast SCR pathway (R4-15) to prevail in Phase 2, relative to the slow SCR dominant in the prior phase or the standard SCR dominant in Phase 2 of Fig. 4-10. The slightly increased NO concentration coincides with the prevailing of surface nitrites due to CO, some of which react with NO₂ to form NO (R4-8). Adding O₂ during Phase 3 causes both NH₃ and NO to vanish due to their oxidation. Turning off NH₃ during Phase 4 sharply increases NO concentration, proving that CO is less effective in NO_x reduction than either NH₃-SCR or HC-SCR. Subsequent O₂ removal in phase 5 has negligible effect on either NO or NO₂ profiles, suggesting that O₂ does not affect NO₂ reduction by CO.

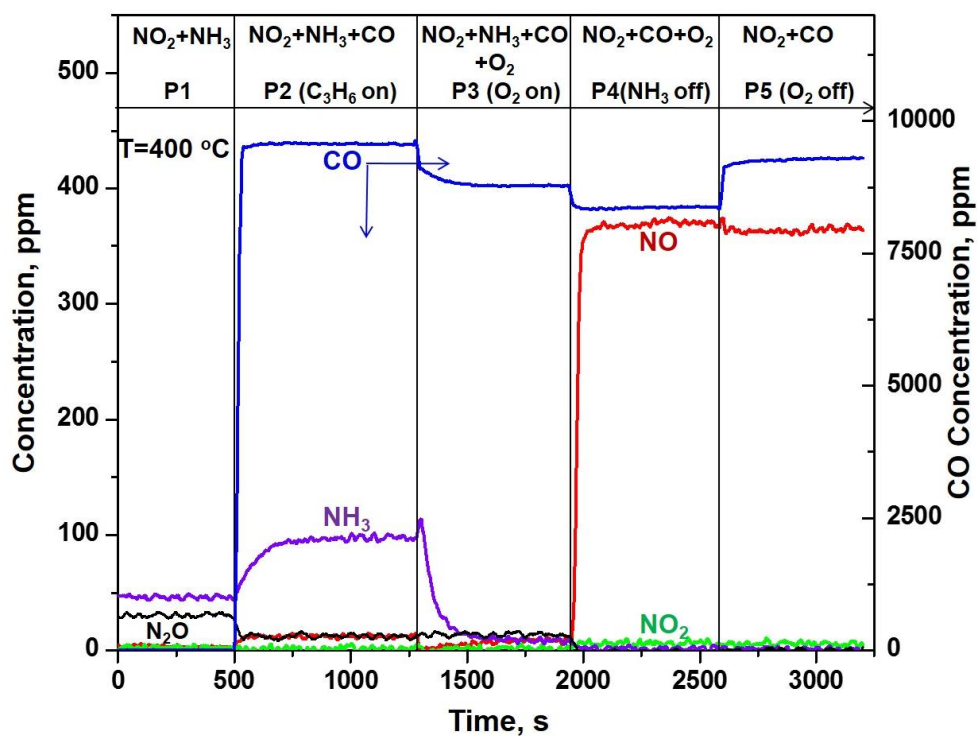


Fig. 4-11 Effluent species concentrations during a five-phase step-response protocol at 400 °C; (500 ppm NO₂, 500 ppm NH₃, 1% CO, 5% O₂ if required, in carrier gas of 2.5% H₂O, 2% CO₂ and balance Ar).

4.5.3 N₂O formation

The recent US EPA 2017-25 greenhouse gas regulations capped the N_2O emission from LD and HD vehicles [5]. A concern regarding SCR reaction with a high feed NO_2/NO_x ratio is the relatively high N_2O emission at low temperatures due to decomposition of ammonium nitrates ($\text{NH}_4\text{NO}_3 \rightarrow \text{N}_2\text{O} + 2\text{H}_2\text{O}$) above 200°C [65]. Figs 4-10 and 4-11 show that the trace amount of N_2O vanishes following either the C_3H_6 or CO induction period in Phase 2. This led us to examine N_2O emission during the slow SCR reaction under previous temperature ramp experiments. Less N_2O was emitted when either C_3H_6 , CO or H_2 was present with C_3H_6 resulting in the lowest N_2O emission (data not shown).

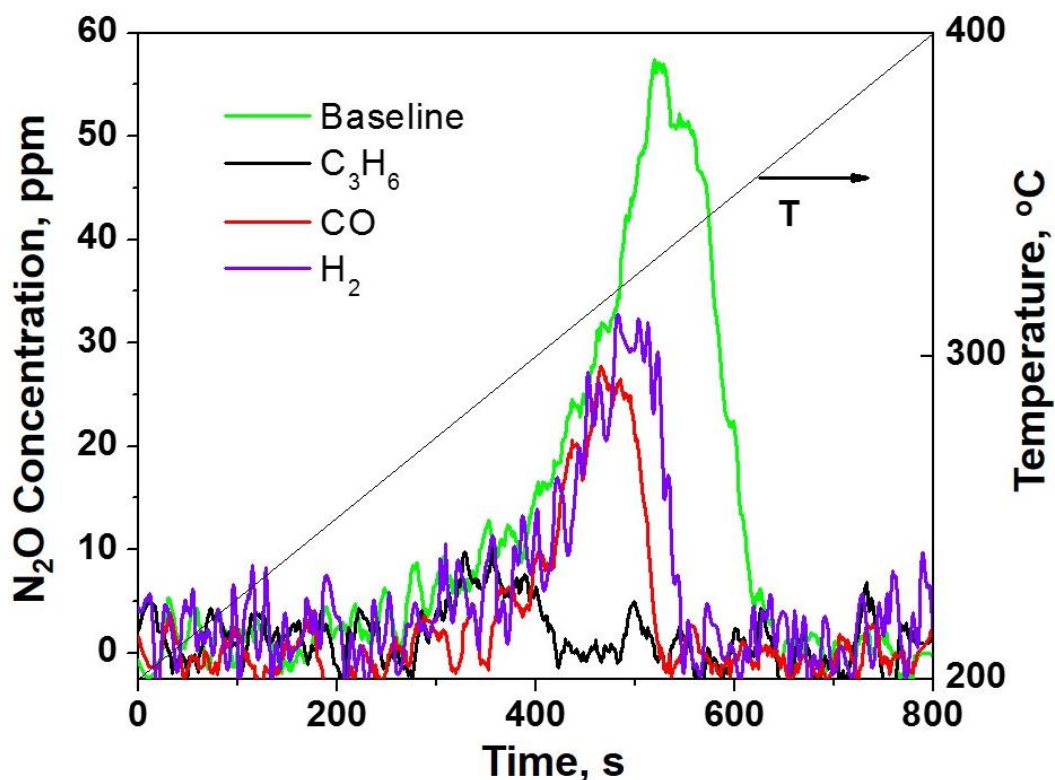


Fig. 4-12 N_2O effluent concentration during TPD of NH_4NO_3 in the absence (baseline) or in the presence of either 500 ppm C_3H_6 , 1% CO or 1% H_2

Ammonium nitrates are commonly considered the main source of N₂O production. Temperature-programmed desorption (TPD) of pre-loaded NH₄NO₃ in the presence of CO or H₂ or C₃H₆ was conducted as shown in Fig. 4-12. As described in the Experimental Section, the clean catalyst was initially loaded with an equal amount of ammonium nitrates by exposing the catalyst to NO₂ and NH₃ for 30 mins at 200 °C. After flushing with Ar, a TPD at 15 °C/min rate was followed either without or with one of the three reducing agents in the carrier gas. For the baseline sample, a peak N₂O desorption is observed at about 320 °C. Note that only a trace amount of NO₂ is recorded (data not shown), confirming the high selectivity of NH₄NO₃ for decomposition to N₂O. N₂O production is greatly reduced relative to the baseline when either C₃H₆, CO or H₂ is present. Table. 4-2 describes the reduced N₂O release in the presence of each reductant. This suggests the consumption of surface NH₄NO₃ by these reductants, which otherwise could decompose to N₂O at elevated temperature. It is likely that each reductant is capable of reducing NH₄NO₃ to NH₄NO₂ which can readily decompose to N₂ instead of N₂O.

Table 4-2 Accumulated N₂O release from TPD of NH₄NO₃^a

Conditions	N ₂ O release, μmol
Baseline	5120
w/H ₂	3414
w/CO	1062
w/C ₃ H ₆	416

^a NH₄NO₃-preloaded catalyst is heated at 15 °C/min from 200 to 400 °C with or without each reductant (1% CO, 1% H₂, and 500 ppm C₃H₆) in carrier gas of 2.5% H₂O, 2% CO₂ and balance Ar.

4.6 Impact of CO, H₂ and C₃H₆ on cyclic NH₃-SCR reduction

The SCR unit in a LNT-SCR configuration is periodically exposed to lean and rich environments. Thus, it is necessary to study the effect of intermittent rich exposure on NH₃-SCR behavior. Lean/rich cycling experiments (baseline) were performed as reported in Table 4-1. These included the 5s exposure to a rich phase of 500 ppm NH₃ and 300 ppm NO_x, followed by 30s exposure to a lean phase of 300 ppm NO_x + 5% O₂ in a carrier gas. Reducing agents (1% CO + 1% H₂ or 500 ppm C₃H₆) were introduced in the rich phase with NH₃ for comparison.

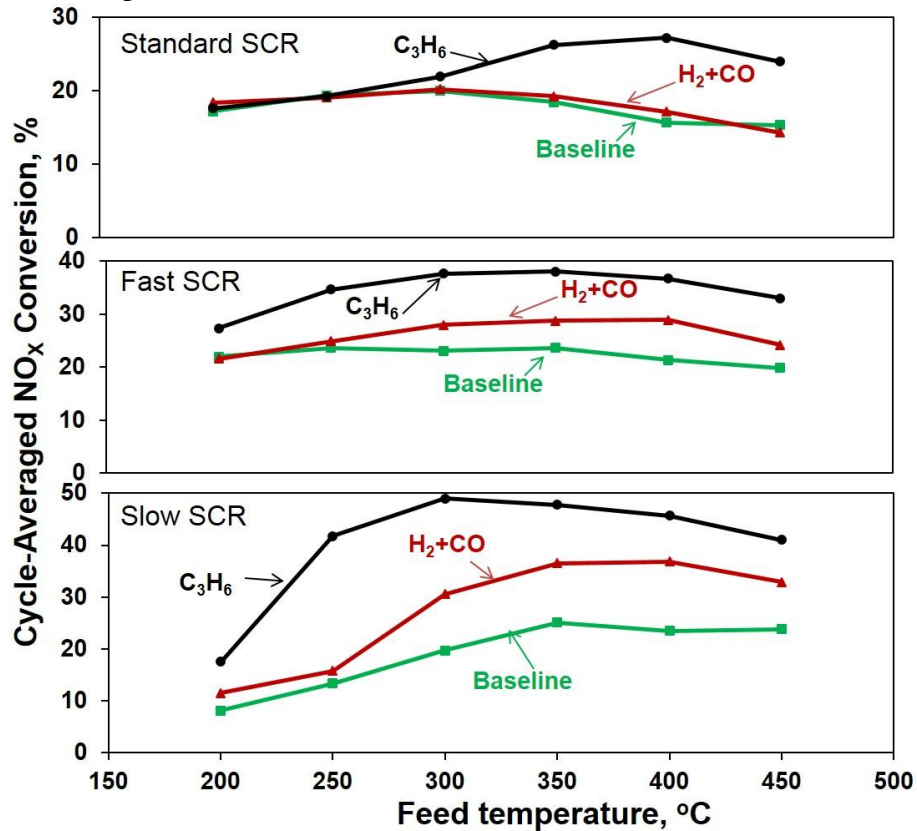


Fig. 4-13 Cycle-averaged NO_x conversion of a) standard, b) fast and c) slow SCR reactions when NH₃ and either C₃H₆ or H₂+CO are present with in the rich phase.

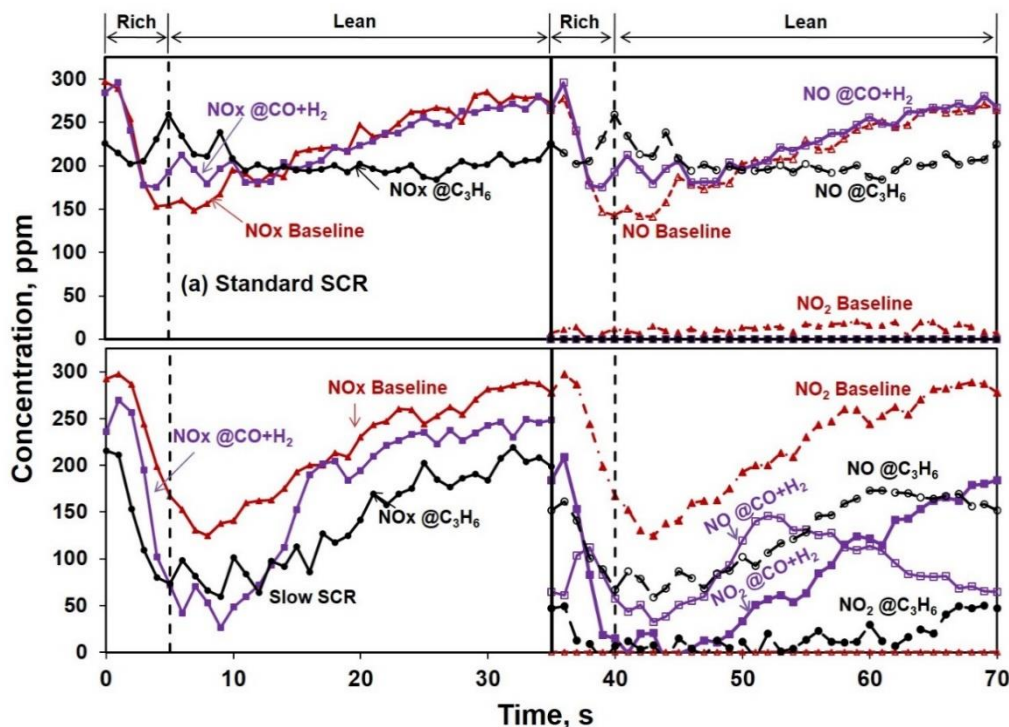


Fig. 4-14 Effluent gas concentration during (a) standard and (b) slow SCR reactions under cyclic condition at 350 °C when NH_3 and either C_3H_6 or H_2+CO are present in the rich phase.

Fig. 4-13 compares the effects of $\text{CO} + \text{H}_2$ and C_3H_6 in the rich phase on the cycle-averaged NO_x conversion. To simplify the study, we have combined the addition of CO with H_2 . Contrary to the steady-state operation for which a negative effect of C_3H_6 was encountered on almost all NH_3 -SCR reactions, except for the low-temperature region of slow SCR reaction, C_3H_6 has a significantly positive impact under cyclic conditions. In Chapter 3, we found that cyclic operation can help mitigate the C_3H_6 poisoning effect due to the removal of organic intermediates through their reaction with NO_x and/or O_2 during the lean phase. This purge contributes to additional NO_x reduction via HC-SCR pathway. Both mitigated C_3H_6 poisoning and additional HC-SCR contribution enhanced NO_x conversion under cyclic condition. This is consistent with the report by Kim et al. [52] of the additive contribution of C_3H_6 and NH_3 to cycle-averaged NO_x reduction during the

standard SCR reaction. $\text{CO} + \text{H}_2$ addition enhances the NO_x conversion but to lower extent for both fast and slow SCR.

Fig. 4-14 shows the periodic temporal effluent concentrations of NO_x , NO , NO_2 for standard and slow SCR reactions at 350 °C. The total NO_x ($\text{NO} + \text{NO}_2$) concentration profiles in one cycle are shown in the left half of the figures, while the right half describes the individual NO and NO_2 profiles. No NH_3 slip happens in any of the cases. Fig. 4-14a shows that the addition of $\text{CO} + \text{H}_2$ during standard SCR reaction has a very minor effect on all baseline NO_x , NO and NO_2 profiles. This is expected because, as shown in Fig. 4-1, CO and H_2 do not react with $\text{NO} + \text{O}_2$. In contrast, C_3H_6 introduction affects the NO_x transient behavior. For the baseline case, the NO_x concentration peaks at the end of the lean phase and drops to its lowest level at the onset of the lean phase. It then gradually increases due to the depletion of stored NH_3 . In contrast, when C_3H_6 is fed, the NO_x concentration peaks at the end of rich phase and then gradually decreases and stabilizes during the lean phase. The accumulation of propene itself or its oxidized intermediates during the rich feed inhibits the NH_3 -SCR pathway. NO_x reduction by NH_3 is retarded and this delays the appearance of NO_x peak at the end of the rich phase. The removal of those intermediates by NO_x and O_2 during the early stage of the lean phase enables the HC-SCR and NH_3 -SCR reactions to gradually decrease the NO_x slip.

For the slow SCR conditions in Fig. 4-14b, all three cases exhibit similar transient NO_x concentration. The smallest NO_x slip occurs for C_3H_6 , followed by $\text{CO} + \text{H}_2$ feed and the baseline case. The higher reactivity of C_3H_6 with NO_2 is higher than that with $\text{NO} + \text{O}_2$, decreasing the smaller amounts of surface intermediates blocking the active sites. Thus, a high NO_2/NO_x ratio can alleviate C_3H_6 poisoning and enable both the HC-SCR and NH_3 -

SCR pathways to proceed without interfering with each another. The lower NO_x slip for the CO + H₂ case, is consistent with their capability to convert NO₂ to N₂ (Fig. 4-2). The temporal NO and NO₂ profiles reveal that only NO₂ breakthrough occurs for the baseline case over the entire cycle, while considerable NO slip occurs for both C₃H₆ and CO + H₂ cases. For C₃H₆ feed case, C₃H₆ and its derivatives stored during the rich feed, continue to promote NO₂ reduction in the ensuing lean feed. For CO + H₂ feed case, since their adsorption on this catalyst is negligible (data not shown), the high amount of surface nitrites formed from nitrates reduction by CO and H₂ during the rich feed is the main cause for the NO production (R4-8) in the lean phase.

4.7 Conclusions

We investigated the roles of CO, H₂ and C₃H₆ reductants in reactions with NO_x, NH₃ storage and oxidation, as well as in NH₃-SCR reactions over a commercial Cu-chabazite SCR catalyst. The main findings are:

- C₃H₆, CO and H₂ promote NO₂ reduction to NO to different extents by distinct pathways. C₃H₆-assisted NO₂ decomposition is the most effective, occurring via organic intermediates. CO reduces nitrates to nitrites that then rapidly react with NO₂ to produce NO. H₂ follows the same nitrate-related pathway as CO for NO₂ reduction but is less effective. H₂ can also reduce Cu cations to metallic Cu that catalyzes H₂-SCR of NO_x to N₂ and NH₃ at high temperatures and under anaerobic condition.
- For NO₂ reaction with H₂, high oxygen levels and low temperatures favor the nitrate-related NO₂ reduction pathway. The opposite trend drives reduction pathway towards H₂-SCR.

- C_3H_6 affects NH_3 -SCR reactions mainly by its interaction with NO_2 . Its main role is to compete with NH_3 for adsorbed NO_2 to produce oxygenates, and release NO . Thus, an increasing NO/NO_x ratio changes the dominant NH_3 -SCR pathway. For example, contingent on the temperature range, a slow SCR reaction can be changed to either a fast or a standard SCR condition.
- CO competes with NO for nitrates decomposition to nitrites, leading to a negligible impact on standard and fast SCR pathways but a positive effect on slow SCR reaction.
- During lean/rich cycling, C_3H_6 addition in the rich phase has a significantly positive effect, increasing cycle-averaged NO_x conversion over the entire temperature range. Both high NO_2/NO_x ratio and sufficiently long lean-phase purge can greatly mitigate propene poisoning, enabling an additive contribution of both HC- and NH_3 -SCR pathways. CO and H_2 also enhance the cycle-averaged NO_x conversion but to a smaller extent.
- All three reductants can limit N_2O production during the slow SCR reaction. This is attributed both to the inhibition of NH_4NO_3 formation or the promotion of NH_4NO_3 consumption.

Chapter 5 Rapid C₃H₆ pulsing for enhanced low temperature NO_x conversion on combined LNT-SCR Catalysts

5.1 Introduction

Toyota researchers reported in recent years an interesting technology called “Di-Air” (standing for diesel NO_x aftertreatment by adsorbed intermediate reductants) that achieves much higher NO_x conversion over a LNT catalyst at elevated temperatures [25, 66]. The unique operational feature of Di-Air is the high frequency injection of HC into a lean exhaust stream with cycle times shorter than ~ 5s flowing continuously over a LNT catalyst. The enhanced NO_x conversion performance was attributed to adsorbed, N-containing HC intermediates, which are generated during the high-frequency HC pulsing, through reaction between adsorbed NO_x and partially oxidized hydrocarbons. These short-lived intermediates are readily converted through reaction with surface and/or gas phase NO_x species to N₂ during the lean part of the cycle. Bisaiji et al. [26] further showed that the high-temperature NO_x conversion of the Di-Air using HC reductant was superior over that of using H₂ or CO. Compared to NSR, the Di-Air operation shifts the N₂ formation from one that occurs primarily during the rich phase to one that primarily occurs during the lean phase. The system was demonstrated to significantly improve the deNO_x performance under high-temperature and high-SV operations conditions for which conventional NSR (cycle time 0.5-2 min) performs unsatisfactorily. In a recent study our group found that fast cycling of propylene enhanced the deNO_x activity of LNT catalysts even at low temperatures, albeit to a smaller extent than at high temperatures [27].

A definitive mechanism has yet to be established for the Di-Air process although progress is being made. A mechanism proposed by Toyota researchers is similar to the aforementioned “non-NH₃” pathway encountered with the LNT-SCR system. Both involve the formation of HC intermediates (C_xH_yO_z, C_xH_yO_zN_i) through reaction of adsorbed NO_x and oxygenated hydrocarbon species that accumulate on the LNT catalyst during the rich purge. Zheng et al. [67] showed that these surface HC intermediates play an important role in the low-temperature NO_x conversion enhancement in the combined LNT-SCR system. Our recent preliminary study showed that a Di-Air process with high-frequency HC pulsing can benefit a combined LNT+ passive SCR system, especially at low temperatures [68].

The aim of this chapter is to gain insight into the working mechanism of rapid propylene pulsing on integrated LNT-SCR catalysts, with the objective to expand the operating temperature window of a conventional NSR system. We investigate the effects of cycle timing (NSR and Di-Air operation), exothermic heat effects, SCR catalyst types (Cu-zeolites and Ag/Al₂O₃), and loadings of Ceria and PGM, on the catalyst system performance in terms of catalytic activity, product distribution and catalyst durability. An overall mechanism for fast HC pulsing on both standalone LNT and combined catalysts is proposed based on recent data and new data. We also show how the deNO_x performance may be enhanced through catalyst configuration design, i.e., layering and zoning.

5.2 Experimental

5.2.1 Catalysts

The monolithic LNT catalysts provided by BASF (Iselin, NJ) have a cell density of 400 cpsi (cells per square inch) and washcoat loading of 4.6 g/in³ monolith, corresponding to a peripheral-averaged thickness of ~80 μm. The catalyst contains

Pt/Rh/BaO/CeO₂/Al₂O₃ with an overall PGM (precious group metal) loading of 90 g/ft³ monolith, 15 wt.% (washcoat basis) BaO and 34 wt.% CeO₂ on a γ -alumina support. In some experiments, a LNT with the same specifics except for no CeO₂ addition was used which was also provided by BASF. Small cylindrical catalyst samples (~55 channels, D = 0.42 in, L = 1 in) were drilled out of a large brick. The in-house synthesized small-pore Cu-SAPO-34 with chabazite (CHA) framework and Ag (2 wt.%)/Al₂O₃ catalyst powders were prepared via solid-state ion exchange [69] and incipient wetness impregnation methods [8], respectively. The as-prepared catalyst powder was washcoated onto the LNT monoliths by a dip-coating technique. A uniform washcoat layer of 0.8-0.9 g/in³ was deposited on top of the LNT layer creating dual-layer catalysts (LNT-SCR, LNT-Ag/Al₂O₃). All catalysts were aged at 700 °C for 33 hours in air, equivalent to 160,000-km aging, prior to bench reactor experiments [25].

5.2.2 Reactor system

The set-up comprised four major components: gas supply, tubular reactor, analytical and data acquisition systems. The flow reactor utilized synthetic exhaust gas mixtures from cylinder-supplied gases (Praxair). Gas flow rates were controlled by mass flow controllers (MKS Instruments). Water was fed by a syringe pump (ISCO Model 500D) and vaporized in a heated line. In all experiments, the total gas flow was 3000 cm³/min, corresponding to a gas hourly space velocity (GHSV) of ca. 74,000 h⁻¹ at standard conditions. The gases were pre-mixed in three separate lines; one line contained inert species (CO₂, H₂O, Ar), another the lean feed components (NO, O₂, Ar), and a third the rich feed components (NO, O₂, C₃H₆, Ar). The monolith catalyst core sample was wrapped with Fiberfrax® ceramic paper and inserted into a quartz tube (OD = 0.75 in.) positioned

inside a ThermocraftTM tube furnace. Local feed gas and catalyst temperatures were measured using two K-Type thermocouples (Omega Engineering Inc.). One thermocouple was placed 0.5 in. upstream of the catalyst to monitor the feed temperature (T_f), while another was positioned at the midpoint of the monolith (radial and axial) to measure the temperature at the center of the catalyst (T_c). Note that T_c is a dependent variable, which varied markedly during the aerobic regenerations. The outlet gas stream flowed through a heated line at ca. 190 °C to the MultiGas 2030 FTIR (MKS Instruments), which measured concentrations of NO, NO₂, N₂O, C₃H₆, NH₃, HCHO, HNCO, CO, CO₂ and H₂O.

A solenoid actuated four-way valve (Valco Inc., Micro-electric two position valve) generated the high-frequency propylene pulses via fast switching between lean and rich feeds. The lean and rich feeds were connected to the inlets of the switching valve, while one outlet of the valve was connected to the main gas line just upstream of the catalyst sample and the other to the vent. The flow rate of the inert gas in the main line was kept at 800 cm³/min, lower than the 2200 cm³/min for the lean or rich reactive feed. The main purpose was to guarantee that the correct amount of reactive feed was injected during the fast switching. HC premixed in the rich line also helps avoid flow maldistribution. This was important as Toyota researchers recently pointed out that high radial uniformity of HC concentration was essential for Di-Air performance [70]. In order to minimize upstream axial mixing of lean and rich streams, the switching valve was placed close to the monolith catalyst (~ 0.6 m upstream), but sufficiently far to enable sufficient preheating of the feed stream. We found that too long a distance between the switching valve injection point and the catalyst resulted in an unacceptable level of axial mixing due to dispersion in the tubing. The axial mixing decreased NO_x conversion during high frequency operation. (We did not

investigate in detail this design variable in the current study so the 0.6 m distance may not be the optimal value.). The injection valve, thermocouples and MFCs were all controlled and monitored using LABVIEWTM software. Time delays between the feed point, reactor and the analytical equipment were accounted for in the data processing through tracer measurements.

Table 5-1 Gas condition for baseline cycling test

Gas	Lean	Rich
NO	300 ppm	300 ppm
C ₃ H ₆	—	1.8%
O ₂	10%	5%
CO ₂	5%	5%
H ₂ O	3.5%	3.5%

Lean-rich cycling experiments were conducted over either the LNT only, LNT-SCR dual-layer, LNT-Ag/Al₂O₃ dual-layer or LNT-SCR dual-brick catalysts. Table 5-1 describes the cycling conditions. Three different cycle timing protocols, 60s lean/10s rich, 30s lean/5s rich, and 6s lean/1s rich, were used. The 60/10 and 30/5 timing are representative of conventional NSR operation while the 6/1 is representative of high-frequency NSR (simulated Di-Air). Due to the system limitation (switching delay time, mixing design to get rectangular plug flow HC pulses) higher injection frequency could not be realized. In the Di-Air process studies of Toyota the air:fuel ratio (A/F) was varied periodically through reductant injection into a flowing lean gas. To mimic this approach, we used a high O₂ concentration of 10%, typical of real diesel exhaust, in the lean feed and

5% in the rich feed. Previous studies found that a rich duty cycle (rich phase duration divided by total cycle time) of ~ 14% achieved a high NOx conversion [71]. Hence, this value was used in all cycling experiments. The stoichiometric number is the molar ratio of the oxidizing to reducing components:

$$S_N = \frac{2[O_2] + [NO]}{9[C_3H_6]} \quad (5-1)$$

A S_N value greater than unity represents a lean mixture, whereas a S_N value less than unity represents a rich mixture. $S_{N,p}$ and S_N denote the stoichiometric number of the feed stream during the rich pulse and the cycle-averaged value, respectively. At each temperature the final ten periodic cycles were averaged after the system reached a periodic state to determine the cycle-averaged NOx and C₃H₆ conversions, product selectivities and T_c [27].

Prior to testing, each catalyst was pretreated by exposing it at 400 °C for 15 min to lean/rich 30/5s and 6/1s cycling conditions, respectively. Different pretreatment methods caused different low-temperature cycle-averaged NOx conversions with the above periodic lean/rich pretreatment superior to that following an oxidative pretreatment (i.e., 5% O₂ for 30 min).

5.3 Effects of combining rapid propylene pulsing with SCR layer addition

Fig. 5-1a compares the cycle-averaged NOx conversion over the standalone LNT catalyst as a function of the feed temperature for cycle times spanning 60/10s to 6/1s for a fixed rich duty cycle (14.3%). The dual-layer LNT-SCR catalyst at the fastest cycling (6/1s) is shown for comparison. For each of the cases the NOx conversion exhibits a rather broad

maximum over a range of feed temperatures. The extent of the fall-off at low temperature is a sensitive function of the cycle timing and SCR top-layer.

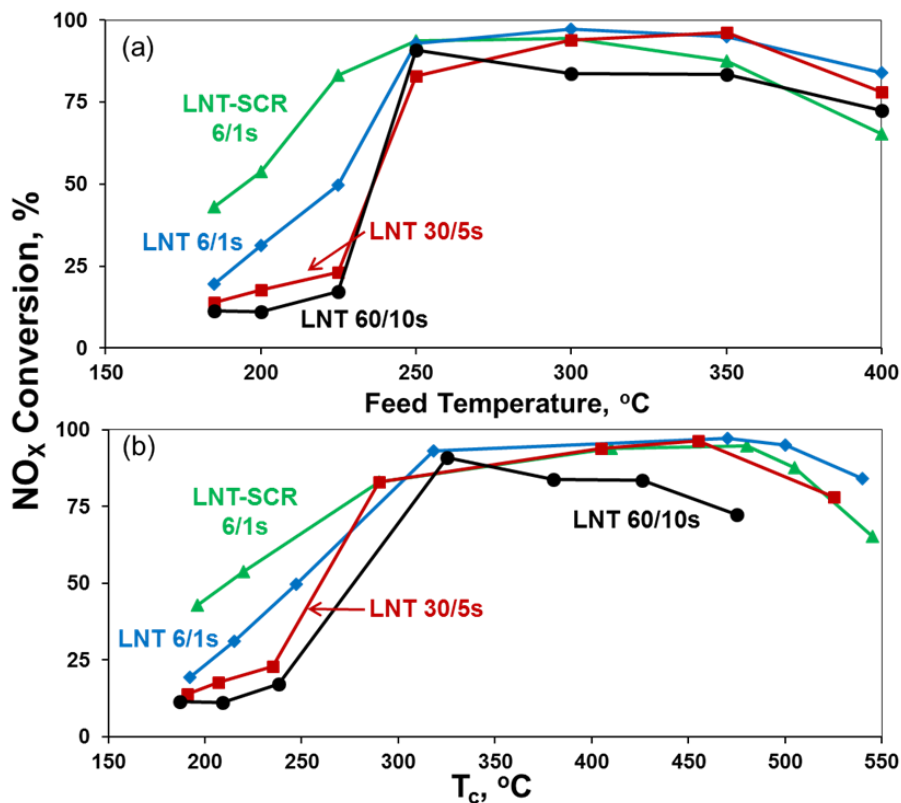


Fig. 5-1 Cycle-averaged NO_x as a function of (a) feed temperature and (b) temperature at the center of monolith, T_c , for LNT alone and dual-layer catalysts with different cycle times.

For the longest cycle time the LNT has a NO_x conversion exceeding 80% between 250 and 350 °C. For feed temperatures below 225 °C the conversion is 10-20% while at 400 °C the conversion is ~70%. As the cycle time is shortened to 30/5s and 6/1s, both the low and high-temperature NO_x conversions increase with the larger increase occurring at low feed temperatures (≤ 250 °C). Finally, adding a Cu-SCR top-layer combined with fast propylene pulsing further increases the low-temperature NO_x conversion. The combination of fast cycling and SCR top-layer decreases the light-off temperature by ca. 50 °C below

that of the standalone LNT with 60/10s cycle timing. For example, for a feed temperature at 225 °C, a 80% NO_x conversion was achieved for the dual-layer with rapid injection, compared to 51% and 24% conversion for the standalone LNT with the fast (6/1s) and slower (30/5s) cycling, respectively. We expand on the noted low temperature enhancement by the faster cycling and addition of the SCR layer below. At high feed temperature (400 °C) faster cycling enhances the NO_x conversion for the standalone LNT, consistent with previous studies [25]. However, addition of the SCR top-layer decreases the NO_x conversion. This decrease is primarily attributed to increased mass transfer resistance which limits C₃H₆ supply to the underlying LNT layer.

The exothermic oxidation of propylene occurs during the propylene injection, and therefore non-isothermal behavior is expected. Kabin et al. [72] reported significant temperature excursion of up to 150 °C during conventional NSR using propylene as a reductant in cases when the rich feed contained up to 5% O₂. Epling et al. [73] reported an evolving and non-uniform axial temperature profile along the LNT monolith owing to the rich purge. This affected the dynamic NO_x storage capacity during a cycle period. Fig. 5-1b shows the same cycle-averaged NO_x conversion plotted as a function of the corresponding cycle-averaged T_c (at the monolith center). A comparison of Fig. 5-1a and 5-1b reveal an expansion in the temperature range due to the substantial temperature rise after ignition (T_f > 225 °C). Although T_c spans a broader temperature window than T_f, the same qualitative trends in the data are apparent. One notable difference is the more significant difference in the high temperature NO_x conversions for the different cycle times. These trends are in line with results reported by Bisaiji et al. [25]. It is noted that the actual

temperature of the catalyst (washcoat) at the monolith midpoint is likely higher than the local gas phase temperature because of gas-to-solid heat transfer limitations.

5.3.1 Effect of rapid propylene injection

Detailed information on the effect of cycle timing is gotten from the instantaneous concentration and temperature profiles. Fig. 5-2 shows the transient effluent NO_x (C₃H₆) concentration and catalyst temperature at the low feed temperature of 225 °C. The first and second columns of the figure are for the standalone LNT with 30/5s and 6/1s cycle timing, respectively. The third column shows results for the LNT-SCR dual-layer catalyst which we discuss later.

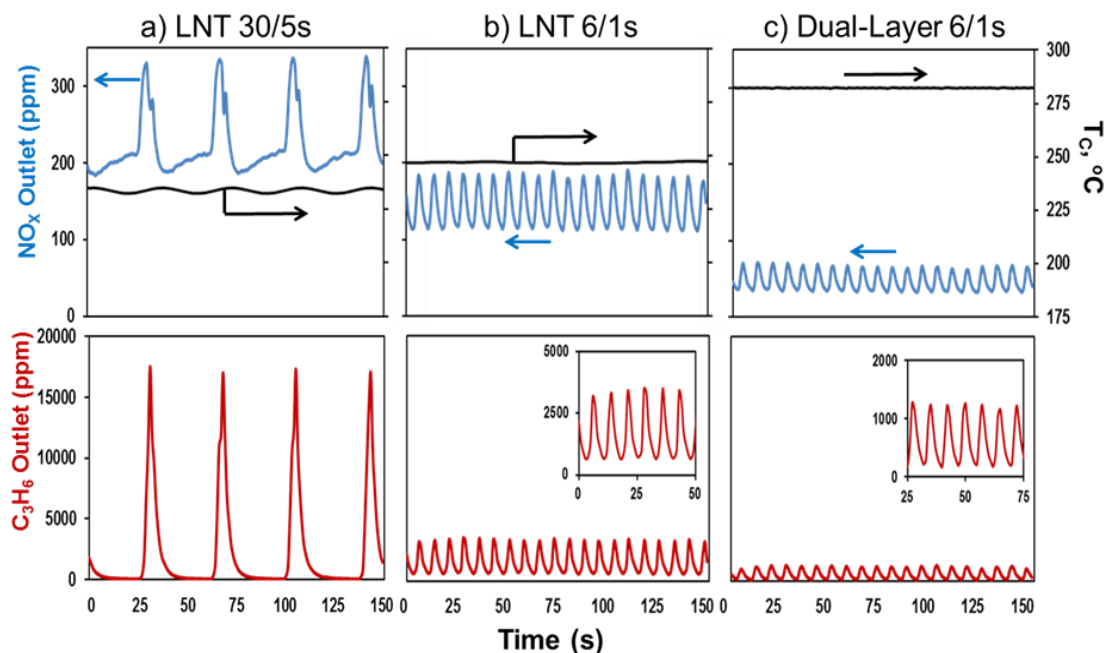
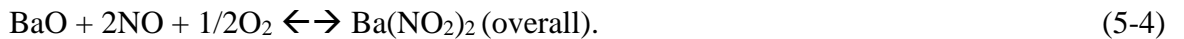


Fig. 5-2 Effluent NO_x/C₃H₆ concentration and catalyst temperature for a set of cycling experiments at 225 °C feed temperature over LNT and dual-layer catalysts.

The cycle-averaged NO_x conversions for the two LNT cases are ~24 and 51%, respectively, while the corresponding cycle-averaged C₃H₆ conversions are ~8 and 40%, respectively. Under the slower NSR cycling (30/5s), NO_x breakthrough gradually increases

during the lean period, followed by a sharp NO_x spike upon switching to rich phase. This trend is typical of conventional NSR operation. Generally, the inefficient low-temperature NO_x conversion is a result of low rates of NO oxidation, NO_x storage, and/or incomplete regeneration. Forzatti et al. [30] suggested that the slow diffusion of NO₂ from Pt to distant BaO storage sites accounts for the slower uptake of NO_x at the later stages of the lean phase. In this context, proximal adsorption sites quickly saturate first then the storage slows down due to the longer diffusion distances on the surface or in the bulk of BaO/BaCO₃ particles. Thus, a prolonged lean phase leads to considerable NO_x slip as observed (Fig. 5-2a). Epling et al. [39] attributed the inefficient low-temperature rich purge using hydrocarbon reductants to both slow kinetics of propylene reaction with the stored NO_x and Pt site poisoning by hydrocarbon intermediates, limiting the regeneration extent.

Lower NO_x and C₃H₆ effluent concentrations are observed along with a higher and steadier catalyst temperature (see middle column of Fig. 5-2) upon increasing the cycling frequency (6/1s). Lietti et al. [74] suggested that at low temperatures NO may be stored in the form of nitrites and that this mechanism requires the cooperative interaction between Pt and nearby storage materials. This mechanism involves the following sequential steps:



This mechanism known as nitrite pathway does not require the formation of NO₂. This suggests that under fast cycling, NO uptake would only be possible through a fast pathway so that only kinetically accessible storage sites would be utilized. That is, fast cycling mitigates the kinetic challenge of low-temperature NO_x uptake by confining NO_x

storage to surface Ba sites in close proximity to Pt via a spillover process. The fraction of Ba that effectively participates in the storage process is smaller than during conventional NSR operation. This diminishes the importance of NO_x storage capacity that is gradually reduced with elevated temperature, thereby extending the operating window to high temperatures (> 400 °C) as shown in Fig. 5-1 and in the Toyota reports [25]. Perng et al. [27] showed that storage and reduction under fast cycling experiments is less sensitive to CO₂. They argued that this is evidence for a NO_x reduction mechanism that does not rely on NO_x storage on BaCO₃ sites that are less effective in trapping NO_x than BaO or Ba(OH)₂.

Once the proximal storage sites are saturated, a short propylene pulse is injected to purge stored NO_x. Bisaiji et al. [25] proposed that the rapid HC pulsing plays a pivotal role in the Di-Air reaction pathway. HC efficiently reacts with adsorbed NO_x and O₂ over Pt to generate N-containing intermediates (denoted by C_xH_yO_zN_t) which can be stabilized by the nearby basic oxide (BaO) component and retained on the catalyst surface until the end of a sufficiently short rich phase. Such active intermediates are then either converted to N₂ directly or react with adsorbed and/or gaseous NO_x generating N₂ during the subsequent lean period. Bisaiji et al. [26] further conducted an *in operando* XAFS (X-ray Adsorption Fine Structure) study to monitor the valence state of Pt and determined that HC intermediates are capable of maintaining Pt in a metallic state through scavenging O adatoms even within several seconds (up to ~ 4s) into the subsequent lean phase. In other words, Pt is kept in a reduced state all the time under rapid HC pulsing. The presence of reduced Pt sites may imply a different pathway via the direct NO decomposition on metallic Pt sites as reported by Burch et al. [38], compared to Toyota's pathway involving organo-

nitrate species as key intermediates. In either pathway, the initial formation of partially oxidized HC intermediate is critical. Bisaiji et al. [25] reported that a high injection frequency sustains the gas phase O_2 at a higher level and that this promotes propylene oxidation, given the positive reaction order with respect to O_2 for propylene oxidation. It is noted that the high ceria content (34 wt.%) in the LNT catalyst used in the current study also acts as oxygen buffer to maintain surface oxygen concentration. The functionality of ceria for fast cycling is further discussed later. In summary, fast injection of propylene encounters relatively high-levels of both stored and gaseous O_2 . This enables improved utilization of the propylene reductant, evidenced by the much lower C_3H_6 breakthrough. In addition, better propylene oxidation results in higher catalyst temperature which, in turn, benefits efficient NO_x storage and regeneration, especially at low temperatures.

5.3.2 Effect of Cu-SAPO-34 top-layer

The deposition of a Cu-SCR layer and fast cycling leads to an even higher NO_x and C_3H_6 conversion. As shown in the right column of Fig. 5-2, the addition of a Cu-SAPO-34 top-layer to the LNT catalyst while maintaining the 6/1s cycling results in a noted drop in the NO_x and C_3H_6 effluent concentrations. The cycle-averaged NO_x conversion is ~ 80%, an absolute increase of 29% from the standalone LNT under fast cycling. Moreover, the resulting T_c is higher by over 30 °C. Due to the higher oxygen level and short rich duration, negligible NH_3 slips from the LNT upon fast cycling over the almost entire temperature range [68]. Thus, the classic NH_3 -pathway cannot account for the increased NO_x conversion on the dual-layer catalyst.

An alternative mechanism for the LNT + SCR system that does not require NH_3 was advanced by Ford researchers [75]. Bisaiji et al. [25] reported the detection of several

stable gas phase intermediates in LNT effluent during rapid HC pulsing, including amines (CH_3NH_2 , $\text{C}_2\text{H}_5\text{NH}_2$, NH_2OH), carboxylic acids (HCOOH , CH_3COOH) and aldehydes (CH_3CHO). In the current study, we observed both HCHO and HNCO in the effluent during fast cycling to the standalone LNT catalyst at a feed temperature of 225°C . Other propene oxidation derivatives in addition to HCHO and HNCO are likely to exist but only HCHO and HNCO were reported due to measurement limitations. It is expected that such intermediates released from the LNT may be trapped and utilized as reductants in the SCR top-layer via a HC-SCR pathway. These species have been previously reported as NO_x reductants via a HC-SCR pathway on zeolite catalysts [43, 46, 76]. For example, Peden et al. [77] reported that the partially oxidized propylene species are more active than propylene for NO_x reduction over Ba- or Na- exchanged zeolite catalysts. In fact, a feed containing aldehyde species like HCHO , CH_3CHO , etc., included in a lean NO_x stream resulted in 80% NO_x conversion over a BaY zeolite catalyst at 200°C . This supports our conjecture that the added SCR layer can utilize released intermediates for additional NO_x reduction.

To gain further insight into the catalytic oxidation chemistry, DRIFTS measurements were conducted to identify and monitor the evolution of surface organic intermediates over powder LNT and SCR catalysts. The DRTFTS spectra of Fig 3-7 in Chapter 3 shows the temporal changes of the in situ DRIFTS spectra when exposing a NO_x pre-adsorbed LNT to a feed of $0.1\% \text{C}_3\text{H}_6 + 1\% \text{O}_2$ at 200°C . After a 1h pre-conditioning, the catalyst was exposed to a feed containing 500 ppm $\text{NO} + 5\% \text{O}_2$. Three intense peaks were observed at 1270 , 1300 and 1575 cm^{-1} , which can be assigned to the bulk nitrates, surface nitrites and surface nitrates, respectively [32, 41]. Upon the introduction of

propylene the spectra exhibited a temporal decrease in the intensity of the surface nitrates peaks at 1300 and 1575 cm^{-1} , and a near-simultaneous evolution of four new bands at 1650, 1680, 2190 and 2215 cm^{-1} . Compared to the nearly constant peak at 1270 cm^{-1} corresponding to bulk nitrates, the dramatic decrease in the spectral intensity of the surface nitrates peak suggests that NO_x stored at surfaces sites close to the Pt are prone to conversion at low temperatures. The bands at 1680, 2190 and 2215 cm^{-1} are assigned to C=N stretching vibration of acetone oxime [43], isocyanate (R-NCO) over barium [44] or cyanide species (R-CN) over alumina [45], and surface isocyanate over alumina [44], respectively. Thus, these surface species measurements together with the gas phase species HNCO and HCHO, as well as the additional species reported by Toyota researchers suggest either a direct release or hydrolysis of activated surface intermediates over the LNT during the rapid HC pulsing into a lean NO_x stream.

Fig. 5-3 shows the temporal DRIFTS spectra when exposing a NO_x pre-adsorbed SCR catalyst to a feed of 0.1% C_3H_6 + 1% O_2 at 200 °C in a separate experiment. The SCR powder used here is Cu-SSZ-13 provided by BASF. Its performance is comparable to our in-house synthesized Cu-SAPO-34 [69]. After feeding propylene for 5 min, a band at 2278 cm^{-1} corresponding to R-CN [62] appears. Prolonged propylene exposure for 30 min results in a decrease in this peak intensity, accompanied with a gradual evolution of two new peaks at 2218 and 2254 cm^{-1} that can be assigned to R-NCO on Cu^+ and zeolite, respectively [61]. About 1 h after propylene admission, the peak for R-CN disappears and peaks for R-NCO stabilize at higher intensities. Isocyanates are well recognized as active intermediates that can rapidly hydrolyze to produce NH_3 or amine to further reduce NO_x . The spectra clearly indicate a slow evolution of surface organic intermediates from R-CN (2278 cm^{-1}) towards

R-NCO (2218 and 2254 cm^{-1}). Compared to nearly immediate evolution of R-NCO species on the LNT, the time taken to form R-NCO on the SCR is much longer. This suggests the formation of NCO may be the RDS for the HC-SCR pathway on the Cu-CHA catalysts, especially at low temperature. Thus, we speculate that the activated HC intermediates provided by the LNT facilitate the formation of R-NCO on the Cu-CHA catalyst, thereby promoting the LNT-assisted HC-SCR reaction. This hypothesis is consistent with the non- NH_3 pathway proposed by Ford researchers [11].

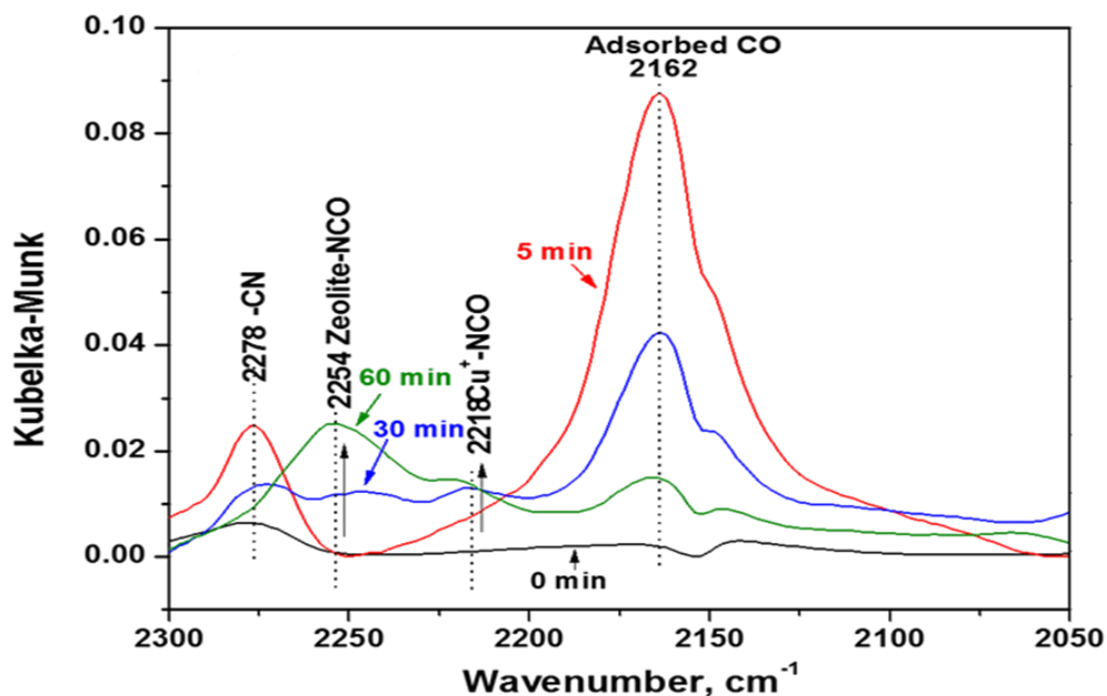


Fig. 5-3 Temporal DRIFTS spectra over SCR catalyst taken at $200\text{ }^{\circ}\text{C}$ after a 1h pre-conditioning by 500 ppm NO + 5% O_2 and purge with He, subsequently exposed to a flow of 0.1% C_3H_6 + 1% O_2 .

5.4 Effect of ceria in LNT layer

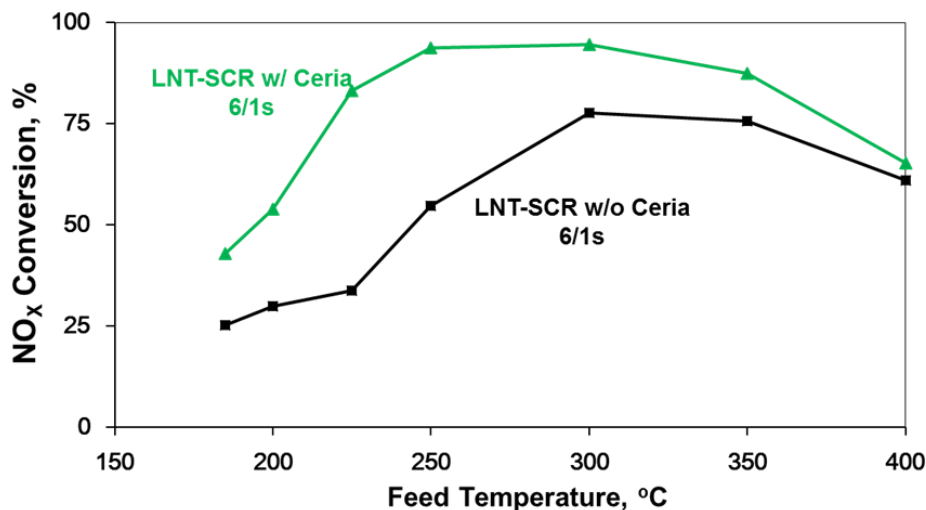


Fig. 5-4 Cycle-averaged NO_x as a function of feed temperature for dual-layer catalysts with and without ceria under fast cycling.

Fig. 5-4 compares the NO_x conversion as a function of feed temperature under fast cycling obtained with two dual-layer catalysts, one with the same LNT formulation having ceria and the second without ceria. The effect of ceria is marked: in its absence the cycle-averaged NO_x conversion is significantly lower over the entire feed temperature range. A large number of previous studies have shown the important role of ceria in automotive emission control, including oxygen storage capacity, low-temperature NO_x storage and stabilization of Pt dispersion, etc [35, 78]. As suggested earlier, ceria supplies oxygen to promote the oxidation of propylene to form surface intermediates that are critical for fast-cycling performance. Yi et al. [24] reported that ceria enhanced the resistance of LNT-SCR dual-layer catalysts to thermal aging by suppressing the migration of Pt and BaO from underlying LNT to the top SCR layer. Recently, Kapteijn et al. [79] argued that ceria might provide active sites for NO_x reduction under fast cycling conditions. Using Temporal Analysis of Products (TAP) they showed that propylene reduces the ceria surface layer

from Ce^{4+} to Ce^{3+} , thereby creating surface layer oxygen vacancies that are active for NO decomposition to N_2 . It is speculated that HC surface species act to maintain the reduced state of surface ceria rather than directly reacting with surface NOx species [79]. Further study is needed, especially operando monitoring of ceria valence state under realistic Di-Air condition and interaction of ceria with Pt and basic storage material. At any rate, ceria certainly plays a crucial role in the activity and durability of LNT and dual-layer catalysts under fast cycling operation.

5.5 Effect of top-layer material

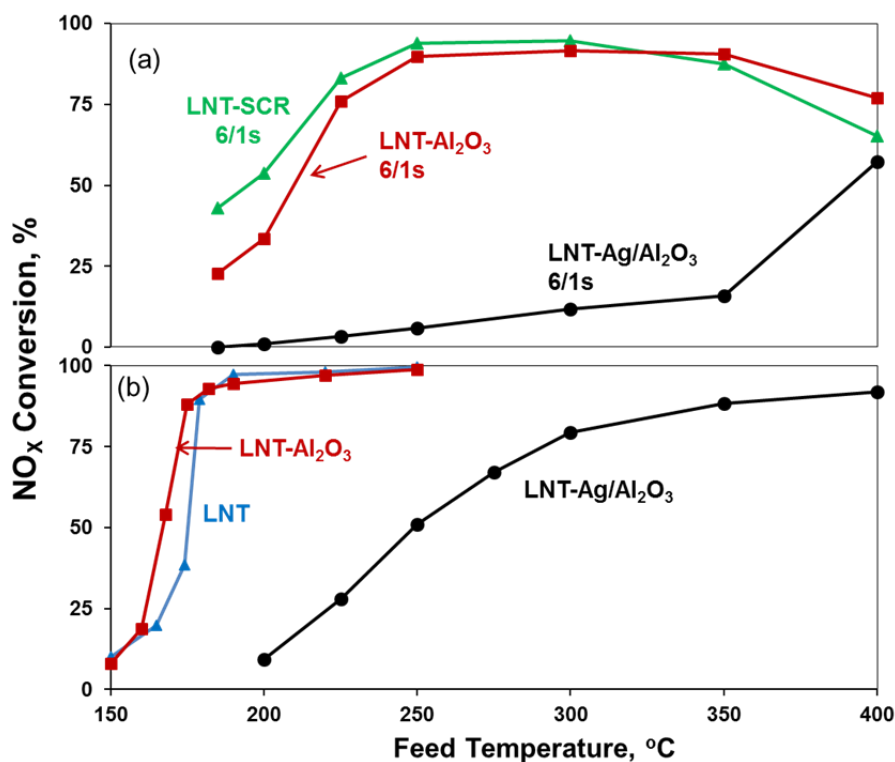


Fig. 5-5 a) NO_x conversions as a function of feed temperature for dual-layer catalysts with either Cu-SAPO-34 or γ -Al₂O₃ or Ag/Al₂O₃. b) Propene oxidation over LNT, LNT-Al₂O₃ and LNT-Ag/Al₂O₃ catalysts

Based on our hypothesis that the added SCR top-layer utilizes hydrocarbon intermediates generated and released from the underlying LNT layer via a HC-based SCR

pathway, we compared the performance of three top-layer materials: Cu-SAPO-34, γ -Al₂O₃ and Ag/Al₂O₃. The Cu-exchanged aluminosilico phosphate SAPO-34 is of interest because it and the related Cu-exchanged SSZ-13 zeolite have very high NH₃-based SCR activity. Ag/Al₂O₃ is of interest because it is a known effective HC-SCR catalyst [80]. The use of unimpregnated γ -Al₂O₃ is intended to check whether the NO_x conversion enhancement might be the result of storage and transport effects only. Fig. 5-5a compares the cycle-averaged NO_x conversions of dual-layer catalysts with the three top-layer materials. The data show that the Cu-SAPO-34 top-layer has the highest NO_x conversion at feed temperatures below 300 °C while the γ -Al₂O₃ top-layer has the highest NO_x conversion at high temperatures (≥ 350 °C) among all the samples.

We consider first the γ -Al₂O₃ results. The lower NO_x conversion obtained with the γ -Al₂O₃ top-layer for $T_f \leq 300$ °C compared to Cu-SAPO-34 top-layer is undoubtedly a result of the lower HC-SCR activity. The added γ -Al₂O₃ top-layer slightly enhances the low-temperature NO_x conversion of LNT. This follows from the study of Panov et al. [77] who reported that γ -Al₂O₃ is able to catalyze the reduction of NO_x by aldehydes, even though less effectively than metal-exchanged zeolite catalysts. This probably in part accounts for the minimal enhancement. In contrast, its higher high-temperature NO_x conversion is attributed to its lower propylene oxidation activity. This enables more propylene to access to the underlying LNT layer.

The results obtained with the Ag/ γ -Al₂O₃ top-layer are somewhat surprising and would appear to contradict the explanations just provided for the selection of γ -Al₂O₃ top-layer. A dramatic performance decline was observed for the dual-layer LNT-Ag/Al₂O₃ catalyst spanning the entire temperature range. Ag/Al₂O₃ is generally regarded as an

effective HC-SCR catalyst so one would expect NO_x reduction chemistry to occur in the top-layer. Rather, it appears that there is significant negative interaction between Ag/Al₂O₃ and LNT layers, apparently from the migration of Ag ions to the LNT base layer. To prove this conjecture, Fig. 5-5b shows the steady-state propylene oxidation light-off for the standalone LNT, LNT-Al₂O₃ and LNT-Ag/Al₂O₃ dual-layer catalysts (1111ppm C₃H₆, 1% O₂, 3.5% H₂O, 5% CO₂). While the LNT and LNT-Al₂O₃ catalysts have similar light-off results, the presence of Ag in the top-layer significantly inhibits the propylene oxidation as evidenced by the increase in the light-off temperature by almost 100 °C. This suggests the poisoning effect of Ag on LNT catalyst, probably due to Ag migration to underlying LNT layer and block Pt sites, especially after high-temperature thermal aging. Further catalyst characterization is needed to verify the deactivation mechanism and will be reported elsewhere.

5.6 N₂O yield and selectivity

One of the challenges with conventional NSR operation is the relatively high levels of N₂O generated at low to intermediate temperatures, especially compared to NH₃-based SCR on metal-exchanged zeolites. N₂O is relatively stable in the atmosphere and is a potent greenhouse gas with a global warming potential ~300 times that of CO₂. The recently enacted US EPA 2017-25 greenhouse gas regulations will require the reduction of N₂O from LD and HD vehicles. Fig. 5-6 shows the N₂O selectivity and yield under both conventional and fast cycling on both single-layer LNT and dual-layer catalysts. For the standalone LNT, the use of fast cycling increases the N₂O selectivity and yield. These data are consistent with the earlier findings by Perng et al. [27]. Interestingly, the addition of the SCR top-layer lowers the N₂O selectivity under fast cycling. This is probably due to lower

N₂O selectivity for NO_x reduction by SCR than LNT catalysts. This encouraging result provides additional incentive for the proposed fast cycling technology. However, the highest N₂O yield below 225 °C of ca. 15% was observed for the dual-layer catalyst, due to the highest NO_x conversion in this temperature range. Efforts still need to be made to further reduce the N₂O formation.

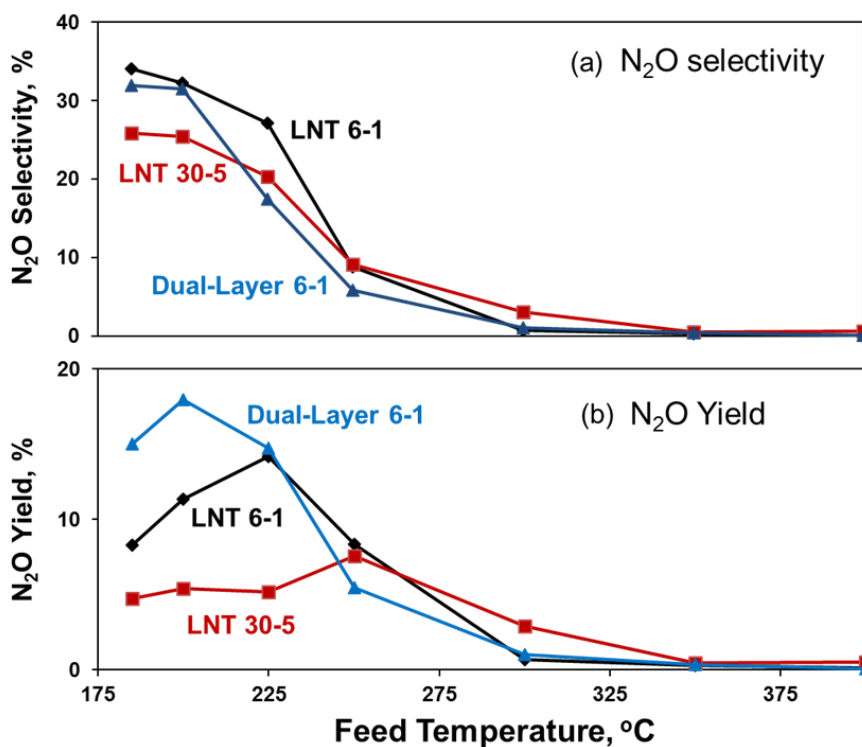


Fig. 5-6 N₂O selectivity (a) and yield (b) as a function of feed temperature for LNT alone and dual-layer catalysts with different cycle times.

5.7 Working mechanism of rapid propylene pulsing

To this point we have reported data for the effects of cycling frequency, reaction exotherm, HC intermediates, top-layer material, and the LNT ceria content to elucidate the performance of dual-layer catalysts under fast propylene pulsing. In contrast to

conventional LNT+SCR system, NH_3 is not a primary reductant of NO_x reduction in the SCR component. Here we describe a likely mechanism spanning the complete cycle.

A schematic of the proposed cyclic mechanism is shown in Fig. 5-7. The high-frequency pulse of propylene into the lean feed facilitates the generation of surface hydrocarbon intermediates on the LNT by the partial oxidation of propylene, both by surface NO_x and oxygen. These intermediates may desorb or accumulate. The oxidation process is enhanced by ceria, possibly through the spillover of oxygen to the precious metal crystallites. As discussed earlier, direct NO decomposition on reduced metal sites is another potential route for N_2 and N_2O formation. The complex set of surface catalyzed reactions generate organic oxygenates and nitrogenates which may react with NO , selectively producing N_2 and a lesser amount of byproduct N_2O . A key feature of this mechanism is the cycle timing. If the sustained supply of injected propylene, alternated with a lean feed, is accomplished at a sufficient frequency, then the desired HC-based SCR and/or NO decomposition may occur before the desorption of these intermediates, without the accumulation of surface nitrites and nitrates, and the production of deep reduction product NH_3 .

The role of the SCR top-layer is to trap partially oxygenated species that desorb from the LNT layer, enabling further production of N_2 through HC-SCR pathway. That a moderate level of additional NO_x reduction occurs even with a $\gamma\text{-Al}_2\text{O}_3$ top-layer suggests that the conversion of the intermediates is fast. Perhaps the elevated temperature caused by the propylene oxidation enhances the reaction rates. The coupled chemical and thermal effects enhance the low-temperature NO_x conversion over that of the standalone LNT.

Clearly, this proposed mechanism should be subjected to further validation with targeted experiments and modeling.

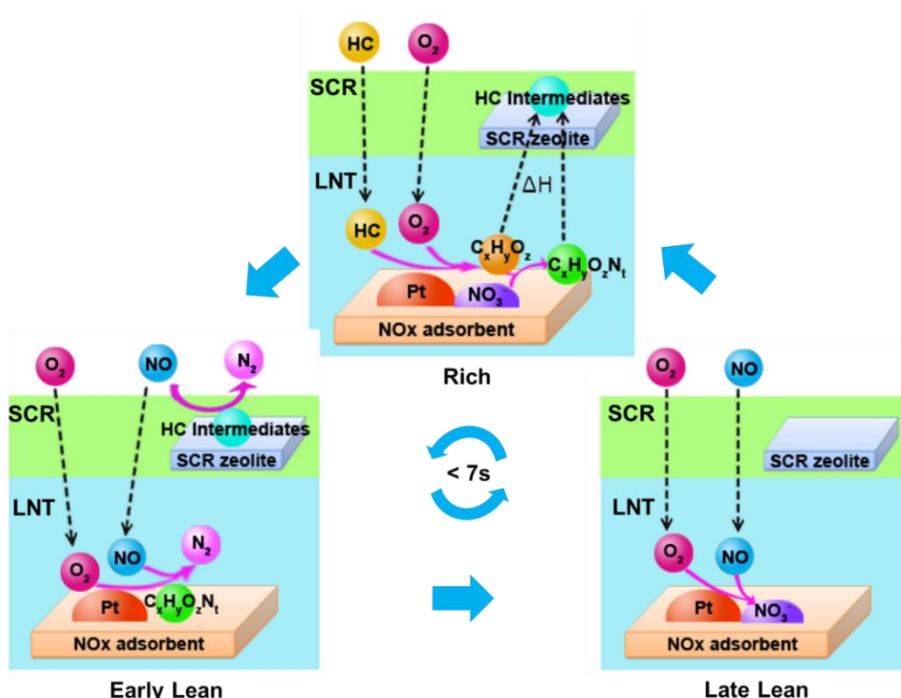


Fig. 5-7 Working mechanism for fast propylene pulsing over dual-layer catalyst.

5.8 Effects of catalyst configuration

A comparison of the cycle-averaged NOx conversions under high frequency operations using either only the LNT or LNT-SCR dual-layer or LNT-SCR dual-brick catalysts, is shown in Fig. 5-8. The three samples had the same LNT loading. The SCR brick had the same composition as the SCR used in the dual-layer catalyst but had a higher washcoat loading (2.4 g/in³) than the dual-layer catalyst (0.8 g/in³). The low-T deNOx performance of the dual-layer was best, while the dual-brick was better than LNT alone. The high low-T performance of the dual-layer catalyst is most likely due to a higher thermal benefit. On the other hand, when it comes to high-T performance, the addition of the SCR layer becomes somewhat detrimental. A high-T conversion decline may be ascribed to

diffusion limitation that limits the propene accessible to the bottom LNT and undesired propene oxidation by the SCR top-layer. This conversion loss at high temperatures may be minimized by either slightly increasing the propene concentration or applying SCR zoning, as discussed in Chapter 3.

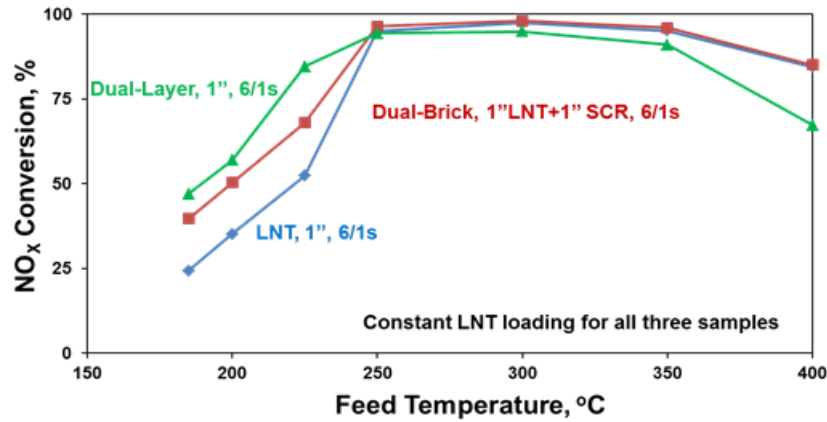


Fig. 5-8 Cycle-averaged NO_x as a function of feed temperature by LNT, dual-layer and dual-brick catalysts under fast cycling.

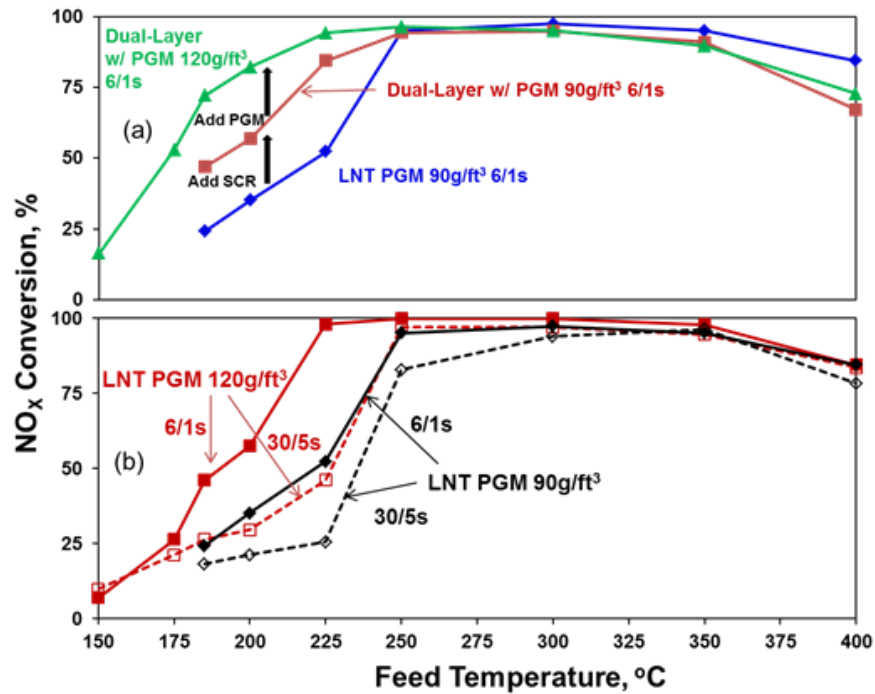


Fig. 5-9 Cycle-averaged NO_x as a function of feed temperature by (a) LNT, dual-layer catalysts with different PGM loading under the same fast cycling and (b) LNT alone with varied PGM loading and varied cycle times.

Based on the reaction mechanism of the rapid HC pulsing, the effective production of partially oxidized hydrocarbon is crucial to the low-T performance. In other words, the fast light-off of hydrocarbon oxidation determines the low-T deNO_x performance. Since higher PGM loading can reduce the light-off temperature of propene oxidation, we increased the LNT PGM loading from 90 to 120 g/ft³ to check if this leads to a better performance. Fig. 5-9a shows the dual-layer catalyst with higher PGM loading decreased the light-off temperature by ca. 25 °C relative to one with lower PGM loading to a feed temperature of ca. 175 °C. It led to about 80% NO_x conversion at feed temperature of 200 °C. The same trend was observed in Fig. 5-9b for LNT alone catalysts. A higher PMG loading decreased the light-off temperature for both fast and slow cycling.

5.9 Conclusions

High frequency propylene pulsing of LNT or dual-layer LNT-SCR catalysts under lean conditions can enhance low-temperature deNO_x efficiency and expand the operating temperature windows of a conventional NSR system. The main findings of this study are:

- High-frequency propylene pulsing expands the operating temperature window of a conventional NSR system in both the low and high-temperature regions.
- The combination of rapid propylene pulsing and the dual-layer catalyst increased low-temperature NO_x and C₃H₆ conversions. This may be useful for advanced fuel-efficient engines with low exhaust temperatures
- HC intermediates generated over the LNT can either directly react with NO_x or act as oxygen scavenger to maintain Pt at reduced states for direct NO decomposition.

- Under fast cycling partially oxidized HC intermediates should be the primary NO_x reductants for SCR, in contrast to classic NH₃-pathway. The evolution of isocyanates is considered as the RDS of HC-SCR over Cu-zeolite catalysts. The activated HC intermediates provided by the underlying LNT may facilitate isocyanates formation, thus promoting LNT-assisted HC-SCR pathway.
- A top-layer of Cu-SAPO-34 is beneficial while Ag/Al₂O₃ is detrimental.
- Ceria plays a crucial role in the activity, durability and likely reaction pathway of LNT and dual-layer catalysts under fast cycling operation.
- Optimization of catalyst configuration (i.e., zoning of SCR and PGM) can improve system performance and decrease the catalyst price.

Chapter 6 Conclusions and recommendations for future study

6.1 Conclusions

Extensive experimental studies have been conducted on lean NO_x emission control by the combined LNT-SCR catalysts. A systems approach to develop and optimize a combined catalytic system is proposed in terms of reaction pathways, catalyst formulation, configuration, regeneration protocol and operating strategy.

6.1.1 Catalyst formulation

There are some unique requirements for LNT and SCR catalysts as components in the combined system, compared to in stand-alone system. A high ceria level (34 wt.%) in the LNT improves the low-temperature (150-250 °C) performance of the dual-layer catalysts, due to enhanced NO_x adsorption and NH₃ generation. Ceria also plays a crucial role in the activity and durability of LNT and dual-layer catalysts under fast cycling operation. On the other hand, oxygen stored on ceria consumes reductants to lower the reductant/NO_x ratio and delays the time at which the catalyst reaches a net reducing state. Both effects inhibit NH₃ formation, especially at high temperatures (> 300 °C). In addition, NH₃ trapped at sites near to the LNT/SCR interface is prone to be oxidized to NO_x in the presence of a high ceria loading. This limits the high-temperature performance of dual-layer catalysts. Thus, the ceria level in the LNT is an important parameter that needs to be tuned to achieve optimum performance of combined catalysts at the targeted temperature window.

A high NH₃ storage capacity is a desirable feature of the SCR component in the combined system, as opposed to a SCR standalone system in which too high NH₃ storage

may lead to NH_3 slippage during a transient temperature excursion. For the dual-layer architecture, a high NH_3 storage capacity of Cu-SSZ-13 addresses the trade-off between high NH_3 storage capacity and low top-layer diffusion limitation by effectively trapping released NH_3 with a minimal loading (thickness). Besides, a unique durability requirement for the SCR component is the need to withstand periodic rich exposure during regeneration of underlying LNT. Reducing agents including H_2 , CO and C_3H_6 negatively affect NH_3 -SCR activities of Cu-SSZ-13 to different extents.

6.1.2 Catalyst configuration

Inherent drawbacks associated with dual-layer architecture include top-layer diffusion limitation, undesired NH_3 oxidation by LNT and inter-layer mixing of catalyst components. Using Na-ZSM-5 with a high Si/Al ratio of 280 instead of the active Cu-zeolite layer enable a quantitative analysis of top-layer diffusion limitation. A combined zoning and layering strategy is applied to mitigate the negative effect caused by the top-layer addition. Zoning of either or both the SCR and LNT in the dual-layer catalysts enables an increase of the low-temperature NO_x conversion, and minimizes the high temperature (300-400 °C) conversion loss caused by the SCR diffusion resistance and undesired NH_3 oxidation by the LNT. The combination of zoned and layered architecture is an effective catalyst design strategy, which enables a potential PGM loading reduction of up to 37.5% with comparable de NO_x performance to that of baseline LNT only catalyst in a laboratory test.

6.1.3 Rich feed composition

Different regeneration strategies lead to different types and composition of rich reductants. Generally, H_2 is the most effective reductant for NO_x reduction and NH_3

generation over the LNT, followed by CO and then HC. When using H₂ and CO as reducing agents, NH₃ is the sole chemical link between LNT and SCR via the classical NH₃-SCR pathway. The presence of HCs like propylene leads to an alternative pathway, the LNT-assisted HC-SCR pathway. Briefly speaking, the LNT promotes the formation of active partially oxidized HC intermediates during the rich purge which are otherwise difficult to produce by the Cu-zeolite layer at low temperatures. These activated intermediates are stored and react with NO_x via HC-SCR pathway in the SCR catalyst during the ensuing lean phase. The non-NH₃ pathway plays a major role in the incremental NO_x conversion over the SCR of dual-layer catalysts at low temperatures (≤ 225 °C) using simulated diesel exhaust feed. The importance of NH₃-pathway increases with temperature (225-300 °C) as NH₃ yield increases and HC intermediates stability decreases.

As the SCR component in the combined system is inevitably exposed to a rich exhaust condition during the LNT regeneration, we investigated the effects of CO, H₂ and C₃H₆ on the NH₃-SCR behavior of Cu-SSZ-13. The three reductants affect to different extent the standard SCR (NO + NH₃ + O₂), the fast SCR (NO + NH₃ + NO₂), and slow SCR (NH₃ + NO₂). Propylene is most effective in promoting NO₂ reduction to NO by formation of organic intermediates. CO effectively reduces nitrates to nitrites that react with NO₂, releasing NO. H₂ follows a similar pathway as CO but is less effective. In addition, H₂ enables a H₂-based SCR pathway through the reduction of Cu cations to Cu⁰ which then catalyzes the NO_x reduction. This pathway is particularly evident at high temperatures and low O₂ levels. As for NH₃-SCR reactions, propylene competes with NH₃ for adsorbed NO₂, which generates NO and thus increases the NO/NO_x ratio. This leads to the dominance of either fast or standard SCR for a slow SCR (NH₃ + NO₂) feed condition when C₃H₆ is

present. CO has only a minor effect on both standard and fast SCR but as a promoting effect on slow SCR. The ineffective reduction of NO₂ to NO by H₂ at low temperatures ($T < 250$ °C) results in a negligible effect on slow SCR. In contrast to steady-state operation, lean/rich cycling enhances cycle-averaged NO_x conversion for each of the NH₃-SCR reactions when adding either C₃H₆ or a CO + H₂ to the rich phase. N₂O generation rate from the slow SCR reaction is decreased when any of the three reductants are present due in part to their reaction with ammonium nitrates. This study underscores the importance of accounting for the impact of reducing agents on conventional NH₃-SCR reaction mechanism when SCR catalyst is subjected to either rich regeneration of integrated systems (LNT + SCR, SCR on DPF) or cold-start.

6.1.4 Lean/rich timing

Conventional NSR cyclic operation comprises a sequential lean phase (typically 30-90 s) and a much shorter rich phase (3-10 s). Spatial temporal analysis of NH₃ evolution over the LNT during the regeneration event reveals that NH₃ was produced behind and at the reductant front. In other words, no NH₃ is emitted from LNT outlet until the reductant front breaks through. This suggests a relatively long rich phase is beneficial for high NH₃ yield, and thus greater SCR contribution to the overall NO_x conversion of the combined catalyst. Prolonged rich phase, however, compromises the fuel economy target and raises concerns on the CO and HC slippage. For example, the recent TWC + passive SCR studies by ORNL researchers reported that NO_x emission can be satisfactorily abated by the use of *in-situ* NH₃ formation from TWC, while the biggest challenge goes for the significant CO and HC slippage. Compared to the relatively long cycle time of typical NSR operation,

Di-Air process developed by Toyota is a potential solution to the trade-off between NO_x conversion and fuel economy.

Fast C₃H₆ pulsing into a lean exhaust stream expands the operating temperature window of a conventional NSR system at both the low and high-temperature regions. The combination of rapid propylene pulsing and the dual-layer catalyst architecture achieves a low-temperature NO_x conversion of up to 80% at a feed temperature of ca. 200 °C and relevant space velocities ($\sim 70\text{ k h}^{-1}$). Fast cycling facilitates the generation of partially oxidized hydrocarbon intermediates over the LNT that can then either directly react with NO_x or act as oxygen scavenger that maintains Pt in a reduced state for direct NO decomposition. The SCR top-layer traps partially oxygenated species that desorb from the LNT layer, enabling further production of N₂ through a LNT-assisted HC-SCR pathway. Optimization of ceria content, top-layer material and catalyst configuration like SCR and PGM zoning can improve system performance and reduce catalyst price.

6.2 Recommendations for future study

Many questions remain about catalyst design and operating strategy of the combined LNT-SCR system. Practical applications require determining the impact of thermal aging and sulfur posing on the combined catalysts. Another important question is the optimal loading ratio of LNT and SCR. The optimal ratio depends on the synergistic interaction between the LNT and SCR components. The optimal ratio varies with system designs and operating strategies as the synergy depends on catalyst configuration and formulation (component, composition, washcoat loading), regeneration method (lean/rich timing, rich lambda, types of reducing agents), reaction conditions (SV, temperatures, NO₂/NO_x ratio), as well as regulatory constraints (fuel penalty, emission of other regulated

pollutants). In this regard, the optimal or most promising systems should be determined prior to optimizing the loading ratio of the LNT to the SCR specific to a certain system. This dissertation has provided information to help understand what are critical system parameters, how critical parameters are measured and how they interconnect. System engineering tools for rigorous critical parameter management like Technology Development for Six Sigma (TDFSS) should be employed to find out an optimal design that strikes the best balance between regulatory requirement, technology capabilities, business goals and customer expectation.

The BASF LNT catalysts used in our study are not optimal for the combined application. Although high ceria loading of 34 wt.% is preferable to ceria-free for dual-layer catalysts under either NSR cycle with simulated diesel exhaust or Di-Air process with fast C₃H₆ pulsing, other components like NO_x storage materials, noble metals in LNT and Cu content and Si/Al ratio in SCR, can be optimized for a better performance. For example, except for the ideal case with pure H₂ as the reductant, a reduction of more than 25 wt.% in LNT loading within dual-layer catalysts degrades the overall deNO_x performance, compared to the LNT standalone baseline. The additional NO_x conversion by SCR layer fails to compensate for the performance loss caused by the reduced LNT loading. Spatial analysis identifies a significant NO_x slippage during the lean phase. It can be ascribed to reduced loading of NO_x storage material (i.e., Ba and Ce). Thus, it is desirable to reduce the expensive PGM loading at constant barium and ceria loading to maintain the NO_x storage capacity, rather than decreasing total LNT loading. This can help determine the potential maximum PGM loading reduction for combined systems. More importantly, a reliable model of combined catalysts that factor in the effects of PGM, ceria, NO_x and NH₃

storage capacity, undesirable NH_3 oxidation, diffusion limitation, etc., is useful to determine the optimal catalyst formulation and configuration of the combined system.

The study regarding the effects of CO , H_2 and C_3H_6 on Cu-SSZ-13 catalyzed NH_3 -SCR reactions, underscores the importance of accounting for the impact of reducing agents on the conventional NH_3 -SCR reaction mechanism when the SCR catalyst is subjected to rich exposure. Current SCR models predict well the behavior of standalone SCR operating under lean conditions. In order to improve the prediction of the performance of the combined catalysts, the SCR model needs to be modified to account for the effects of rich reducing agents. Such modified SCR models can be applied also to other combined system like SCR on filter or standalone SCR during the cold-start, desulfation and regeneration of upstream DPF.

Future studies on fast cycling will focus on the impact of different HC species and injection frequency on the performance of both LNT alone and combined LNT-SCR catalysts. Preliminary results show that the type of HC species is critical for low-temperature enhancement. Preferred are light olefins, which have a relatively low light-off oxidation temperature and stronger affinity to Pt. Propane that weakly adsorbs on Pt and has a higher light-off temperature, limit the performance enhancement by fast cycling and SCR-layer addition. HC mixture of short- and long-chain alkane and alkene may benefit from fast cycling operation. In addition to experimental work, modelling of fast cycling is needed to determine the optimal injection frequency and design of injector and mixer to enhance radial uniformity and minimize axial mixing.

REFERENCES

- [1] T. Johnson, *SAE Int. J. Engines* 7 (2014) 1207-1227.
- [2] N. Zacharof, U. Tietge, P. Mock, “CO₂ Emissions from New Passenger Cars in The EU: Car Manufacturers' Performance in 2014,” International Council on Clean Transportation, 2015.
- [3] M. Zammit, C.L. DiMaggio, C.H. Kim, C. Lambert, G.G. Muntean, C.H. Peden, J.E. Parks, K. Howden, “Future Automotive Aftertreatment Solutions: The 150 °C Challenge Workshop Report,” U.S. DRIVE Advanced Combustion and Emission Control, 2013.
- [4] G.D. Neely, J.V. Sarlashkar, D. Mehta, *SAE Int. J. Engines* 6 (2013) 1009-1020.
- [5] T. Johnson, *SAE Int. J. Engines* 6 (2013) 699-715.
- [6] P. Granger, V.I. Parvulescu, *Chem. Rev.* 111 (2011) 3155-3207.
- [7] F. Gao, J.H. Kwak, J. Szanyi, C.H. Peden, *Top. Catal.* 56 (2013) 1441-1459.
- [8] S. Satokawa, J. Shibata, K.-i. Shimizu, A. Satsuma, T. Hattori, *Appl. Catal. B: Environ.* 42 (2003) 179-186.
- [9] W.S. Epling, L.E. Campbell, A. Yezerets, N.W. Currier, J.E. Parks, *Catal. Rev.* 46 (2004) 163-245.
- [10] T. Morita, N. Suzuki, N. Satoh, K. Wada, H. Ohno, *SAE Tech. Paper* 2007-01-0239 (2007).
- [11] L. Xu, R.W. McCabe, *Catal. Today* 184 (2012) 83-94.
- [12] T.C. Watling, M.R. Ravenscroft, G. Avery, *Catal. Today* 188 (2012) 32-41.
- [13] L. Castoldi, N. Artioli, R. Matarrese, L. Lietti, P. Forzatti, *Catal. Today* 157 (2010) 384-389.

- [14] L. Xu, R. McCabe, M. Dearth, W. Ruona, *SAE Int. J. Fuels Lubr.* 3 (2010) 37-49.
- [15] Y. Zheng, Y. Liu, M.P. Harold, D. Luss, *Appl. Catal. B: Environ.* 148 (2014) 311-321.
- [16] K. Wada, N. Suzuki, N. Satoh, T. Morita, S. Yamaguchi, H. Ohno, *SAE Tech. Paper* 2007-01-1933 (2007).
- [17] N. Waldbuesser, J. Guenther, H. Hoffmann, O. Erlenmayer, F. Duvinage, C. Enderle, J. Schommers, D. Waeller, *SAE Tech. Paper* 2010-01-1172 (2010).
- [18] E.C.W. Hai-Ying Chen, Joseph M. Fedeyko, Julian P. Cox and Paul J. Andersen, *SAE Tech. Paper* 2010-01-0302 (2010).
- [19] T. Wittka, B. Holderbaum, P. Dittmann, S. Pischinger, *Emiss. Control Sci. Technol.* 1 (2015) 167-182.
- [20] G.D. Neely, D. Mehta, J. Sarlashkar, *SAE Int. J. Engines* 7 (2014) 1302-1310.
- [21] J. Jeon, H. Seo, K. Lee, S. Kwon, K. Bae, *SAE Tech. Paper* 2014-01-1529 (2014).
- [22] Y. Matsuo, S. Ishimaru, M. Amano, N. Komatsu, S. Aoyagi, H. Dan, T. Endo, Y. Matsuzono, T. Ito, M. Nagata, *SAE Tech. Paper* 2013-01-0536 (2013).
- [23] G. Koltsakis, O. Haralampous, I. Koutoufaris, *SAE Tech. Paper* 2010-01-0893 (2010).
- [24] Y. Liu, Y. Zheng, M.P. Harold, D. Luss, *Appl. Catal. B: Environ.* 132-133 (2013) 293-303.
- [25] Y. Bisaiji, K. Yoshida, M. Inoue, K. Umemoto, T. Fukuma, *SAE Int. J. Fuels Lubr.* 5 (2011) 380-388.
- [26] Y. Bisaiji, K. Yoshida, M. Inoue, N. Takagi, T. Fukuma, *SAE Int. J. Fuels Lubr.* 5 (2012) 1310-1316.

- [27] C.C. Perng, V.G. Easterling, M.P. Harold, *Catal. Today* 231 (2014) 125-134.
- [28] J.A. Pihl, J.E. Parks, C.S. Daw, T.W. Root, *SAE Tech. Paper* 2006-01-3441 (2006).
- [29] R.D. Clayton, M.P. Harold, V. Balakotaiah, *Appl. Catal. B: Environ.* 81 (2008) 161-181.
- [30] P. Forzatti, L. Lietti, L. Castoldi, *Catal. Lett.* 145 (2015) 483-504.
- [31] L. Cumananatunge, S. Mulla, A. Yezerets, N. Currier, W. Delgass, F. Ribeiro, *J. Catal.* 246 (2007) 29-34.
- [32] T. Szailer, J. Kwak, D. Kim, J. Hanson, C. Peden, J. Szanyi, *J. Catal.* 239 (2006) 51-64.
- [33] P. Forzatti, L. Lietti, I. Nova, S. Morandi, F. Prinetto, G. Ghiotti, *J. Catal.* 274 (2010) 163-175.
- [34] P. Dasari, R. Muncrief, M.P. Harold, *Top. Catal.* 56 (2013) 1922-1936.
- [35] R.J. Gorte, *AIChE J.* 56 (2010) 1126-1135.
- [36] F. Posada, A. Bandivadekar, J. German, *SAE Tech. Paper* 2013-01-0539 (2013).
- [37] W.P. Partridge, J.M. Storey, S.A. Lewis, R.W. Smithwick, G.L. DeVault, M.J. Cunningham, N.W. Currier, T.M. Yonushonis, *SAE Tech. Paper* 2000-01-2952 (2000).
- [38] R. Burch, J. Breen, F. Meunier, *Appl. Catal. B: Environ.* 39 (2002) 283-303.
- [39] M. Al-Harbi, D. Radtke, W.S. Epling, *Appl. Catal. B: Environ.* 96 (2010) 524-532.
- [40] J. Wang, Y. Ji, Z. He, M. Crocker, M. Dearth, R.W. McCabe, *Appl. Catal. B: Environ.* 111-112 (2012) 562-570.
- [41] C. Sedlmair, K. Seshan, A. Jentys, J. Lercher, *J. Catal.* 214 (2003) 308-316.
- [42] J.-Y. Luo, H. Oh, C. Henry, W. Epling, *Appl. Catal. B: Environ.* 123 (2012) 296-305.

- [43] H.-Y. Chen, T. Voskoboinikov, W. Sachtler, *Catal. Today* 54 (1999) 483-494.
- [44] H. Abdulhamid, J. Dawody, E. Fridell, M. Skoglundh, *J. Catal.* 244 (2006) 169-182.
- [45] M. Huuhtanen, T. Kolli, T. Maunula, R.L. Keiski, *Catal. Today* 75 (2002) 379-384.
- [46] O. Gorce, F. Baudin, C. Thomas, P. Da Costa, G. Djéga-Mariadassou, *Appl. Catal. B: Environ.* 54 (2004) 69-84.
- [47] N. Collins, J. Cooper, D. Morris, A. Ravenscroft, M. Twigg, *SAE Tech. Paper* 2005-01-2158 (2005).
- [48] A. Kumar, K. Kamasamudram, A. Yezerets, *SAE Int. J. Engines* 6 (2013) 680-687.
- [49] C. He, Y. Wang, Y. Cheng, C.K. Lambert, R.T. Yang, *Appl. Catal. A: Gen.* 368 (2009) 121-126.
- [50] I. Heo, Y. Lee, I.-S. Nam, J.W. Choung, J.-H. Lee, H.-J. Kim, *Micropor. Mesopor. Mat.* 141 (2011) 8-15.
- [51] J.-Y. Luo, A. Yezerets, C. Henry, H. Hess, K. Kamasamudram, H.-Y. Chen, W.S. Epling, *SAE Tech. Paper* 2012-01-1096, 2012.
- [52] M.-Y. Kim, J.-S. Choi, M. Crocker, *Catal. Today* 231 (2014) 90-98.
- [53] Y. Huang, Y. Cheng, C. Lambert, *SAE Int. J. Fuels Lubr.* 1 (2009) 466-470.
- [54] M.A. Smith, C. Depcik, J. Hoard, S. Bohac, D. Assanis, *SAE Tech. Paper* 2013-01-1062 (2013).
- [55] P. Namkhang, P. Kongkachuichay, *J. Nanosci. Nanotechnol.* 15 (2015) 5410-5417.
- [56] F. Gao, E.D. Walter, E.M. Karp, J. Luo, R.G. Tonkyn, J.H. Kwak, J. Szanyi, C.H.F. Peden, *J. Catal.* 300 (2013) 20-29.
- [57] P.G. Savva, C.N. Costa, *Catal. Rev.* 53 (2011) 91-151.

- [58] J. Xue, X. Wang, G. Qi, J. Wang, M. Shen, W. Li, *J. Catal.* 297 (2013) 56-64.
- [59] I. Lezcano-Gonzalez, U. Deka, B. Arstad, A. Van Yperen-De Deyne, K. Hemelsoet, M. Waroquier, V. Van Speybroeck, B.M. Weckhuysen, A.M. Beale, *Phys. Chem. Chem. Phys.* 16 (2014) 1639-1650.
- [60] D. Wang, L. Zhang, K. Kamasamudram, W.S. Epling, *ACS Catal.* 3 (2013) 871-881.
- [61] F. Solymosi, T. Bansagi, *J. Catal.* 156 (1995) 75-84.
- [62] A. Pelmenchikov, R. Van Santen, J. Janchen, E. Meijer, *J. Phys. Chem.* 97 (1993) 11071-11074.
- [63] C. Prestipino, L. Capello, F. D'Acapito, C. Lamberti, *Phys. Chem. Chem. Phys.* 7 (2005) 1743-1746.
- [64] A. Grossale, I. Nova, E. Tronconi, D. Chatterjee, M. Weibel, *J. Catal.* 256 (2008) 312-322.
- [65] K. Kamasamudram, C. Henry, N. Currier, A. Yezerets, *SAE Int. J. Engines* 5 (2012) 688-698.
- [66] M. Inoue, Y. Bisaiji, K. Yoshida, N. Takagi, T. Fukuma, *Top. Catal.* 56 (2013) 3-6.
- [67] Y. Zheng, D. Luss, M.P. Harold, *SAE Int. J. Engines* 7 (2014) 1280-1289.
- [68] Y. Zheng, M. Li, M. Harold, D. Luss, *SAE Int. J. Engines* 8 (2015).
- [69] D. Wang, F. Gao, C.H. Peden, J. Li, K. Kamasamudram, W.S. Epling, *ChemCatChem* 6 (2014) 1579-1583.
- [70] T. Uenishi, K. Umemoto, K. Yoshida, T. Itoh, T. Fukuma, *Int. J. Automotive Eng.* 5 (2014) 115-120.

- [71] R.L. Muncrief, K.S. Kabin, M.P. Harold, *AIChE J.* 50 (2004) 2526-2540.
- [72] K.S. Kabin, R.L. Muncrief, M.P. Harold, *Catal. Today* 96 (2004) 79-89.
- [73] W.S. Epling, A. Yezerets, N.W. Currier, *Catal. Lett.* 110 (2006) 143-148.
- [74] L. Lietti, M. Daturi, V. Blasin-Aube, G. Ghiotti, F. Prinetto, P. Forzatti, *ChemCatChem* 4 (2012) 55-58.
- [75] L. Xu, R. McCabe, P. Tennison, H.-W. Jen, *SAE Int. J. Engines* 4 (2011) 158-174.
- [76] Y. Zheng, M.P. Harold, D. Luss, "Effects of CO, H₂ and C₃H₆ on Cu-SSZ-13 Catalyzed NH₃-SCR", *Catal. Today*, 2015, in press.
- [77] A.G. Panov, R.G. Tonkyn, M.L. Balmer, C.H. Peden, A. Malkin, J. Hoard, *SAE Tech. Paper* 2001-01-3513 (2001).
- [78] J.-Y. Luo, W.S. Epling, G. Qi, W. Li, *Catal. Lett.* 142 (2012) 946-958.
- [79] Y. Wang, J.P.d. Boer, F. Kapteijn, M. Makkee, "The Role of Ceria in NO_x Reduction by Hydrocarbons and The Possible Reaction Pathway," 24th North American Catalysis Society Meeting, 2015.
- [80] S. Tamm, H.H. Ingelsten, A.E. Palmqvist, *J. Catal.* 255 (2008) 304-312.

